

Bio-based ground improvement through Microbial Induced Desaturation and Precipitation (MIDP)

Pham, Vinh

DOI

[10.4233/uuid:3997066a-0ad6-4de2-9c79-e5e474bae20f](https://doi.org/10.4233/uuid:3997066a-0ad6-4de2-9c79-e5e474bae20f)

Publication date

2017

Document Version

Final published version

Citation (APA)

Pham, V. (2017). *Bio-based ground improvement through Microbial Induced Desaturation and Precipitation (MIDP)*. [Dissertation (TU Delft), Delft University of Technology]. <https://doi.org/10.4233/uuid:3997066a-0ad6-4de2-9c79-e5e474bae20f>

Important note

To cite this publication, please use the final published version (if applicable). Please check the document version above.

Copyright

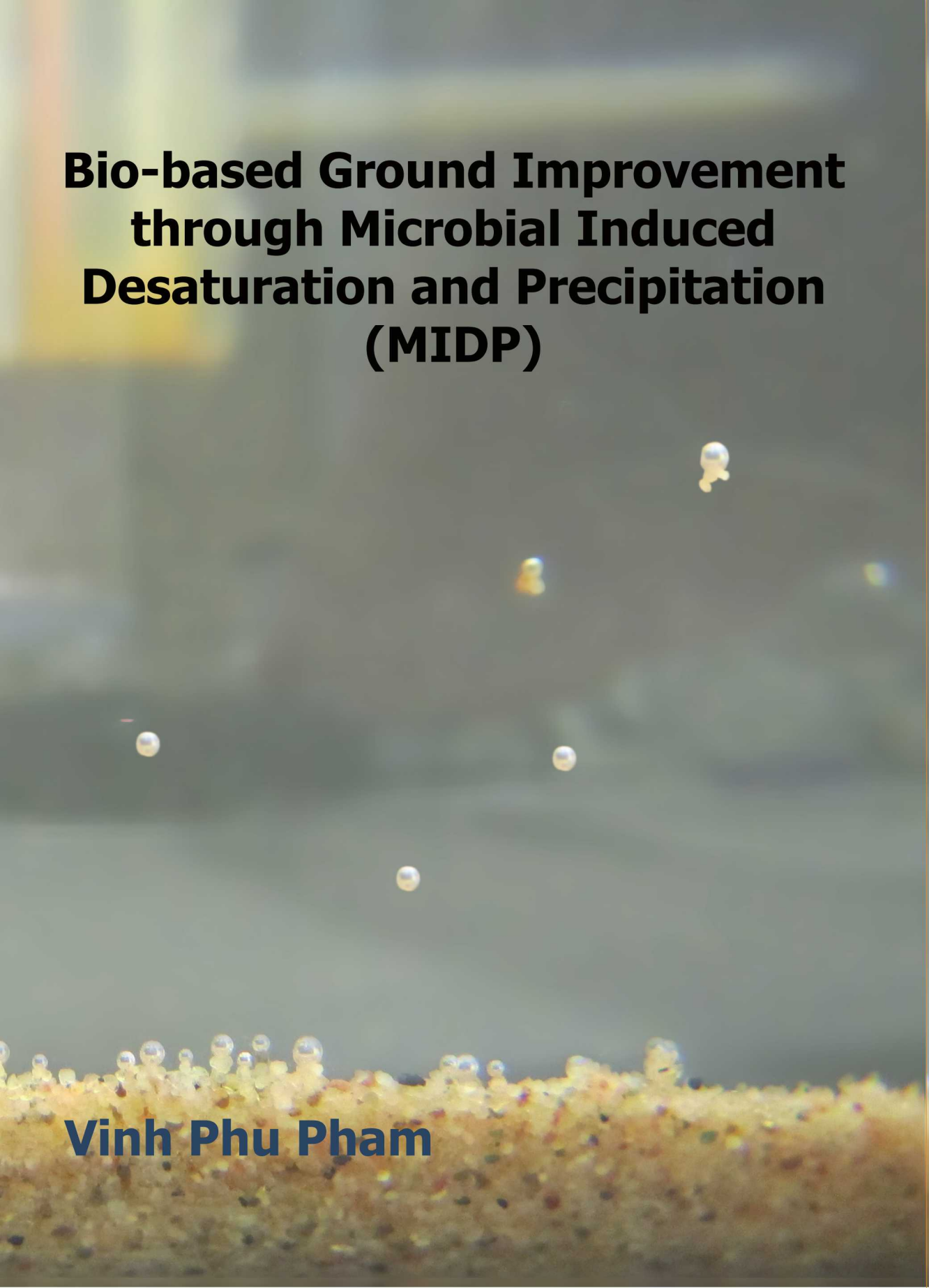
Other than for strictly personal use, it is not permitted to download, forward or distribute the text or part of it, without the consent of the author(s) and/or copyright holder(s), unless the work is under an open content license such as Creative Commons.

Takedown policy

Please contact us and provide details if you believe this document breaches copyrights. We will remove access to the work immediately and investigate your claim.

Bio-based Ground Improvement through Microbial Induced Desaturation and Precipitation (MIDP)

Vinh Phu Pham

A microscopic view of soil particles, likely sand or silt, with numerous small, clear water droplets attached to their surfaces. The background is a soft, out-of-focus greyish-blue, suggesting a liquid environment. The droplets vary in size and are scattered across the field of view, with a higher concentration near the bottom edge where they appear to be coating the particles.

Propositions

accompanying the dissertation

Bio-based ground improvement through Microbial Induced Desaturation and Precipitation (MIDP)

by

Vinh P. Pham

1. Denitrification based MICP is a coupled process, in which denitrification and calcium carbonate precipitation influence and are beneficial to each other: denitrification produces dissolved inorganic carbon and alkalinity required to precipitate calcium carbonate, whereas the precipitation generates favourable growth conditions for denitrifying bacteria by neutralizing its alkaline tendency.
2. Biochemical and mechanical interaction of the reaction products of denitrification based MICP process is an advantage to their applications in practice.
3. The key to an optimum treatment strategy of denitrification based MICP is to minimize the lag phase of the denitrifying bacteria.
4. Minimizing accumulation of the denitrification intermediates is required not only to reduce the risk of their toxicity but also to increase the calcium carbonate precipitation yield.
5. 'What we see is all there is' - Daniel Kahneman, so 'To see a thing, you must first believe it possible' – Ted Nield.
6. 'Everything is everywhere, it's the environment that selects' – Baas Becking, is only the starting point; as the "chosen" ecology modifies the original environment and thus the selecting conditions.
7. Things are often perfect the way they are, the issue is how to find the perfect spot to fit each of these things in.
8. Experimentalists and numerical modellers are like the realists and the dreamers. 'The dreamers need the realists to keep them from soaring too close to the sun, and the realists without the dreamers might not ever get off the ground' – from Modern Family.
9. Doing a PhD is to train the students to be advanced in being aware about things they do not know yet, and still, confident about their progress.

These propositions are considered opposable and defendable, and have been approved as such by the promoters Prof. di. ir. Timo J. Heimovaara and Dr. ir. Leon A. van Paassen.

Stellingen

behorende bij het proefschrift

Bio-based ground improvement through Microbial Induced Desaturation and Precipitation (MIDP)

door

Vinh Pham

1. Microbiologisch ge-Induceerde Desaturatie en Precipitatie (MIDP) is een gekoppeld proces, waarbij de twee deelprocessen, denitrificatie en calciumcarbonaat precipitatie, elkaar gunstig beïnvloeden: de productie van alkaliniteit door denitrificatie stimuleert de neerslag van calciumcarbonaat, terwijl de consumptie van alkaliniteit door calciumcarbonaat precipitatie neutraliseert de zuurgraad en creëert daarmee gunstige omstandigheden voor de groei van denitrificerende bacteriën.
2. De biochemische en mechanische interactie tussen de reactieproducten is voordelig voor toepassingen van het MIDP proces in de praktijk.
3. De sleutel tot een optimale behandelingsstrategie van het MICP proces op basis van denitrificatie is de aanpassingsfase van de denitrificerende bacteriën te minimaliseren.
4. Het minimaliseren van accumulatie van de tussenproducten van het denitrificatie proces is niet alleen nodig om het risico op hun toxiciteit te verminderen, maar ook om de opbrengst van calciumcarbonaatafbreking te verhogen.
5. 'Wat we zien is alles wat er is' - Dannieel Kahneman, dus 'Om iets te zien moet je het eerst geloven dat het bestaat.' - Ted Nield.
6. 'Alles is overal, het is de omgeving die selecteert' - Baas Becking, is slechts het beginpunt; Aangezien de "gekozen" ecologie de oorspronkelijke omgeving en daarmee de selectievoorwaarden wijzigt.
7. Dingen zijn vaak perfect zoals ze zijn. Het probleem is hoe je de perfecte plek kunt vinden om elk van deze dingen in te passen.
8. Experimentalisten en numerieke modellers houden zich als realisten en dromers. 'De dromers hebben de realisten nodig om te voorkomen dat ze dichtbij de zon vliegen, terwijl de realisten zonder de dromers waarschijnlijk nooit van de grond zouden komen' – uit "Modern Family".
9. Een promotie onderzoek traint studenten om zich sterk bewust te zijn van dingen die ze nog niet kennen, maar tegelijk nog steeds zelfverzekerd te zijn over hun voortgang.

Deze stellingen worden oponeerbaar en verdedigbaar geacht en zijn als zodanig goedgekeurd door de promotoren Prof. Dr. Ir. Timo J. Heimovaara en Dr. Ir. Leon A. van Paassen.

Bio-based ground improvement through
Microbial Induced Desaturation and
Precipitation (MIDP)

Vinh Phú Phạm

Bio-based ground improvement through Microbial Induced Desaturation and Precipitation (MIDP)

Proefschrift

ter verkrijging van de graad van doctor
aan de Technische Universiteit Delft,
op gezag van de Rector Magnificus prof.ir. K.C.A.M. Luyben;
voorzitter van het College voor Promoties,
in het openbaar te verdedigen op
dinsdag 4 juli 2017 om 12:30 uur

door

Vinh Phú PHẠM
Master of Science in Civil Engineering, Delft University of Technology,
Netherlands
geboren te Hanoi, Vietnam

This dissertation has been approved by the promotor:
Prof.dr.ir T.J. Heimovaara and Dr.ir L.A. van Paassen

Composition of the doctoral committee:

Rector Magnificus	chairmen
Prof.dr.ir T.J. Heimovaara	Delft University of Technology
Dr.ir L.A. van Paassen	Arizona State University

Independent members:	
Prof.dr. J. Chu	Nanyang TU, Singapore
Prof.dr. K.G. Gavin	Delft University of Technology
Prof.dr. C. Jommi	Delft University of Technology
Prof.dr.ir. P.L.J. Zitha	Delft University of Technology
Dr. H.M. Jonkers	Delft University of Technology



ISBN: 978-94-028-0695-3

Cover picture by: Minh L. Vu
Printed by: Ipskamp Printing

This research was funded by the Dutch Ministry of Economic Affairs, through STW perspective program BioGeoCivil (11337), and performed in close collaboration of Deltares, Van Hattum en Blankevoort – Volker Stevin and Delft University of Technology.

For my parents, my husband, and our son..

Contents

Summary	5
Samenvatting.....	8
Acknowledgement.....	12
1. Potential of denitrification for MICP and soil desaturation as a ground improvement method	15
1.1. Inducing calcium carbonate precipitation in sandy soil through biological pathways	16
1.2. Process characteristics and challenges of MIDP by denitrification.....	18
1.3. Thesis objective.....	19
1.4. Thesis structure	20
2. Denitrification ecology and stoichiometry.....	23
2.1. Nitrate reduction and denitrification ecology	24
2.1.1. <i>Denitrification among different pathways of nitrate reduction</i>	24
2.1.2. <i>The intermediates of denitrification</i>	26
2.2. Kinetic growth and inhibition factor of denitrification.....	27
2.3. Stoichiometry of complete denitrification	28
2.3.1. <i>Metabolism and Gibbs energy</i>	28
2.3.2. <i>Stoichiometry of catabolism</i>	29
2.3.3. <i>Stoichiometry of anabolism</i>	30
2.3.4. <i>Gibbs energy change of the overall specific growth reaction</i>	30
2.3.5. <i>Maximum specific growth rate</i>	31
2.3.6. <i>Overall specific growth reaction</i>	31
2.4. Conclusion	32
3. Applying MICP by denitrification in soils: a process analysis	33
3.1. Introduction	34
3.2. Materials and Methods	34
3.2.1. <i>Substrate solutions</i>	34
3.2.2. <i>Liquid batch experiments</i>	35
3.2.3. <i>Sand column experiments in a triaxial cell at varying pressure conditions</i>	36
3.2.4. <i>Sand column experiments with multiple batches of substrate solution</i>	37
3.3. Results	39
3.3.1. <i>Liquid batch experiments</i>	39
3.3.2. <i>Triaxial tests at different pressure conditions</i>	42

3.3.3. <i>Sand column experiment with multiple substrate flushes at ambient pressure</i>	44
3.4. Discussion	48
3.4.1. <i>Mass balance</i>	48
3.4.2. <i>The effect of substrate composition on process efficiency</i>	49
3.4.3. <i>The effect of pressure conditions on gas formation and distribution</i>	50
3.4.4. <i>The relationship between the distribution of gas and calcium carbonate</i>	50
3.4.5. <i>Conversion</i>	51
3.5. Conclusions	51
4. Biogenic gas formation by denitrification-based MICP in sandy soils	53
4.1. Introduction	54
4.2. Simplified calculation method to predict the gas saturation in porous media generated by denitrification.	54
4.3. Experimental method and materials.....	56
4.3.1. <i>Experiment set-up and variables</i>	56
4.3.2. <i>Bacteria cultivation and substrate concentrations</i>	58
4.4. Experimental results	59
4.4.1. <i>Water saturation and hydraulic conductivity changes</i>	59
4.4.2. <i>Results of the sand behaviour under undrained monotonic loading</i>	61
4.5. Discussion	63
4.5.1. <i>Comparing the simplified model with experimental results</i>	63
4.5.2. <i>Effect of soil matrix and pressure conditions on gas formation and stability</i>	65
4.6. Conclusion.....	67
5. Evaluating strategies to improve process efficiency of denitrification based MICP	69
5.1. Introduction	70
5.2. Materials and methods.....	72
5.2.1. <i>Bacteria cultivation</i>	72
5.2.2. <i>Sand types</i>	72
5.2.3. <i>Substrate concentrations, resident duration and number of flush</i>	72
5.2.4. <i>Equipment</i>	73
5.2.5. <i>Experimental procedure</i>	74
5.3. Results	76
5.3.1. <i>Substrate consumption of the stock inoculum in liquid batch</i>	76
5.3.2. <i>Water saturation changes and permeability reduction of the sand samples in the triaxial tests</i>	77

5.3.3.	<i>Flow rates during flushing after each treatments.....</i>	<i>78</i>
5.3.4.	<i>Substrate consumption and production rate in the sand columns throughout the treatments</i>	<i>80</i>
5.3.5.	<i>Amount of precipitated CaCO₃.....</i>	<i>83</i>
5.3.6.	<i>Soil behaviour under monotonic loading</i>	<i>85</i>
5.3.7.	<i>ESEM images of a sand lump</i>	<i>86</i>
5.4.	<i>Discussion.....</i>	<i>86</i>
5.4.1.	<i>Effect of initial concentrations on the conversion rate and yield</i>	<i>86</i>
5.4.2.	<i>Effect of other process conditions on conversion rate and yield.....</i>	<i>88</i>
5.4.3.	<i>Gas production and its stability in the sand</i>	<i>90</i>
5.4.4.	<i>Impact of the reaction products on the sand.....</i>	<i>91</i>
5.4.5.	<i>Implications for practical application of denitrification-based MICP.....</i>	<i>92</i>
5.5.	<i>Conclusion</i>	<i>93</i>
6.	<i>Model of 2-step denitrification-based MICP</i>	<i>95</i>
6.1.	<i>Introduction</i>	<i>96</i>
6.2.	<i>Theory.....</i>	<i>96</i>
6.2.1.	<i>Kinetic growth and inhibition mechanisms.....</i>	<i>96</i>
6.2.2.	<i>Stoichiometry of two2-step denitrification and the overall reaction</i>	<i>98</i>
6.2.3.	<i>Dependence of the stoichiometry on the specific growth rate of the metabolism.....</i>	<i>99</i>
6.2.4.	<i>Equilibrium calculation.....</i>	<i>100</i>
6.3.	<i>Model implementation</i>	<i>100</i>
6.3.1.	<i>Model structure</i>	<i>100</i>
6.3.2.	<i>Testing cases and model variables.....</i>	<i>103</i>
6.3.3.	<i>Evaluate performance of the model by the 'grey modelling' toolbox</i>	<i>104</i>
6.4.	<i>Results and discussion.....</i>	<i>104</i>
6.4.1.	<i>Result of the 2-step denitrification stoichiometry analysis.....</i>	<i>104</i>
6.4.2.	<i>Case I – Considering substrate limitation with fixed kinetic constants</i>	<i>106</i>
6.4.3.	<i>Case II –Considering substrate limitations and inhibitions with fixed and calibrated parameters</i>	<i>111</i>
6.4.4.	<i>Predicting results of calcite and pH.....</i>	<i>115</i>
6.4.5.	<i>Utilization of results</i>	<i>115</i>
6.4.6.	<i>Model limitations and recommendations for future work.....</i>	<i>117</i>
6.5.	<i>Conclusions</i>	<i>118</i>
7.	<i>Conclusion.....</i>	<i>119</i>
	<i>List of figures.....</i>	<i>122</i>

SUPPLEMENTAL DATA	125
S1. Supplemental data of the single treatment experiments – Pore and back pressure changes during the reacting period.....	125
S2. Supplemental data of the multiple treatment experiments	126
S2.1. <i>Change of pore water volume and hydraulic conductivity</i>	126
S2.2. <i>Concentrations and volumes of the substrates in the flushes</i>	128
S2.3. <i>Breakthrough curves of electrical conductivity EC of the outflows during flushing</i>	130
S2.4. <i>Substrate consumption during the treatments</i>	132
S2.5. <i>Estimating the amount of Ca²⁺ reacted for CaCO₃ precipitation from the concentration measurements</i>	136
S2.6. <i>ESEM images and XRF analysis results of large precipitated crystals</i>	138
S2.7. <i>Pore pressure response during the resident time</i>	143
References	144
Curriculum Vitae	152

Summary

Improving and altering soil foundation conditions is a common task in construction and civil engineering. It often involves increasing soil strength or stiffness or reducing hydraulic conductivity to reduce soil deformation during and after construction. Besides conventional ground improvement methods, there are several biological processes that can improve ground properties by precipitating calcium carbonate. Microbially Induced Carbonate Precipitation, MICP, using microbially catalysed hydrolysis of urea has been demonstrated at field scale and has shown to be suitable as a ground improvement method. Research and development on this subject is ongoing aiming to optimize and scale up the method for various practical applications. Another biological process that can be used for MICP is denitrification which is the subject of this thesis. In this process indigenous denitrifying bacteria are supplied with a solution containing calcium fatty acids and calcium nitrate, which allows them to precipitate calcium carbonate and forms cementing bonds between the sand grains, resulting in increase of strength and stiffness. Besides precipitating calcium carbonate they also produce nitrogen gas. The formation of gas reduces the water saturation, which may be utilized to increase the soil resistance to dynamic loading. Hence denitrification based MICP or Microbially Induced Desaturation and Precipitation, MIDP, has two ways in which it alters ground properties and therefore expands the potential of biological processes to improve the ground conditions for different applications.

Using denitrification for MIDP has several challenges. In the denitrification reaction, nitrate is reduced to (di)nitrogen gas through the three intermediates: nitrite, nitric oxide and nitrous oxide. All these intermediates are harmful to living organisms and the environment so their accumulation should be avoided. Using the nitrogen gas production in applications such as liquefaction mitigation has another challenge which is about how to control the gas formation, distribution and its stability. The final challenge for MIDP when it is used to create cementing bonds between soil particles is its low rate of calcium carbonate precipitation in comparison with MICP using urea hydrolysis.

In this thesis, several factors, which affect the feasibility of the MIDP process for ground improvement applications have been evaluated at laboratory scale to improve understanding about the process and enhance the process performance. The study aims to find the optimum treatment conditions, minimizing NO_2^- accumulation, increase the precipitation rate, and monitor the gas formation and its effect on the soil behaviour at different environmental conditions.

Results of liquid batch incubation studies in chapter 3 show that denitrification based MICP is a coupled process, in which denitrification and calcium carbonate precipitation processes influence and are beneficial for each other. Calcium carbonate precipitation is a direct consequence of denitrification in a solution containing dissolved calcium ions, through the production of inorganic carbon and alkalinity in the denitrification reaction. In exchange, the precipitation reaction helps to neutralize the alkaline tendency of denitrification. These feedback loops enhance the process stability and resulted in a reduced amount of temporarily accumulated nitrite.

To minimize nitrite accumulation, both the substrate ratio and concentration to be used are important. Using acetate as carbon source, the theoretical range of acetate over nitrate ratio, A/N, was calculated in chapter 2 and is between 0.6 and 1.25, which corresponds to the stoichiometry of zero and maximum growth respectively. The consumption ratio found in the batch liquid experiment in chapter 3 was 0.8, but sand column experiments in chapter 5 demonstrated that the A/N ratio varied between the two extremes. In the experiment using a relatively high substrate concentration, consumed A/N ratio approached the low extreme, nitrite accumulated until the end of the experiments resulting in strong inhibition. When using a relatively low substrate concentration at the same initial supplied ratio, the consumed A/N ratio approached the high extreme, there was no nitrite at the end of the experiments. Microbial activity was maintained throughout this experiment, resulting in the highest reaction rate that corresponded with precipitation rates up to 0.26 weight%-CaCO₃ per day. This value is higher than the observed values in literature and improves the potential of using this process for ground improvement applications. It is expecting that limiting nitrite accumulation not only improves the conversion rate, but also increases the precipitation yield. To obtain an efficient substrate conversion with limited nitrite accumulation and reasonable high precipitation rate, these results suggest that it is important to maintain a high microbial activity and minimize its lag phase.

In order to study the kinetics of denitrification, a theoretical model is proposed in chapter 6, which includes the effect of nitrite accumulation, product yield evaluation and main inhibiting mechanism identification. The model assumes the denitrification process to be a two-step reaction and includes nitrite as an intermediate product. Simulations using this model confirmed that an A/N ratio of 0.6 is not suitable to generate complete denitrification and results in nitrite accumulation. The A/N ratio which can generate complete denitrification was calculated to be between 0.9 and 1.25. The model also confirms preventing the accumulation of nitrite improves the conversion rate and increases the inorganic carbon production over total consumed acetate and nitrate. Hence, both the model and the experiments emphasize that it is important to consider and put the effort in minimizing nitrite accumulation and maintaining a high microbial activity to improve yield and rate of denitrification-based MICP.

The formation and stability of the gas phase in sandy soil was also studied in the laboratory experiments presented in chapters 4 and 5. The produced gas volume is a function of the amount of supplied substrates, the stoichiometry of the reaction and the pressure conditions, while the gas percolation threshold of the soil is function of pore size distribution and confining pressure. These parameters need to be considered to design applications using the gas phase. The experiments showed that one single batch treatment with relatively low substrate concentrations is sufficient to desaturate the sand to the gas percolation threshold. This maximum value for the gas saturation was reached within 1 or 2 days and ranged from 21 to 50% depending on pore size. Part of the gas formed in one reaction period is mobile and was removed by flushing, but the remaining part is stable, resulting in a minimum of gas saturation of about 10 to 15% throughout the experiments. The gas stability appeared to be dependent on the relative proportion of the produced gas volume with the gas percolation threshold of the soil.

The effect of gas formation and calcium carbonate precipitation on the mechanical behaviour has been evaluated in the triaxial set-up as described in chapter 4 and 5. The presence of nitrogen gas in the sand damped pore pressure build up in response to undrained monotonic loading and showed an increase in small strain stiffness. Precipitation of calcium carbonate caused an increase in stiffness and dilatancy in response to drained monotonic loading. During the treatments with multiple flushes in which microbial growth was favoured also a significant decrease in the soil hydraulic conductivity was observed, which eventually clogged the sand column. The resulting response is attributed to the combination of the precipitation, gas formation and biomass accumulation. To a certain extent the process can be directed towards one of the three products by adjusting the treatment regime in order to obtain the desired properties for specific applications.

Overall in this thesis, MIDP has shown its capability to alter hydro-mechanical behaviour of sandy soils at laboratory scale, and can be applied for a wide range of ground improvement applications. Appropriate substrate concentrations and supplying regimes are required to maintain a good microbial activity with negligible accumulation of toxic intermediate nitrogen compounds and obtain a high conversion rate and product yield. The formation, distribution and persistence of the gas phase are also affected by substrate regime, environmental conditions and grain size distribution of the soil. With the proposed models and simplified calculation methods presented in this thesis, these controlling factors can be studied to design the treatment procedure. Process upscaling and optimization for different applications are required for future work.

Samenvatting

Grondverbeteringstechnieken worden regelmatig toegepast bij civiel technische werken. Het betreft vaak methoden waarbij de sterkte en de stijfheid van de grond worden verbeterd om grote vervormingen tijdens en na de constructie te voorkomen. Naast traditionele technieken, zijn er ook biologische processen die leiden tot verbetering van grondeigenschappen. Grondverbetering door Microbiologisch ge-Induceerde Calciumcarbonaat Precipitatie (MICP) door hydrolyse van ureum is op grote schaal aangetoond en wordt momenteel verder ontwikkeld voor verschillende toepassingen. In dit proefschrift is een ander biologisch proces onderzocht: MICP op basis van denitrificatie. In dit proces wordt een oplossing van calcium acetaat en calcium nitraat in de bodem geïnjecteerd. Oxidatie van het organisch materiaal door in de bodem aanwezige denitrificerende bacteriën leidt in aanwezigheid van de calcium ionen tot neerslag van calciumcarbonaat kristallen, die een cementerende binding vormen tussen de zandkorrels en de sterkte en stijfheid van de grond verhogen. Het nitraat (NO_3^-) wordt gereduceerd tot stikstofgas (N_2). De aanwezigheid van samendrukbaar gas in de poriën, beperkt de opbouw van wateroverspanningen bij dynamische belasting van de grond, waarmee de weerstand tegen verweking wordt verhoogd. Het MICP proces op basis van denitrificatie, oftewel Microbiologisch ge-Induceerde Desaturatie en Precipitatie (MIDP) verandert dus op twee manieren de grondeigenschappen, waarmee het potentieel van biologische processen als grondverbeteringstechniek wordt uitgebreid.

Het MIDP proces kent enkele uitdagingen. De reductie van nitraat tot stikstofgas verloopt via drie tussenproducten: nitriet (NO_2^-), distikstofmonoxide (N_2O -lachgas) en stikstofmonoxide (NO). Aangezien alle drie deze tussenproducten schadelijk zijn voor levende organismen en het milieu, moet ophoping worden voorkomen. Ten tweede is het voor de toepassing van stikstofgas als verwekings-mitigerende maatregel van belang de vorming, verspreiding en stabiliteit van de gasfase te kunnen controleren. Tenslotte is bij de toepassing van kalkvorming als cement de reactiesnelheid van het denitrificatie proces een stuk lager dan de het proces op basis van hydrolyse van ureum.

In deze studie zijn de factoren die de haalbaarheid van het MIDP proces als grondverbeteringstechniek beïnvloeden op laboratoriumschaal onderzocht. Doel van het onderzoek is het inzicht in proces te verbeteren en de optimale behandelingsprocedure te ontwikkelen, die wordt gekenmerkt door een beperkte ophoping van nitriet, een maximale omzettingssnelheid en efficiënt gebruik van grondstoffen, waarbij de consumptie van het substraat, de productie van stikstof

en kalk en het effect daarvan op de grondeigenschappen kunnen worden gecontroleerd en gemonitord voor variërende initiële grondeigenschappen en omgevingscondities.

Resultaten van vloeistof incubatiestudies in hoofdstuk 3 laten zien dat MIDP uit twee deelprocessen bestaat die elkaar gunstig beïnvloeden. De productie van alkaliniteit en inorganisch koolstof door de denitrificerende bacteriën leidt in nabijheid van opgeloste calcium ionen tot calciumcarbonaat precipitatie. Tegelijkertijd ontrekt de neerslag van calciumcarbonaat alkalinitiet en inorganisch koolstof uit de oplossing waardoor de zuurgraad wordt gebufferd. Koppeling van de twee processen resulteert in gunstige condities voor de groei van denitrificerende bacteriën en beperkt de accumulatie van toxische tussenproducten.

Om de ophoping van nitriet te beperken is het belangrijk de juiste verhouding en concentraties van substraten toe te passen. In hoofdstuk 2 is de substraat verhouding berekend met acetaat als koolstofbron. De theoretische acetaat-nitraat (A/N) ratio ligt tussen 0,6 en 1,25 die respectievelijk overeenkomt met condities van nul en maximale groei van de bacteriën. Tijdens de vloeistof incubatiestudies in hoofdstuk 3 bleek de optimale A/N ratio 0,8 te zijn, maar tijdens de experimenten in de zandkolom beschreven in hoofdstuk 5 variëerde de consumptie ratio tussen beide extreme waarden. In het experiment met een relatief hoge substraatconcentratie, werd de reactie sterk vertraagd door de ophoping van nitriet en benaderde de A/N ratio de lage extreme waarde, die gekenmerkt wordt door beperkte microbiële groei. Bij relatief lage substraatconcentraties benaderde de substraat ratio de maximale waarde. Nitriet concentraties bleven laag en de microbiële activiteit in deze proef bleef gehandhaafd, wat resulteerde in de hoogste reactie snelheid oplopend tot circa 2,6 g Calciumcarbonaat per kg grond per dag. Deze waarde hoger is dan de tot nu toe gerapporteerde waarden in de literatuur en verbetert het potentieel van MIDP als grondverbeteringstechniek. Het beperken van nitriet accumulatie verbetert niet alleen de reactiesnelheid, maar verhoogt ook de kalk opbrengst. De resultaten bevestigen dat een hoge microbiële activiteit noodzakelijk is om een efficiënte omzetting van substraat met beperkte nitriet accumulatie en redelijke hoge neerslagsnelheid te krijgen.

In hoofdstuk 6 is een theoretisch model beschreven dat is ontwikkeld om de kinetiek van denitrificatie inclusief het effect van nitriet accumulatie te bestuderen en inzicht te krijgen in de stoichiometrie van de reactie voor verschillende microbiële groeisnelheden en inhibitie condities. In dit model is aangenomen dat het denitrificatie proces in twee reductie stappen verloopt met nitriet als enige tussenproduct. Simulaties met dit model bevestigen dat een A/N ratio van 0,6 leidt tot onvolledige omzetting van nitraat en ophoping van nitriet. Een A/N ratio tussen 0,9 en 1,25 leidt tot volledige denitrificatie. Het model bevestigt ook dat het voorkomen van de nitriet accumulatie leidt tot hogere omzettingssnelheid en

hogere calciumcarbonaat productie. Kortom, zowel het model als de experimenten bevestigen dat het essentieel is ophoping van nitriet te voorkomen en actieve microbiële groei te stimuleren om een hoge reactiesnelheid en efficiënte omzetting te krijgen.

De vorming en stabiliteit van de gasfase is ook bestudeerd in de laboratoriumexperimenten, die zijn beschreven in hoofdstuk 4 en 5. Het volume van de gasfase is een functie van de hoeveelheid toegediend substraat, de stoichiometrie van de reactie en de waterdruk, terwijl de gas percolatie limiet is een functie van de korrelgrootte verdeling en de effectieve steundruk. Deze parameters moeten worden beschouwd bij het ontwerp van een behandelingsprocedure, waarbij de gasfase wordt gebruikt om de geotechnische eigenschappen van de grond te verbeteren. De experimentele resultaten tonen aan dat een enkele behandeling met relatief lage substraatconcentraties voldoende is om de verzadigingsgraad van het zand te verlagen tot de gas percolatie limiet. Deze maximale waarde voor de gas verzadiging werd bereikt binnen 1 tot 2 dagen en varieerde van 21 tot 50% afhankelijk van de poriegrootte. Een deel van het gas dat in één reactieperiode werd gevormd was mobiel en werd bij het spoelen direct verwijderd. Het resterende deel van ongeveer 10 tot 15% was stabiel en bleef na spoelen achter in de poriën. De stabiliteit van de gasfase bleek afhankelijk van de relatieve hoeveelheid geproduceerd gas ten opzichte van de percolatie limiet.

Het effect van gasvorming en precipitatie op de hydro-mechanische eigenschappen is ook bestudeerd in de experimenten beschreven in hoofdstuk 4 en 5. De aanwezigheid van samendrukbaar stikstof gas dempt de toename van wateroverspanning bij ongedraineerd belaste en verhoogt de stijfheid bij kleine rek. Neerslag van calciumcarbonaat verhoogt de stijfheid en dilatantie bij gedraineerd belaste. Tijdens de behandeling met meerdere spoelingen waarbij microbiële groei werd gestimuleerd nam ook de waterdoorlatendheid af, wat uiteindelijk tot verstopping leidde. De hydro-mechanische repons wordt dus toegeschreven aan de combinatie van de precipitatie, gasvorming en groei van biomassa. Tot op zekere hoogte kan het MIDP proces richting een van de drie producten worden gestuurd, door aanpassing van de behandelingsprocedure om de gewenste eigenschappen voor specifieke toepassingen te verkrijgen.

In conclusie, met dit proefschrift is op laboratoriumschaal bevestigd dat de hydro-mechanische eigenschappen van zand met het MIDP proces kunnen worden beïnvloed en dat het proces mogelijk kan worden gebruikt als grond verbeteringstechniek voor uiteenlopende toepassingen. Substraatconcentraties en injectie strategie dienen op passende wijze te worden gekozen om microbiële activiteit te stimuleren, ophoping van toxische tussenproducten te voorkomen en een hoge omzettingssnelheid en productopbrengst te verkrijgen. De vorming, verspreiding en persistentie van de gasfase wordt beïnvloed door het substraat regime, omgevingscondities en korrelgrootteverdeling van de bodem. Met de modellen en vereenvoudigde berekeningsmethoden gepresenteerd in dit

proefschrift kunnen deze controlerende factoren worden bestudeerd om behandelingsprocedures te ontwerpen. Opschaling en optimalisatie van het proces voor specifieke toepassingen vereist aanvullend onderzoek.

Acknowledgement

Looking back my Phd progress I realized that with all the people that I had met, will all the circumstances that I experienced, they have come to help and shape me in this current state. I'm very grateful for all I have been through, and this acknowledgment is a note to express my gratitude to them.

One of the major things that I enjoyed the most during my PhD besides that I was free with my schedule, is our lively discussion every times I had with you, Leon. I learned from you the open-mindedness, and admire your supportiveness to people when they are in difficult situations, including me. In my understanding, you won't let a bad output influence your judgment about people and their effort. This is particularly special to me because I'm often result oriented. So actually at some point it helped me to feel comfortable about my progress. Thank you very much for giving me the chance to pursue this PhD, for your supervision on daily basis, and for how you are.

This thesis and my PhD is completed also thanks to my promotor Timo. With the limited time we have had together, our meeting were always efficient and helped to improve the work I was doing. Your schedule is always full, but even then you offered to correct my writing paragraphs by paragraphs when I was preparing the Go no go report in my first year. I really appreciate your time and support that you had for me.

Accomplishment of this thesis is also attributed to other people from both the faculty and Deltares. Thank you very much Wouter because you always made me feel welcome by your enthusiasm, and you always had some nice suggestions for me each time we met. I really enjoyed my time at Deltares since the time I did my master thesis with your supervision 5 years ago until now. And the technical support of Arno, Jolanda, Lambert and Gert, besides helping me to achieve all the importance results in this thesis, helped me to gain confidence in the lab, and I learned much practical stuff from them. And as I barely have experience in modelling, Andre was the one that helped me with it and I had very nice fitting figures. And it was also great to have him as a PhD peer.

And this thesis is not completely mine, it also had the work of Akiko in it as my PhD inherited her work in Delft. And also thank to you Akiko, I know more about the beautiful Japan. I'm very glad that I had chance to know you and we keep in touch. It would be great if we could be officemates again like the old time in

Deltares, but we will see. I really hope and will try so that we can have opportunities to work together in the future.

My PhD journey cannot be completed without friendships and PhDships. The feeling when finishing a day late and exhausted and there sis Phuong brought me a piece of cake, and the fun when we tried cooking, sewing, knitting together. And now we have babies to be added into the categories. And with Hoang Anh, our time being roommates was not long but really memorable. I gained much boardgame experience thank to you and Thien. Your PhD journey is quite the opposite of mine in some ways, and it is interesting to exchange the perspective. And also to Luke, Miranda, Roderick, Nor, Richard, Arash, brother Thang, brother Duong and sis Quynh Anh, Ninh, Nga, Linh, Son, Tham, my piano teacher Marlijn, and all of my PhD friends and other Vietnamese friends, I am very glad that I met you and grateful for our precious time.

And the last persons but the most important ones that this thesis is dedicated to, are my husband and my family. Their support and love are the source of my energy to accomplish this thesis and move on in life. I am lucky to have them by my side, and with our new family member coming, I think I am ready for the new journey ahead.

1. Potential of denitrification for MICP and soil desaturation as a ground improvement method

Ground improvement is commonly applied in construction and civil engineering, which aims to ensure the stability of a foundation to support the structures above such as buildings, dams or highways. There are various techniques of ground improvement, corresponding with different soil types, structural load and depth that can be listed: compaction, preloading and drainage, stabilization by mixing with lime or cement, jet grouting, deep mixing or compaction piles (Das, 2007). Besides these conventional methods, there is another approach which aims to learn from the natural transition of soil into rock and tries to apply (and accelerate) this natural ground improvement process. In nature, this transition can be stimulated by many different organisms which can produce carbonate and alkalinity and therefore create favourable conditions to induce calcium carbonate (CaCO_3) precipitation, which can cement the soil and increase its strength. Following this approach, various researchers and studies have reached significant progress proving the applicability of such methods for ground improvement purposes. Even so, there are still many challenges to be solved before natural and bio-based ground improvement techniques can be applied in practice. One of the biological processes that can be used to induce CaCO_3 precipitation is denitrification and this is the subject of this thesis.

This first chapter will present an overview of the process in the context of using this approach for ground improvement purposes and the motivation to choose denitrification as the source for CaCO_3 precipitation.

1.1. Inducing calcium carbonate precipitation in sandy soil through biological pathways

Attention to microbial induced carbonate precipitation (MICP) has increased in recent years thanks to its potential of bonding soil particles. The bonding effect has been considered for a wide range of geotechnical and environmental applications (DeJong et al., 2013, Phillips et al., 2013a). There are several biological processes that can trigger MICP as generalized by Zhu and Ditttrich (2016), namely photosynthesis, ureolysis, denitrification, ammonification, sulfate reduction and methane oxidation. In principle all these metabolic pathways, which are conducted by different microbial groups, result in an increase of dissolved inorganic carbon (DIC) and increase the alkalinity in the environment. In the presence of dissolved calcium and available nucleation sites, calcium carbonate (CaCO_3) precipitation will take place. For the interest of ground improvement techniques, most studies on MICP were based on the hydrolysis of urea, more recently followed by the denitrification.

It has been demonstrated at laboratory scale (Montoya et al., 2013, Chu et al., 2012, Harkers et al., 2010, Whiffin et al., 2007, DeJong et al., 2006) and field scale (DeJong et al., 2009, Van Paassen et al., 2010, Paassen, 2011, Burbank et al., 2011) that MICP by urea hydrolysis can significantly strengthen granular soils, which leads to a wide range of potential applications (Phillips et al., 2013b). However commercial applications of MICP by urea hydrolysis are still limited, partly due to the costs for cultivation of ureolytic bacteria and the required removal of ammonium chloride, which is formed as a by-product of the process. MICP by denitrification has been considered as a potential alternative bio-mediated ground improvement process, as it has several advantages over urea hydrolysis (Karatas, 2008, Paassen et al., 2010, Kavazanjian et al., 2015). When nitrate is completely reduced to nitrogen gas, no adverse by-products are formed for which removal effort is required. The required substrates for denitrification are sufficiently soluble to limit the number of injections that are required to reach a target amount of calcium carbonate. Substrates for denitrification can even be produced from waste streams and the conversion does not require cultivation of very specific organisms. In fact indigenous populations of denitrifying bacteria can be used or stimulated in situ (Van der Star et al., 2009, Paassen, 2009b, Martin et al., 2013).

The full system of reactions for denitrification-based MICP can be divided in three part: (i) biological denitrification, (ii) acid-base equilibrium reactions and (iii) phase separation. This system is described in Figure 1-1. Biological denitrification is the irreversible reaction, in which microorganisms consume nitrate (NO_3^-) or nitrite (NO_2^-) and a carbon source, which is acetate ($\text{C}_2\text{H}_3\text{O}_2^-$) in this study. When the denitrification reaction is complete dinitrogen (N_2) and dissolved inorganic carbon (DIC) are produced. Through acid-base equilibria, ions can be present in an aqueous solution as different soluble species depending on the chemical composition and the pH of the solution. Inorganic carbon dissociates

1. Potential of denitrification for MICP and soil desaturation as a ground improvement method

into carbon dioxide (CO_2), bicarbonate (HCO_3^-) and carbonate (CO_3^{2-}) and forms complex species with cations in solution. Bicarbonate is the main product at neutral pH. At a suitable pH and with dissolved calcium ions (Ca^{2+}) in excess, calcium carbonate will precipitate and transfer to the solid phase. In a soil this would decrease porosity and permeability, increase bulk and dry density and support particle bonding, which may increase strength and stiffness. On the other side phase separation can also occur, when produced nitrogen or carbon dioxide transfer to the gas phase. Introducing a gas phase into the system can form a water barrier, reducing hydraulic conductivity or reduce water saturation, reducing bulk liquid stiffness, which can improve the undrained strength of a soil (Rebata-Landa and Santamarina, 2011).

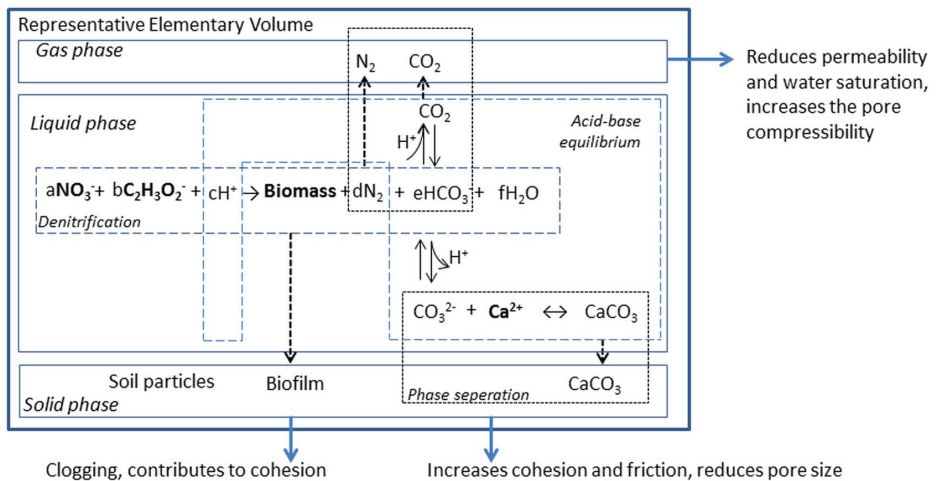


Figure 1-1. Calcium carbonate precipitation induced by denitrification and its potential impact on a unit volume of soil.

The reaction products of denitrification-based MICP expand the potential improvement options of bio-based ground improvement. Besides the possibility to strengthen the soil through mineral precipitation, soil resistance to dynamic loading is also enhanced by the induced gas phase. Based on this characteristic, the method is considered to be applicable to desaturate the soil for liquefaction mitigation and research in this direction has been developing (Kavazanjian et al., 2015, He and Chu, 2014). Employing denitrification for MICP therefore can also be called microbially induced desaturation and precipitation – MIDP. In conditions that microbial growth is favourable leading to biofilm and biomass accumulation, soil hydraulic conductivity can be significantly reduced, showing the potential of leakage and piping mitigation.

1.2. Process characteristics and challenges of MIDP by denitrification

Denitrification in its natural environment and its applications in waste water treatment has been well studied in literature (Ferguson, 1994, Knowles, 1982). The denitrification process alone increases the alkalinity in its surroundings. In a natural system denitrification is often coupled with an acidifying process such as nitrification and consequently the overall ecosystem stays in balance. Denitrification is part of the nitrogen cycle, which is presented in in Figure 1-2.

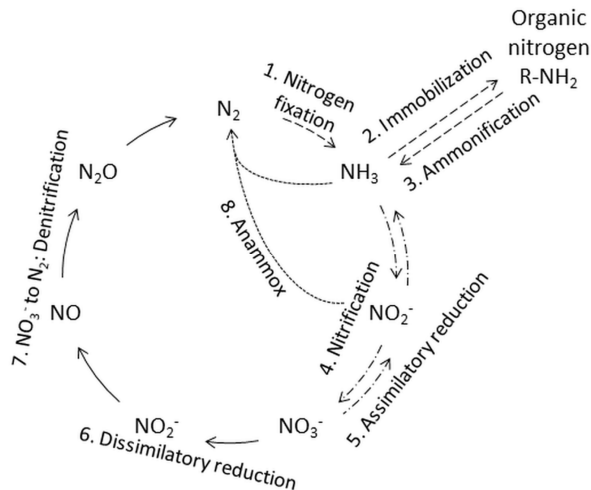


Figure 1-2. Denitrification in the nitrogen cycle, figure reproduced from (Payne, 1981) and (op den Camp et al., 2006)

When denitrification is in balance with other processes in its environment, the pH is buffered. Consequently, denitrifying bacteria function properly and their activity is maintained, in which nitrate is reduced to N_2 with negligible amount of its intermediates. In contrast, when pH is not buffered and shifted away from neutral, nitrate reduction to N_2 is often not complete and resulting in the accumulation of intermediate compounds. The intermediates of denitrification, which are nitrite NO_2^- , nitric oxide NO and nitrous oxide N_2O , are harmful to living organisms and the environment and are all unwanted (Madigan et al., 2012, Zumft, 1997). Therefore, one of the challenges in studying denitrification-based MICP, or MIDP, is to ensure a complete denitrification without accumulation of its toxic intermediates. In MIDP, precipitation of calcium carbonate is the process that helps to neutralize the alkaline tendency of denitrification. However, to what extent these processes are coupled and how this effect can be useful is not clearly stated in the literature.

Not only the activity of denitrifying micro-organisms, but also the formation and transportation of the reaction products are influenced by the environmental conditions. The soil matrix is an important factor that controls the gas formation

and transportation, affects the substrate availability for denitrifying bacteria, and influences distribution of the reaction products. So another challenge for this study is to monitor the process in the soil and quantify the effect of environmental conditions. Addressing these challenges is important to upscale the process from laboratory to pilot and large scale testing and develop the process towards practical applications.

In terms of application, employing the gas production for ground improvement purposes raises the question about stability and persistence of the gas phase. It is often considered that gas bubbles are mobile and can easily vent out of the soil, or even can lead to collapse of the foundation if the gas pressure is allowed to build up and a sudden release of trapped gas can actually result in a blow out or trigger liquefaction, causing damage to overlying structures (Davis, 1992, Reed, 2002). Therefore, being able to control the gas formation and distribution, and endure its stability is an important step to bring this process into applications.

For calcium carbonate precipitation, the reported rate for denitrification based MICP is limited within several weight-% in a treatment duration of several months, which is significantly lower than the rate obtained in MICP based on urea hydrolysis. This low precipitation rate might not be suitable to generate significant soil strength improvement, so increasing the precipitation rate is desirable on one hand. On the other hand, optimizing the process for applications which do not require significant strength improvement but require stabilization at small strain, such as increasing stiffness or dilatancy under dams or road stabilization may still prove potential applications.

1.3. Thesis objective

This investigation aims to improve understanding about the coupled processes of denitrification and CaCO_3 precipitation and its controlling factors, which are the tools to enhance the process performance and improve the applicability of MIDP. To obtain this goal, the performed research includes:

- A literature study and theoretical analysis of the process mechanism, its reaction stoichiometry and kinetics, which is required to define the appropriate substrate recipes to interpret the results and evaluate the process performance;
- Experimental investigation at laboratory scale to validate the proposed theoretical approach and study the influences of the controlling factors on the process performance and the resulting soil behaviour.

The following factors have been evaluated: (i) substrate concentrations and ratios, (ii) substrate supplying strategies, in consideration of the environmental conditions which are: (iii) pressure conditions and (iv) grain sizes. The experiments aim to find the optimum treatment conditions, minimizing NO_2^-

accumulation and maximizing product yield and strengthening effect, monitor the gas formation and its effect on the soil behaviour at different environmental conditions, and improve the precipitation rate. Also a theoretical model has been developed, which can be used to simulate the coupled processes of denitrification and precipitation in a liquid batch environment, in which the correlation of denitrification reactivity and precipitation yield was addressed.

1.4. Thesis structure

After this introduction chapter, the content of this thesis is divided into 5 chapters, following by the last chapter summarizing the main results and conclusions.

In the second chapter an overview of denitrification ecology is provided which is based on a literature study, and a simplified description of the denitrification process is presented assuming complete denitrification whereby NO_3^- is directly reduced to N_2 . The stoichiometry of the metabolic reactions is calculated using a thermodynamic approach. The results were used to select the substrate ratios for the batch liquid incubation experiments presented in chapter 3, in which impact of substrate composition on the process performance in liquid environment was studied.

The formation of gas in a sandy soil can be affected by the environmental conditions. In this study the effect of average grain size and pressure conditions on the formation of gas were evaluated using a modified triaxial test set-up. Sand columns were inoculated with denitrifying bacteria and supplied with substrate solutions. The consumption of substrates and production of gas is monitored and the impact of partial saturation by biogenic gas formation on the soil behaviour is evaluated based on changes in water saturation and hydraulic conductivity. Results of these experiments are presented and discussed in chapter 4 and 5.

The precipitation of calcium carbonate in sandy soils was studied by treating the sand with multiple flushes while varying substrate concentrations and flushing frequencies in order to determine the preferred treatment strategy. The results of these experiments are presented in chapter 5. These experiments were also used to evaluate persistence of the gas phase during flushing and the coupled effect of the reaction products on the process performance and mechanical properties of the treated sand are discussed.

In chapter 6 a model is proposed, which can be used to simulate the coupled processes of denitrification, precipitation and gas formation in a liquid environment. Going further than the simplified model presented in chapter 2, in this model, denitrification is considered to consist of two separated metabolic reactions with nitrite (NO_2^-) as the only intermediate. The stoichiometry of these two reactions is considered to be either fixed or dependent on the specific growth rate of the biomass. The two approaches are compared to evaluate the necessity of considering this rate-dependency of the stoichiometry in the model. Secondly the

1. Potential of denitrification for MICP and soil desaturation as a ground improvement method

model can be used to calculate amount of the reaction products and shows the relation between inhibition through nitrite accumulation, stoichiometry and product yields.

Finally in chapter 7 the main conclusions are summarized and recommendations for further research and developments are provided.

1. Potential of denitrification for MICP and soil desaturation as a ground improvement method

2.

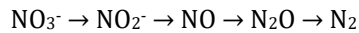
Denitrification ecology and stoichiometry

Denitrification and other processes in the nitrogen cycle can be said to be conventional subjects of biotechnology. In order to be able to employ denitrification for MICP, this chapter studies the basic understanding of denitrification, its intermediates and kinetic growth from literature. Its theoretical stoichiometry is calculated using the microbial energy approach, reflecting the correlation of the stoichiometry with the metabolic state of the denitrifying inoculum.

2.1. Nitrate reduction and denitrification ecology

2.1.1. Denitrification among different pathways of nitrate reduction

Denitrification has been intensively studied since the late 19th century both in natural systems and for industrial applications (Voorhees, 1902, Payne, 1981, Knowles, 1982, Kuenen and Robertson, 1988, Wang et al., 1995, Soares, 2000, Archana and Sobti, 2012) It is the pathway that brings fixed nitrogen, which is the nitrogen bound with other elements in a form that plants and animals are able to use, back to the atmosphere in the form of N₂ to close the global N cycle (Payne, 1981, Robertson and Groffman, 2015). The transformation is carried through 4 reduction steps of nitrogen with the three intermediates:



These reductions are carried mostly by microbes in the soil-water ecology with correspondent enzymes (Robertson and Groffman, 2015). Potential energy of the NO₃⁻/N₂ couple among some others in the redox tower is close to the maximum value generated by aerobic respiration using oxygen (Chp. 4, Madigan et al., 2012). So when nitrate is available instead of oxygen, soil microbes will use nitrate as a terminal electron acceptor in their metabolism to generate energy for growth and maintenance. Most of the denitrifiers are heterotrophic bacteria, which use organic carbon in their oxidative metabolism with nitrate. Large quantities of denitrifying bacteria are found in various soil and ground water conditions, especially in the rhizosphere (Knowles, 1982, Kuenen and Robertson, 1988). The bacteria can likely selectively modify themselves to adapt in different environments, so closely related bacteria can have different denitrification capacity related to different combination of the reductases enzymes (Shapleigh, 2009).

Beside the pathway of reducing to N₂, nitrate can be reduced further to inorganic ammonia NH₃ or organic amino acids which is the source of biosynthetic nitrogen. These reductions are categorized as assimilatory reduction which results in ammonia for cell synthesis, and dissimilatory reduction which results in inorganic products (Kuenen and Robertson, 1988, Zumft, 1997). Denitrification, which is dissimilatory nitrate reduction to N₂, is carried out by bacteria with an oxidative metabolism, while bacteria metabolism of dissimilatory nitrate reduction to ammonia is fermentative (Tiedje, 1988) and was found more often in carbon-rich marine sediment (Cole, 1990). Comparison of nitrate reduction through different pathways was illustrated by (Payne, 1981) and presented in Figure 2-1.

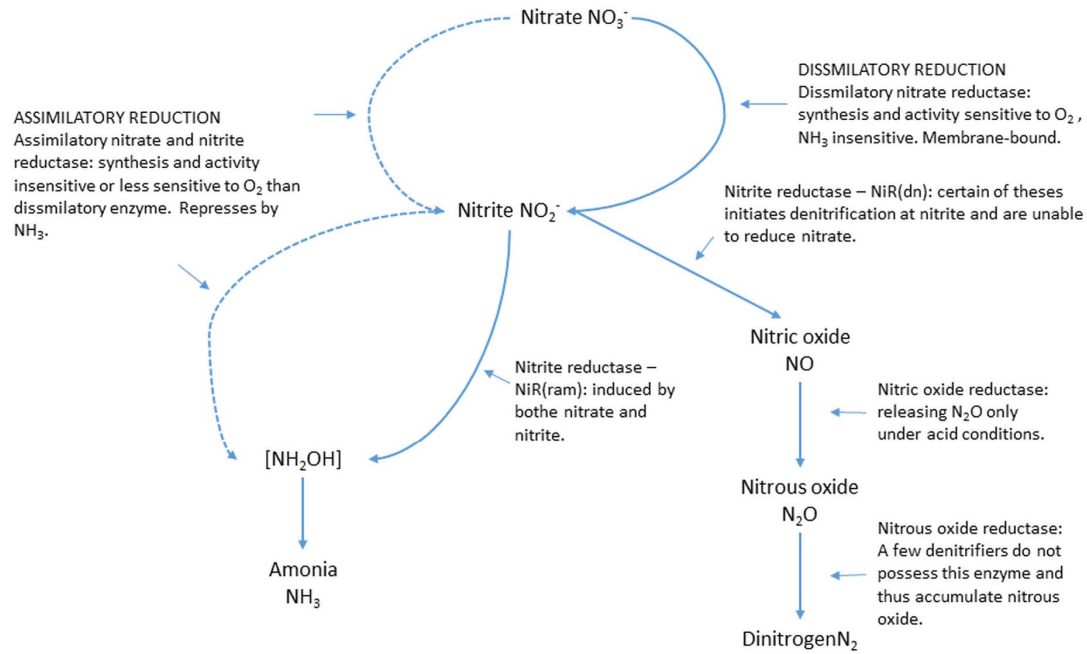


Figure 2-1. Comparison of nitrate reduction through different pathways, reproduced from (Payne, 1981)

Denitrification is highly interactive with other biogeochemical processes in its surrounding environment. In the nitrogen cycle, its reactivity is strongly coupled with nitrification (Kuenen and Robertson, 1988), especially in the aspect of neutralizing pH of the environment and maintain the overall ecology balance (Šimek and Cooper, 2002). Denitrification itself produces alkalinity and causes an increase in pH value, magnitude of this increase depends on the buffering capacity of the environment. When standing alone or when the balance with its environment is shifted, the rise in pH can lead to self-inhibition and accumulation of its toxic intermediates (Glass and Silverstein, 1998).

Denitrification is an oxidative metabolism using nitrate as the oxidizer instead of oxygen in the same metabolic mechanism, therefore fully aerobic conditions are not preferable for denitrification due to the electron competition. At partially saturated oxygen conditions, denitrifying bacteria were found to be able to adapt to oxygen fluctuation and limitation (Robertson et al., 1995), but expression of the reductase enzymes are sensitive to oxygen concentration, especially for the nitrite reductase (Körner and Zumft, 1989, Ferguson, 1994). So for a complete denitrification to nitrogen gas with negligible accumulation of the intermediates, maintaining an anaerobic condition is important.

2.1.2. *The intermediates of denitrification*

In denitrification, nitrate needs to be reduced through four reduction steps with 3 intermediates to reach the final product nitrogen gas. All the intermediates, nitrite (NO_2^-), nitric oxide (NO) and nitrous oxide (N_2O) are harmful to living organisms and their environment. Nitrite is toxic inhibiting microbial growth, and for that characteristic nitrite has been well known and being used as food preserver in strictly low concentration. For NO, a concentration at micro-molar range causes damage to cellular metabolism, and at 1mM and above it results in loss of cell division and viability (Zumft, 1997). For the environment, the major impact comes from N_2O because this is a strong greenhouse gas. Besides, the reaction of N_2O to NO and then NO_2^- in the upper atmosphere results in acid rain and should be avoided (Chp. 4, Madigan et al., 2012).

Although denitrification has the risk of toxic accumulating toxic intermediates, its sequential reduction whereby one intermediate generated from a reductase enzyme being the source for the following reduction step makes NO_2^- and NO accumulations interdependent. Nitrite reduction can only proceed when NO concentration is maintained below its toxicity level, and when NO expresses the inhibition, denitrification temporarily stops at NO_2^- so that NO will not accumulate while continuously being converted further to N_2O and N_2 . In other words, the denitrification system has its own mechanism to minimize the accumulation of its toxic intermediates (Ferguson, 1994, van Spanning et al., 2007), and the extracellular NO concentration in steady state denitrification stays in the low nanomolar range (Zumft, 1997).

Besides the presence of oxygen that affects expression of the reductase enzymes as mentioned in section 2.1.1, substrates concentrations, the ratio between nitrate and carbon sources, and pH are the main environmental factors that influence accumulation of the intermediates. Optimized pH for denitrification was reported to be in range of 7.0 – 8.0. Lowering pH will increase the N_2O fraction, which is the main product of denitrification at pH 4.0 (Knowles, 1982). On the other side, alkaline conditions facilitate temporary NO_2^- accumulation when nitrate is the limited substrate, whereas at neutral condition denitrification could still be inhibited by a high nitrate concentration of 200 mM (Glass and Silverstein, 1998). If carbon is the limited, the excess and partial reduction of nitrate can result in permanent nitrite accumulation in a batch incubation (Almeida et al., 1995, Pham et al., 2016a). In steady-state denitrification in an environment which is not strongly acidic, NO_2^- is the main intermediate of denitrification and other intermediates but NO_2^- can be neglected.

When employing denitrification for MICP, accumulation of toxic intermediates can occur depending on the selected substrate regimes, such as supplying high substrate concentrations because they are preferred to minimize the number of flushes. Nevertheless, experimental results by Paassen et al. (2010) and Erşan et al. (2015) show that the intermediate accumulation can be limited and become negligible at a certain experimental conditions. Finding the right conditions to limit NO_2^- accumulation is one of the challenges which will be dealt with later in the thesis.

2.2. Kinetic growth and inhibition factor of denitrification

Denitrification is a rate-dependent process, in which biomass concentration X is the driving parameter of the system and used to define the specific substrate uptake, growth and production rates of microbial growth kinetic:

$$\text{Specific substrate uptake } C_s \text{ rate: } q_s = \frac{1}{C_x} \frac{dC_s}{dt}$$

$$\text{Specific growth rate of biomass } X: \mu = \frac{1}{C_x} \frac{dX}{dt}$$

$$\text{Specific production } C_p \text{ rate: } q_p = \frac{1}{C_x} \frac{dC_p}{dt}$$

When a substrate is not limited, the biomass is able to consume the substrate at a rate which is close to the maximum specific substrate uptake rate, q_s^{max} , and the substrate consumption is tightly coupled to microbial growth. When the substrate is limited, the specific uptake rate is also reduced and described by the substrate limitation kinetics (Monod, 1949):

$$q_s = q_s^{max} \cdot \frac{C_s}{C_s + K_s}$$

where K_s is the saturation constant for substrate uptake at which the rate is half of the maximum. For nitrate uptake, K_s was reported to be around 1-10 mg N- NO_3 , so

at the common nitrate load of several mM, the overall process is zero-order growth, $q_s \sim q_s^{max}$ (Halling-Sorensen and Jorgensen, 1993). The specific growth rate is dependent on the limiting substrate and expressed as:

$$\text{Eq. 1.} \quad \mu = \mu^{max} \cdot \frac{C_s}{C_s + K_s}$$

where μ^{max} is the maximum specific growth rate and is an bioenergetic parameter of the microbial metabolism. For NO_3^- and NO_2^- , their toxicity to microbial growth can be described by substrate inhibition expression of Andrews (1968):

$$\text{Eq. 2.} \quad \mu = \mu^{max} \cdot \frac{C_s}{C_s + K_s + \frac{C_s^2}{K_I}}$$

where K_I is its inhibition constant. NO_3^- is reported to show inhibition at concentration of 0.2M (Glass and Silverstein, 1998), so this value is considered to be the theoretical value of $K_{I-\text{NO}_3}$. Theoretical value of $K_{I-\text{NO}_2}$ is 0.0007, which is taken following Wang et al. (1995).

Stoichiometric coefficient of substrate S over biomass X , Y_{SX} , represent the ratio between the consumed substrate over the newly produced biomass:

$$Y_{SX} = \frac{dC_s}{dX} = \frac{q_s}{\mu}$$

So the specific substrate uptake rate can also be expresses as:

$$q_s = \mu^{max} \cdot Y_{SX} \cdot \frac{C_s}{C_s + K_s}$$

It can also be reformulated as:

$$\text{Eq. 3.} \quad q_s = \mu^{max} \cdot Y_{SX} \cdot I$$

where I is the total inhibition factor ranging between 0 and 1. It can counts for the substrate limitation taken from Eq. 1 or substrate inhibition taken from Eq. 2. Other inhibition factor such as pH, temperature, cross inhibition of NO_3^- to NO_2^- reduction and NO_2^- to NO_3^- reduction can also be added into this total inhibition factor (Soto et al., 2007, Wang et al., 1995).

2.3. Stoichiometry of complete denitrification

2.3.1. Metabolism and Gibbs energy

Stoichiometry of complete denitrification can be identified by a methodology suggested by Heijnen and his colleagues (Heijnen and Kleerebezem, 2010, Heijnen et al., 1992). The method divides a metabolic reaction into an anabolic reaction, which describes the production of biomass, and a catabolic reaction which generates the energy for the cells to produce new biomass in the anabolic reaction (Haynie, 2008). The stoichiometry of the anabolic and catabolic redox reactions are determined separately by solving the mass and electron balance for each reaction. The ratio between the catabolic and anabolic reactions is determined by

solving the energy balance, i.e. the produced energy from the catabolic reaction is equal to the energy required for biomass production and cell maintenance. The actual ratio depends on the growth rate of the micro-organisms which can range from maximum growth conditions, where micro-organisms grow exponentially, to zero growth conditions, where the total amount of micro-organisms does not increase, but maintaining the population still requires energy. The actual growth rate is controlled by the process and environmental conditions such as the availability of substrates and nutrients and the presence of inhibiting compounds (the condition of negative growth rate or cell decay, e.g. in case there are no substrates available is not considered here).

The overall metabolism is established through 1 C-mol new biomass generated in the anabolic reaction and the number of times the catabolic reaction is needed, f_{cat} , for the correspondent required energy:

$$\text{Metabolism} = \text{Anabolism} + f_{cat} \cdot \text{Catabolism}$$

Eq. 4.
$$Y_G^{gr} = Y_G^{an} + f_{cat} \cdot Y_G^{cat}$$

where Y_G^{gr} is the Gibbs energy of the metabolism, Y_G^{an} is the Gibbs energy of anabolism and Y_G^{cat} is the Gibbs energy of catabolism. For each reaction, its Gibbs energy is calculated as:

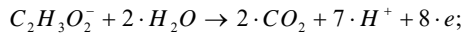
Eq. 5.
$$Y_G = \sum Y_i \times G_i^{(1)}$$

where Y_i is stoichiometric coefficient and $G_i^{(1)}$ is corrected Gibbs energy of the substance i in the reaction. Y_i of the consumed substances are negative, and that of produced substances are positive. Considering that the reactions are at standard conditions of pH and temperature except supplied substrate concentrations, correction for the Gibbs energy of nonstandard concentration C_s is:

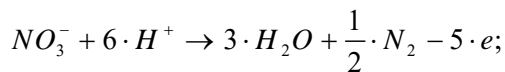
Eq. 6.
$$G_s^{(1)} = G_s^{(0)} + R \cdot T \cdot \ln(C_s)$$

2.3.2. Stoichiometry of catabolism

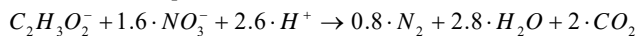
In the generalized model of metabolism, the catabolic reaction is a redox reaction generating the required energy for the cells to maintain themselves and convert nutrients into new biomass. It is based on the half reactions of the electron donor, acetate, and the electron acceptor, nitrate. Oxidation of acetate is:



Reduction of nitrate to dinitrogen is:



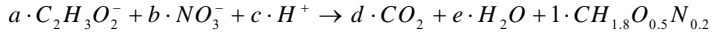
So the catabolism components is:



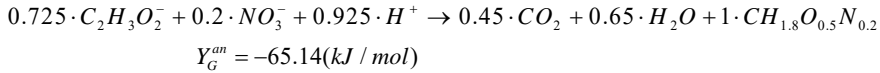
Gibbs energy of this catabolic reaction calculating using Eq. 5 and Eq. 6, Y_G^{cat} is 782.9 (kJ/mol).

2.3.3. Stoichiometry of anabolism

The anabolic reaction describes the production of 1 C-mol biomass from the supplied C-source and N-source:



The stoichiometric coefficients are solved by the mass balance of all the elements and the charge balance of all the ions. Results of the anabolism component is:



2.3.4. Gibbs energy change of the overall specific growth reaction

The Gibbs energy of the overall specific growth reaction is described as function of the actual specific growth rate μ and the Gibbs energy requirement for maintenance:

$$\text{Eq. 7.} \quad Y_G^{gr} = Y_G^{max} + \frac{m_G}{\mu}$$

where Y_G^{max} is the needed Gibbs energy to make 1 C-mol biomass (kJ/C-molX), and m_G is the Gibbs energy needed for biomass maintenance (kJ/C-molX/h). The Gibbs energy to make 1 C-mol biomass was suggested to be a function of the carbon chain length (NoC_{Cs}) and the degree of reduction of the carbon chain source (γ_{Cs}) for heterotrophic growth:

Eq. 8.

$$-Y_G^{max} = 200 + 18 \cdot (6 - NoC_{Cs})^{1.8} + \exp \left\{ \left[(3.8 - \gamma_{Cs})^2 \right]^{0.16} \cdot (3.6 + 0.4 \cdot NoC_{Cs}) \right\}$$

The Gibbs energy requirement for maintenance purpose m_G was suggested to primarily depend on the temperature according to the following function:

$$\text{Eq. 9.} \quad m_G = -4.5 \cdot \exp \left\{ \frac{-69 \cdot 10^3}{R} \left(\frac{1}{T} - \frac{1}{298} \right) \right\}$$

For acetate, $NoCCs$, which is the number of carbon, is 2, and γ_{Cs} , which is the reduction degree of all element of acetate, is 4. Accordingly, the correspondent Y_G^{max} and m_G are -432.1 (kJ/C-molX) and -4.5 (kJ/C-molX/h), respectively. Therefore, Eq. 7 can be written as:

$$\text{Eq. 10.} \quad Y_G^{gr} = -432.1 - \frac{4.5}{\mu} (kJ / C - molX)$$

2.3.5. Maximum specific growth rate

The microbial metabolism, which is controlled by the rate of Gibbs energy made available per unit biomass q_G , is hypothesized to be limited by a maximum rate of electron transport in the catabolic energy production q_e^{max} :

$$q_e^{max} = -3 \cdot \exp \left\{ \frac{-69 \cdot 10^3}{R} \left(\frac{1}{T} - \frac{1}{298} \right) \right\}$$

Eq. 11.
$$q_G^{max} = q_e^{max} \cdot \frac{-Y_G^{cat}}{\gamma_D}$$

where γ_D is the number of electrons transferred in the catabolism, which is 8 (e-mol/C-molX/h) in this case using acetate, and q_e^{max} is equal to 3 (e-mol/C-molX/h) at 298 K. As the generated Gibbs energy from catabolism is used for growth and maintenance, Eq. 7 under maximum growth rate condition is in the form of:

Eq. 12.
$$q_G^{max} = (-Y_G^{max}) \cdot \mu_{max} + m_G$$

Eventually, maximal specific growth rate can be calculated with the following equation:

Eq. 13.
$$\mu_{max} = \frac{q_G^{max} - m_G}{-Y_G^{max}}$$

It gives the result of 0.76 (h⁻¹).

2.3.6. Overall specific growth reaction

Bioenergetic consumption of the bacteria is a function of its microbial activity, which is described by Eq. 7. With the known Gibbs energy of catabolism and anabolism, their proportions in the Gibbs energy of the overall metabolism, f_{cat} , can be derived using Eq. 4. At maximum growth μ_{max} , f_{cat} is about 0.48, while at maintenance $\mu=0$ f_{cat} is approaching to infinite, indicating that the proportion of energy from catabolism using to produce new cell is zero. This relation of Gibbs energy components is also applied on the stoichiometric coefficients of the reaction substances to calculate the stoichiometry of each reduction reaction:

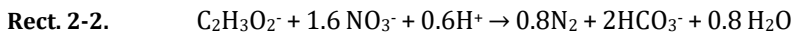
$$Y_{Si} = Y_{Si}^{an} + f_{cat} \cdot Y_{Si}^{cat}$$

where i is assigned for substances of the reactions. This interpretation indicates that stoichiometry of denitrification is also dependent on its specific growth rate μ . At maximal growth the overall metabolic stoichiometry is:

Rect. 2-1.



For zero growth conditions the overall metabolic stoichiometry is equal to the catabolic reaction:



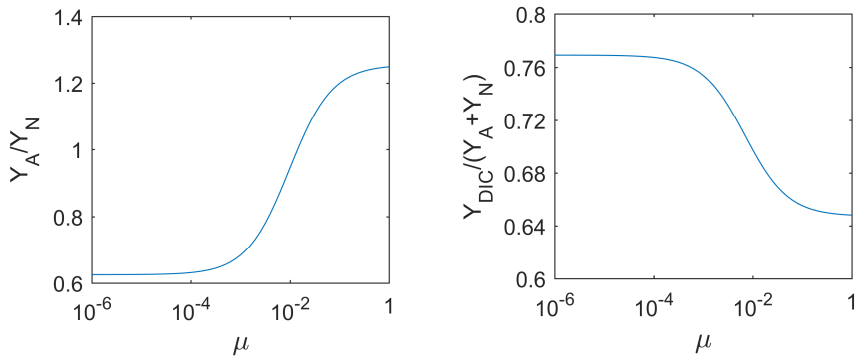


Figure 2-2. Stoichiometry of complete denitrification at different growth rate μ

The ratio of acetate over nitrate, Y_A/Y_N , and DIC over the total acetate and nitrate, $Y_{DIC}/(Y_A+Y_N)$, varying between these two boundaries is presented in Figure 2-2. The substrate consumption ratio Y_A/Y_N is seen to be in the range of 1.25 corresponding with Rect. 2-1 down to 0.625 corresponding with Rect. 2-2, and is proportional with the specific growth rate. In contrast, DIC production is favoured in maintenance mode so its upper boundary, which is 0.65, is expected when there is no growth (Rect. 2-1) and its lower boundary, which is 0.77, is correspondent with maximal growth expressed by Rect. 2-2.

2.4. Conclusion

Denitrification is an important process in the nitrogen cycle that convert nitrate (NO_3^-) to nitrogen gas (N_2). Accumulation of its intermediates needs to be limited due to their toxicity to living organisms and environment. Environmental conditions including oxygen concentration, pH, available nitrate and carbon sources and the ratio between them are important factors that influence accumulation of the intermediates. If its intermediate amounts are negligible, the denitrification reaction will have the consumption ratio of acetate over nitrate Y_A/Y_N to be 0.625 – 1.25, corresponding with the dissolved inorganic carbon production $Y_{DIC}/(Y_A + Y_N)$ of 0.77 – 0.65. These ranges are correspondent with the microbial metabolism from purely maintenance to maximal growth.

3.

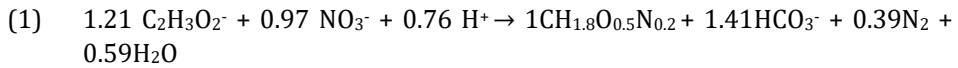
Applying MICP by denitrification in soils: a process analysis

In this chapter the process of Microbially Induced Carbonate Precipitation (MICP) by denitrification is investigated in relation to its potential use as ground improvement method. Liquid batch experiments indicated that the substrate solution had an optimum C/N ratio of 1.6 and confirmed that combining nitrate reduction and calcium carbonate precipitation leads to an efficient conversion, at which the pH is buffered slightly below 7 and accumulation of toxic intermediate nitrogen compounds is limited. Sand column experiments confirmed that the volume and distribution of the gas phase strongly depend on the stress conditions. The produced gas volume is inversely related to the pore pressure and can be predicted based on a mass balance analysis assuming conservation of mass and using theoretical laws of physics. At low pore pressure, the gas formed and accumulated at the top of the column whereas the calcium carbonate precipitation occurred mostly at the bottom near the substrate inlet, an excess amount of gas was produced which vented from the sand columns and induced cracks in the sand at low confining pressures, which negatively affects the sand stabilizing effect of the calcium carbonate minerals.

This chapter has been published online as Pham, V.P., Nakano, A., van der Star, W.R.L., Heimovaara, T.J. & van Paassen, L.A. (2016) "Applying MICP by denitrification in soils: a process analysis". *Environmental Geotechnics*, 10.1680/jenge.15.000780, (Article in press).

3.1. Introduction

MICP by denitrification is considered to have significant potential as a ground improvement method, through biogenic gas production and the formation of cementing calcium carbonate crystals (Kavazanjian et al., 2015, Hamdan et al., 2016). Still, the demonstrated reaction rate of this process is low compared with urea hydrolysis. Selecting the right substrate composition is essential. Too much nitrate may lead to accumulation of intermediate compounds which can be toxic for the bacteria and inhibit growth (Almeida et al., 1995) or increased emissions of nitrous oxide which is a very strong greenhouse gas (Chung and Chung, 2000), while leaving a large excess of acetate would be inefficient. Denitrification metabolism as presented in chapter 2 is between the state of maximum growth (1)- Rect. 2-1, and purely maintenance, (2)- Rect. 2-2:



Accordingly, the amount of required acetate at zero growth is 0.6 mole per mole of nitrate, while the acetate to nitrate (Ac/N) ratio at maximum growth is 1.25 (corresponding with carbon to nitrogen (C/N) ratios range from 1.2 to 2.5).

Besides, the formation, distribution and mobility of gas in porous media strongly depend on the soil characteristics and environmental conditions. Pore pressure in the underground strongly affects the produced gas volume and solubility (Rebata-Landa and Santamarina, 2011) and the accumulation and storage of gas is affected by the substrate supply regime (Ine's M. Soares et al., 1991). If too much gas is produced it could trigger liquefaction on very loose sand instead of mitigating it (Grozic et al., 1998).

For these reasons three sets of experiments were executed to evaluate the process performance of MICP through denitrification for a selection of process variables and test conditions related to its application as ground improvement method:

1) batch experiments in a mixed liquid culture in which substrate composition was varied to study the preferable substrate ratio and understand the process mechanisms;

2) sand column experiments in a triaxial cell, operated at different pore and confining pressure conditions to study the gas formation at different water level and soil depth;

3) sand column experiments at ambient pressure and low confinement with multiple sequential batches of substrates to investigate the precipitation efficiency of the treatment

3.2. Materials and Methods

3.2.1. Substrate solutions

The substrate solutions which were used throughout the experiments contained calcium acetate and calcium nitrate (Sigma Aldrich) at varying concentrations (Figure 3-1). Besides those main substrates all media further contained the following nutrients: 0.003 mM $(\text{NH}_4)_2\text{SO}_4$, 0.0024 mM MgSO_4 , 0.006 mM KH_2PO_4 , 0.014 mM K_2HPO_4 and 1 mL/L trace element solution SL12B (Overmann *et al.* 1992) to avoid nutrient limitation during bacterial growth.

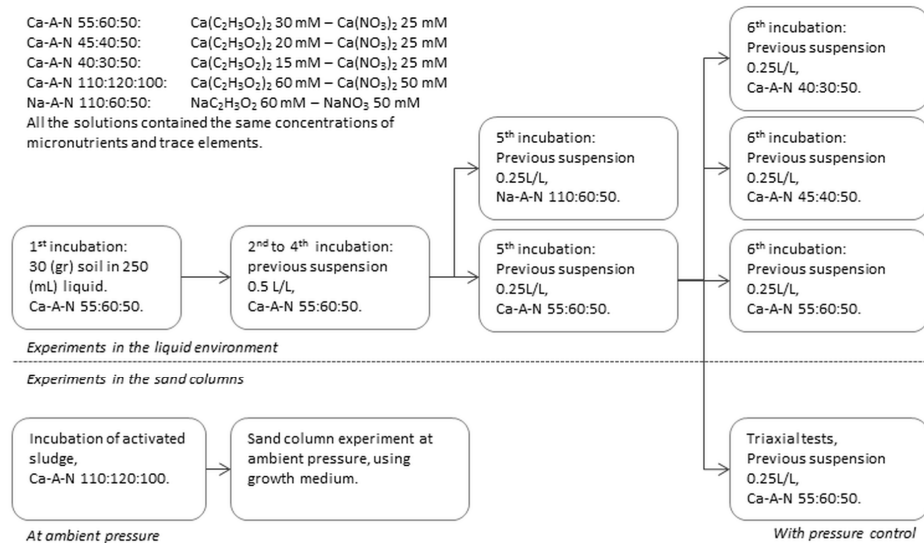


Figure 3-1. Liquid batch incubation testing

3.2.2. Liquid batch experiments

As inoculum for the first batch experiment, a soil sample was taken from the Botanical Garden of the Delft University of Technology. Denitrifying organisms typically occur in soils, which are wet and anaerobic and have sufficiently high organic content and a source of nitrate, such as wetlands or agricultural fields (Keddy, 2010). The sample was taken from a depth of 2 m using a hand auger. The black color and wet condition of the sample indicated that favorable conditions for denitrifiers were met.

The experiments were performed in 250 mL glass bottles (Duran GLS80). Electrodes were inserted through the cap to measure the pH and electrical conductivity (EC) and tubes were connected to sample liquid and to monitor the gas volume. In the first incubation, 30 g soil was suspended in 250 mL growth-medium. After three days of incubation all nitrate and nitrite were consumed and the bottle was shaken to stimulate the detachment of micro-organisms from the soil particles. Afterwards the liquid containing free denitrifying cells (without the solid fraction which had been allowed to settle) was collected and transferred into a new bottle for further experiments. All five subsequent incubations used the

inoculum from the previous incubation with the concentrations as shown in Figure 3-1. Substrates which were used in these batches were 30 mM $\text{Ca}(\text{C}_2\text{H}_3\text{O}_2)_2$ and 25 mM $\text{Ca}(\text{NO}_3)_2$, corresponding with calcium, acetate and nitrate concentrations of 55, 60 and 50 mM, respectively (Ca-Ac-N 55:60:50). In the fifth batch calcium salts in one of the two incubations were replaced by sodium salts (Na-Ac-N 110:60:50). In the sixth batch, the acetate to nitrate ratio was varied. Explicit concentrations of substrates and inoculums of these experiments are presented in Figure 2.

Liquid from the bottles was regularly sampled to analyze the concentration of different solutes, the electrical conductivity (EC) and the pH. All liquid samples were filtered through a 0.45 μm membrane and subsequently diluted to the measureable range before measurements. Nitrate, nitrite, and calcium were determined spectrophotometrically (Lasa 100, Hach Lange) with standard test kits LCK339, LCK341, LCK327, respectively). Total carbon (TC) was measured with the Dohrmann Chromatograph DC190. Acetate consumption was determined indirectly with TOC, which is the result from the TC measurements but pre-treated with HCl to remove the inorganic carbon (Schumacher 2002). All incubations were performed in a climate room at 25°C. The pH and EC were measured on all samples and continuously in the incubating bottles.

The gas produced during the experiment was captured using a water clock, made by placing a graduated cylinder upside down in a water bath. Before starting the incubation, N_2 gas was flushed through the bottle to ensure anoxic conditions and set the partial pressure of N_2 in the gas phase at 100%. The pressure of the gas was kept constant at ambient pressure by manually adjusting the height of the cylinder. Liquid sampling and gas volume measurements were done on a daily basis. The amount of nitrogen gas ($\text{N}-\text{N}_2$) was calculated from the measured gas volume using the ideal gas law at 1 atm and 298K, assuming nitrogen gas was the only produced gas.

3.2.3. Sand column experiments in a triaxial cell at varying pressure conditions.

Sand column experiments were performed at varying pressure conditions, using a triaxial test set-up as described in the standard ISO/TS 17892-9:2004 (CEN, 2004). A uniform fine grained siliceous sand (0.125-0.355 mm) was used (Sibelco, S60) with a silica content of 99.5% and a specific gravity of 2.65 g/cm³. The minimum and maximum dry bulk density (ASTM D4253 and ASTM D4254) range from 1.57 ± 0.01 to 1.66 ± 0.02 g/cm³. Sand columns were prepared using a split mould with a rubber membrane inside. The mould was filled in three layers. For each layer, first the suspension containing the bacteria and substrates was poured into the mould, followed by dry sand, ensuring that the sand always remained below the fluid level. The sample was not tamped, thus resulting in a very loosely packed sand with an average dry bulk density of 1.50 ± 0.1 g/cm³.

The suspension was prepared by mixing a 0.25L/L inoculum harvested at the end of the 5th incubation of the liquid batch experiments, with concentrated substrate solution and demi water. The overall substrate concentration of the suspension was 30 mM $\text{Ca}(\text{C}_2\text{H}_3\text{O}_2)_2$ and 25 mM $\text{Ca}(\text{NO}_3)_2$ (Ca-A-N 55:60:50). This corresponds to an A:N ratio of 1.2, which was selected to ensure there would be sufficient carbon source in case the conditions in the sand would be favorable for bacterial growth changing the metabolic stoichiometry towards maximum growth.

The tests were performed at three different pressure conditions. First, two back pressure conditions were selected to evaluate the effect of pore pressure on gas volume, while the effective confining pressure was kept constant: a low back pressure of 50 kPa with 100 kPa cell pressure and a high back pressure of 300 kPa with 350 kPa cell pressure. Next a third test was performed in which the back pressure was set at 345 kPa while the cell pressure was kept set at 350 kPa to evaluate the process at a low confinement pressure. A control test was performed at 50 kPa back and 100 kPa cell pressure using the growth medium without bacteria.

Once the cell and back pressures were set at the designated stress levels, the sample was left to react, while the volume change in the controllers was monitored. The pore pressure coefficient (or B-factor), which is the ratio of the change in pore pressure over the change in cell pressure and which is related to the degree of water saturation of the sample (Skempton, 1954), was measured at the beginning and at the end of the treatment. At the end of each experiment, the sample was flushed from bottom to top with de-aired water using a third pressure controller, while the back pressure was lowered to obtain a constant head difference of 20 kPa. While flushing, the flow rate was measured to calculate the hydraulic conductivity of the sample.

After flushing the high pressure samples the volume of the expelled and flushed liquids was determined by emptying the back pressure controller. For the low pressure conditions the back pressure controller was emptied before flushing the sample to collect the 'expelled' water and after flushing it was emptied again to collect the 'flushed' water. Samples were taken from the expelled and flushed liquids to determine the concentrations of NO_3^- , NO_2^- , Ca^{+2} , TC. During the first experiment biomass growth was observed in the cell water. Consequently for the other two tests also the volume and concentrations in the cell water were determined

3.2.4. Sand column experiments with multiple batches of substrate solution.

Sand column experiments were performed at ambient pressure conditions in which multiple batches of substrate solution were flushed through the columns in the total period of 65 days.

3. Applying MICP by denitrification in soils: a process analysis

The sand columns were prepared using plastic (PVC) columns with a length of 180 mm and inner diameter of 65 mm as described by (Harkers et al., 2010). The column was filled with a uniform fine siliceous sand (d_{50} : 0.166 mm; Itterbeck fine, Smals IKW, SZI 0032,). The top and bottom of the column were filled with 1 cm of fine gravel (d_{50} : 2.5mm). The sand and gravel were packed by tamping under water to an average dry density of 1.57 g/cm³. Before treatment, the sand column was flushed with several pore volumes of distilled water.

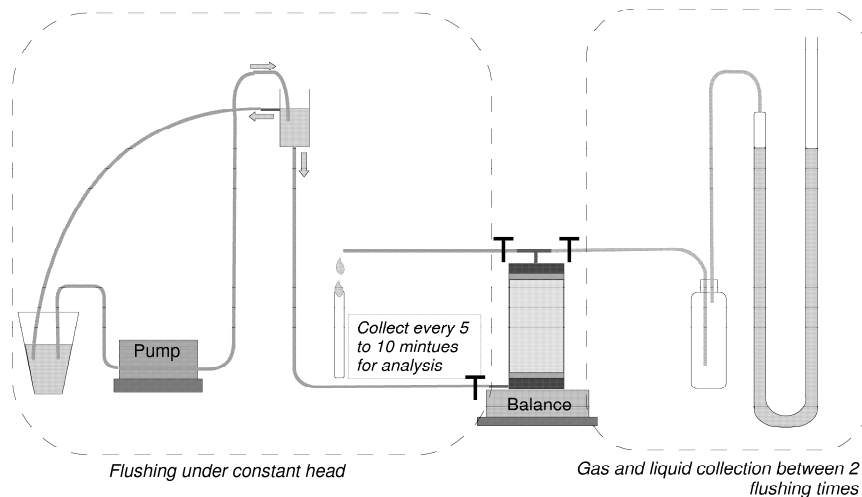


Figure 3-2. Set-up of the sand column with multiple substrate flushes at ambient pressure

The inoculum for this experiment was obtained from activated sludge collected at the municipal wastewater treatment plant Harnaschpolder (Delft, The Netherlands). The sludge was suspended in substrate solution containing 60 mM $\text{Ca}(\text{C}_2\text{H}_3\text{O}_2)_2$ and 50 mM $\text{Ca}(\text{NO}_3)_2$ (Ca-A-N 110:120:100) and the suspension was incubated for 6 days in which nitrate was fully consumed. The suspension containing the biomass, without the sludge (which was allowed to settle) was used as the inoculum for the column set-up. For the column experiment, 250mL of the suspension containing the inoculum 0.5L/L was mixed with substrate solutions reaching concentrations as indicated in Figure 3-1, and flushed into the column. Subsequently the column was flushed 9 times with 250 mL of substrate solution, after which the column was flushed with one pore volume of distilled water to wash the remaining solutes from the column. For the 1st to 3rd flush, the acetate to nitrate ratio was kept high (about 1.6) in order to stimulate bacterial growth and prevent accumulation of toxic intermediate nitrogen compounds. For all subsequent flushes the acetate to nitrate ratio was about 1.2, which corresponds to the reaction stoichiometry at maximum growth (reaction 1). All liquids were flushed in upward flow under a constant head difference of 20cm and the effluent

replaced by newly flushed medium was collected from the top during each flush. The set-up is presented in Figure 3-2

During each flush, the flow rate was determined by collecting the effluent from the top of the setup at regular time intervals and the hydraulic conductivity was determined using Darcy's law. pH, EC and the solute concentrations of these samples were measured. After each flush, the inlet at the bottom was closed and the column was left for 7 to 9 days to react. During this period, the produced gas and expelled liquid were collected. The mass of expelled liquid was measured after the reaction period before the next flush. After treatment the sand column was first analyzed using X-ray CT scanning, then the PVC tube was cut open over the length of the sample and removed. The sample was sliced into 9 parts and dried in the oven at 105 °C. The dry samples before and after treatment were analyzed with an Environmental Scanning Electron Microscope (Philips ESEM XL30). The calcium carbonate concentration was determined for 1.5-2.0 grams of the dried samples at different locations in the column using the acid dissolution method described by (Whiffin et al., 2007)

3.3. Results

3.3.1. Liquid batch experiments

Figure 3-3 shows the difference between incubation with calcium based substrates and sodium based substrates. The reduction in TC and Ca²⁺ concentrations in Figure 3-3a and the drop of EC in Figure 3-3c indicate that calcium carbonate precipitation took place. Due to the precipitation of carbonate the pH is buffered between 6 and 7, which reduces the accumulation of nitrite to a maximum level of 10 mM during the first week compared to 30 mM of nitrite for the sodium based substrate solution. In the sodium based system (Figure 3-3d) no precipitation took place, hence TC remains constant. The small amount of Ca²⁺ was due to the small fraction which was still present in the inoculum obtained from the fourth incubation. Due to MICP, this amount was quickly depleted. The decrease in nitrate and nitrite, and the increase in nitrogen gas (panel b and e) are evidence that denitrification still took place in both systems. In absence of calcium ions, denitrification leads to an alkaline environment, as shown in Figure 3-3f where the pH rose within 3 days to a level between 9 and 9.5.

3. Applying MICP by denitrification in soils: a process analysis

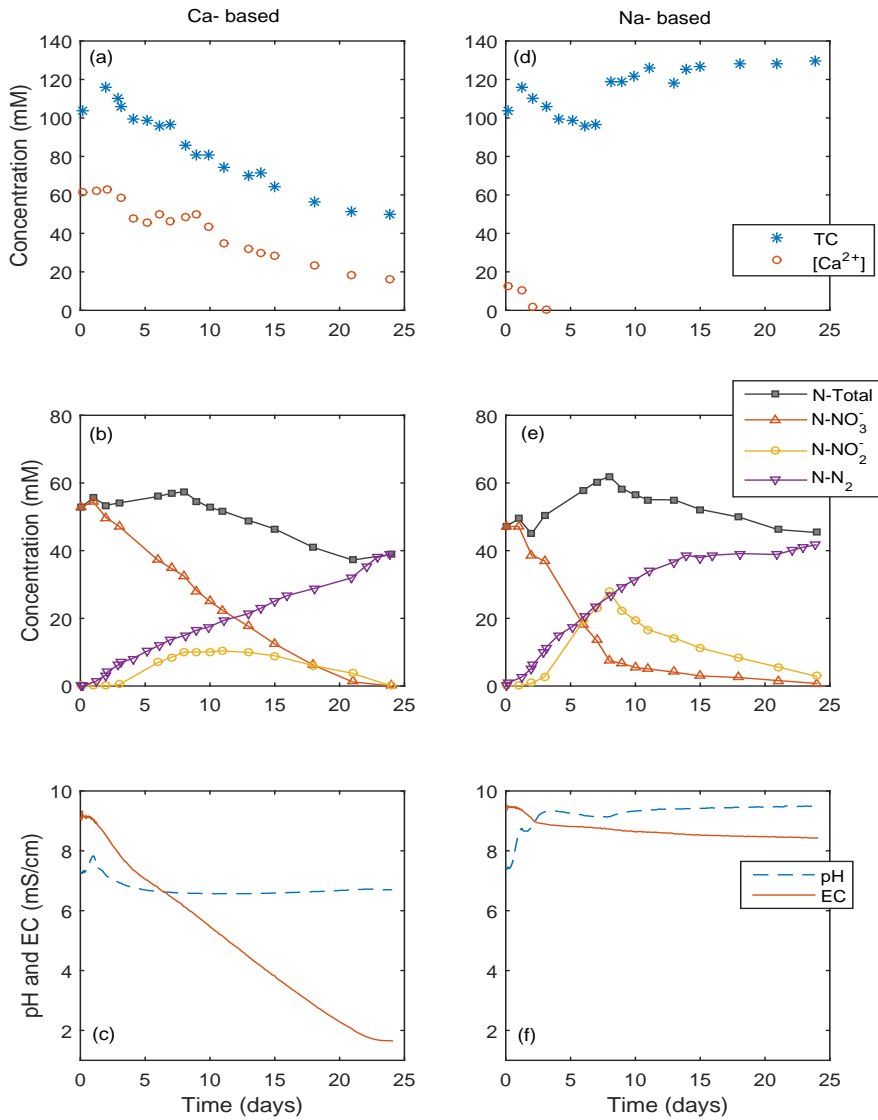


Figure 3-3. Comparison of changes in chemical composition during denitrification in the presence (left column) and absence (right column) of calcium ions during the 5th incubation. Legends indicate chemical compounds (TC is total dissolved carbon).

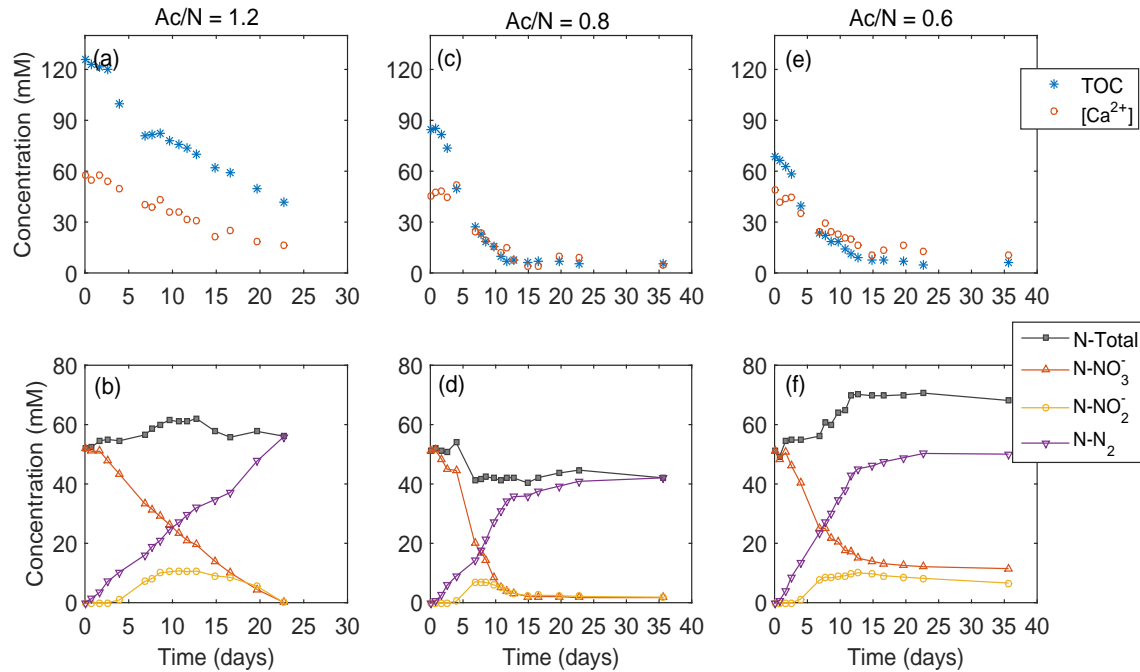


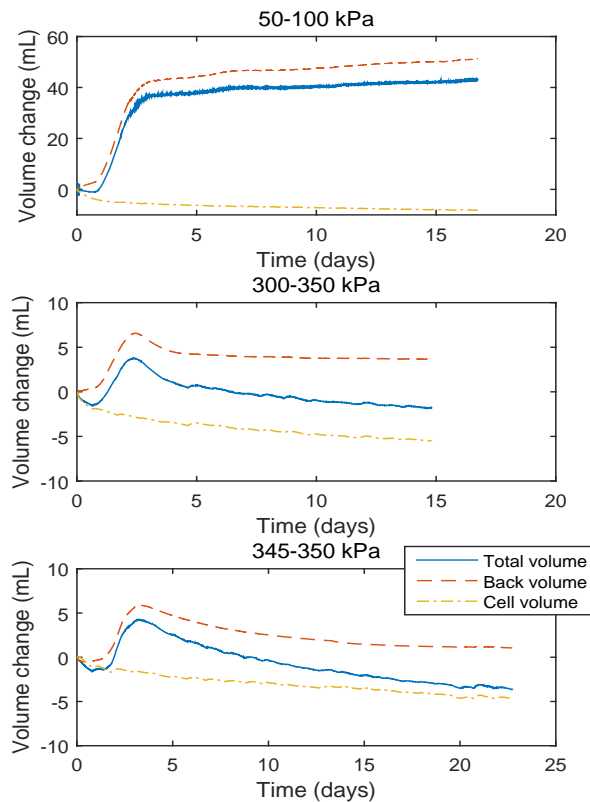
Figure 3-4. Comparison of changes in chemical composition during denitrification in the presence of calcium at 3 different acetate:nitrate ratios in the 6th incubation. Left column: Ca:A:N = 55:60:50, A/N = 1.2; middle column: Ca:A:N = 45:40:50, A/N = 0.8 and right column: Ca:A:N = 40:30:50, A/N = 0.6. Legends indicate chemical compounds (TOC is total organic carbon).

3. Applying MICP by denitrification in soils: a process analysis

Figure 3-4 shows the results of the incubations where the acetate to nitrate ratio was varied. The experiment using the growth medium with an A/N ratio of 1.2, which is close to the reaction stoichiometry for maximum growth of the bacteria (Rect. 2-2), resulted in an excess of calcium and acetate at the end of the experiment. The A/N ratio of 0.6, which corresponds to the stoichiometry of the catabolic reaction (zero growth, Rect. 2-1), resulted in an excess of nitrate and accumulation of nitrite. For the A/N ratio of 0.8, all substrates are converted most efficiently.

3.3.2. Triaxial tests at different pressure conditions

The volume change in the pressure controllers during the incubation experiments in the triaxial cell is shown in Figure 3-5.



4.

Figure 3-5. Volume changes in the triaxial tests at cell pressure – back pressure values of : (a) 350 kPa – 300 kPa; (b) 350 kPa – 345 kPa; (c) 100 – 50 kPa. The total volume change is the difference between the measured volume changes in the pressure cells.

The total volume change is the sum of the volume change in the cell and back pressure controllers and represents the change of the sample volume. All tests showed that the volume in the back pressure controller increased rapidly during the first 3 days. At the same time however volume of the cell pressure controller decreased in all experiments. As a result, the sample volume decreased before it started to rise. After 4 days the volume in the back pressure controller of the experiment with 50 kPa back pressure continued to rise slowly, while for the two tests with higher back pressures the volume started to decrease from the 3rd day onwards, resulting in a significantly lower volume change at the end of the experiment. The change in sample volume even became negative at the end of the experiment. The resulting volume changes and B-factor are presented in Table 3-1.

Table 3-1. Volume changes, B-factor and hydraulic conductivity at the end of the reaction in the triaxial tests

Experiments	Controller volume [mL]						B-factor		Hydraulic conductivity [10 ⁻⁵ m/s]
	Day 3			Day 15					
	Back	Cell	Total	Back	Cell	Total	Initial	end	
Control	0	-2.2	-2.2	1.3	-4.5	-3.2	0.98	0.98	5.9
50-100 (kPa)									
300-350(kPa)	6.4	-3.0	3.4	3.7	-5.5	-1.8	0.98	0.60	5.9
345-350(kPa)	7.4	-1.6	5.8	1.4	-3.5	-2.1	0.96	0.86	5.7
50-100(kPa)	42	-5.5	36.5	50	-7.9	42.1	0.58	0.04	5.8

Table 3-2. Volume and solute concentration of different liquids in the triaxial tests

Experiments	Liquid	Liquid	NO ₃ ⁻	NO ₂ ⁻	Ca ⁺²	TC
		Volume				
		[mL]	[mM]	[mM]	[mM]	[mM]
300-350 (kPa)	Initial Suspension	97	50.0	0	51.9	103.7
	Expelled liquid	n.d.	n.d.	n.d.	n.d.	n.d.
	Flushed liquid	206	2.9	0.04	0.69	9.25
	Cell water	n.d.	n.d.	n.d.	n.d.	n.d.
345-350 (kPa)	Initial Suspension	97	52.7	0	61.6	104
	Expelled liquid	n.d.	n.d.	n.d.	n.d.	n.d.
	Flushed liquid	206	0	0	1.5	7.7
	Cell water	3630	0.15	0.15	0.59	1.73
50-100 (kPa)	Initial Suspension	97	51.8	0	57.6	126
	Expelled liquid	35 (55) ¹	1.44	0.01	3.42	2.2
	Flushed liquid	207 (212) ¹	0.11	0	1.83	4.08
	Cell water	3633	0.1	0.158	0.66	0.92

The volumes and solute concentrations of the different liquid fractions are presented in Table 3-2. In the low pressure the back pressure controller indicated 55 mL was expelled from the sand column. However, the controller only contained 35 mL of liquid. Similarly, during flushing 212 mL was flushed out, of which only 207 mL was collected. It was assumed that the rest of the controller volume was filled with gas.

3.3.3. *Sand column experiment with multiple substrate flushes at ambient pressure*

The breakthrough-curves of EC, pH and the solute concentrations, which were measured during each flush are shown in Figure 3-6. The initial part of each breakthrough curve can be considered as a vertical profile from the top to the bottom through the sand column. The flush was continued until complete breakthrough, indicated by sharp increases in the EC and substrate concentrations. In the first two flushes of the fresh medium, the EC profile showed a relatively constant value of 4- 5 mS/cm over the height of the column, indicating there were no differences in solute concentration in the whole column. From the 4th flush onwards, the EC profiles started to show a decrease from top to bottom, reaching maximum values ranging from about 8 mS/cm at the top to about 3 mS/cm at the bottom, which indicates that during the final flushes a large part of the substrates in the upper half of the column were not converted yet when the next flush was applied.

The solute concentrations show a similar distribution. Nitrate was almost completely consumed over the full height of the column in the first 4 flushes, as only small concentrations of nitrite (< 1.3 mM) was measured and about 20 mM calcium was still present. The gradient of the substrate distribution in the column was very clear in the last 2 flushes. During these flushes, the remaining nitrate at the top of the column was 20 to 30 mM (indicating a conversion of only about 50%), while at the bottom it was completely consumed. The calcium and acetate concentrations showed a similar distribution. Incomplete nitrate conversion in the last flushes caused a considerable amount of nitrite accumulation.

During the reaction period between each flush, 31 to 53 ml of fluid was expelled from the pores due to gas production inside the column. The hydraulic conductivity, which was calculated from the measured flow rate during flushing, showed a significant difference between the first flush and all other flushes. In the second and later flushes initially no liquid flowed out of the column. The injected liquid first filled up the unsaturated pore space, before flowing out of the column. During each flush the flow rate gradually increased. The hydraulic conductivity at the end of the second and all later flushes was 50 to 70% lower than during the first flush. The increase in hydraulic conductivity can be explained by an increase in saturation as the trapped gas was gradually flushed out together with the liquid (increasing the relative permeability).

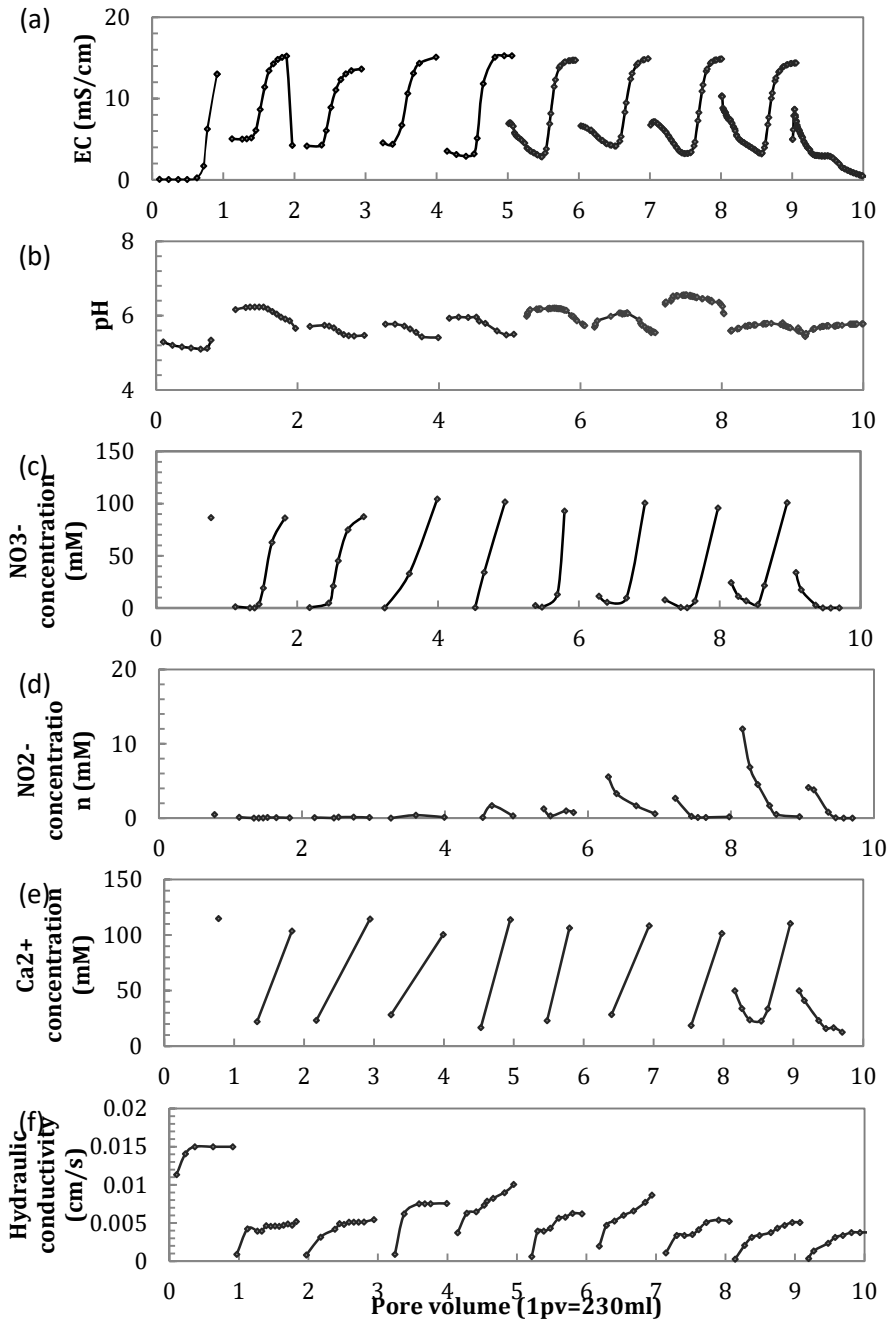


Figure 3-6. Measured values of (a) EC, (b) pH, (c) [NO₃⁻], (d) [NO₂⁻], (e) [Ca²⁺] and (f) Hydraulic conductivity for the sand column experiment at ambient pressure.

3. Applying MICP by denitrification in soils: a process analysis

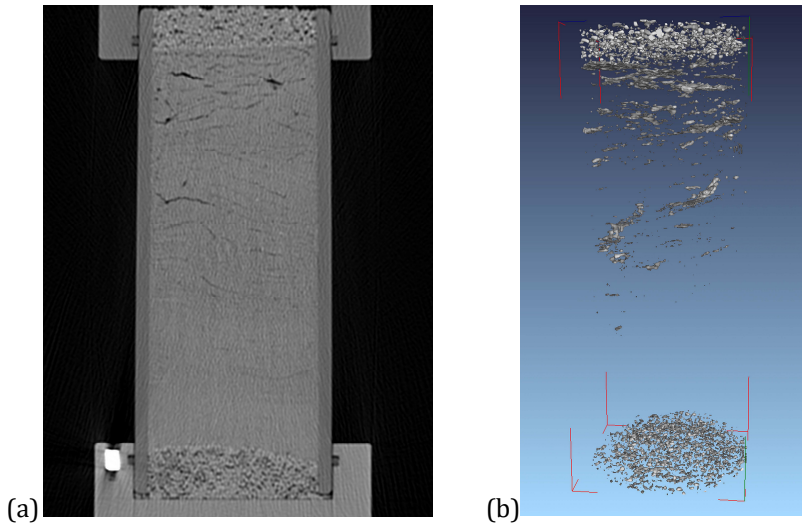


Figure 3-7. Result of the gas distribution in the sand column treated at ambient pressure with multiple substrate flushes: (a) the X-ray CT scanned images and (b) the constructed 3D image.

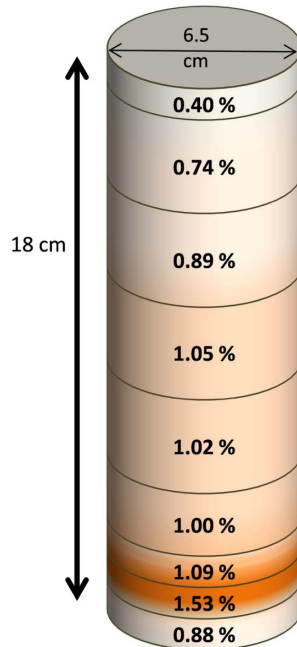


Figure 3-8. CaCO₃ distribution in the sand column treated at ambient pressure

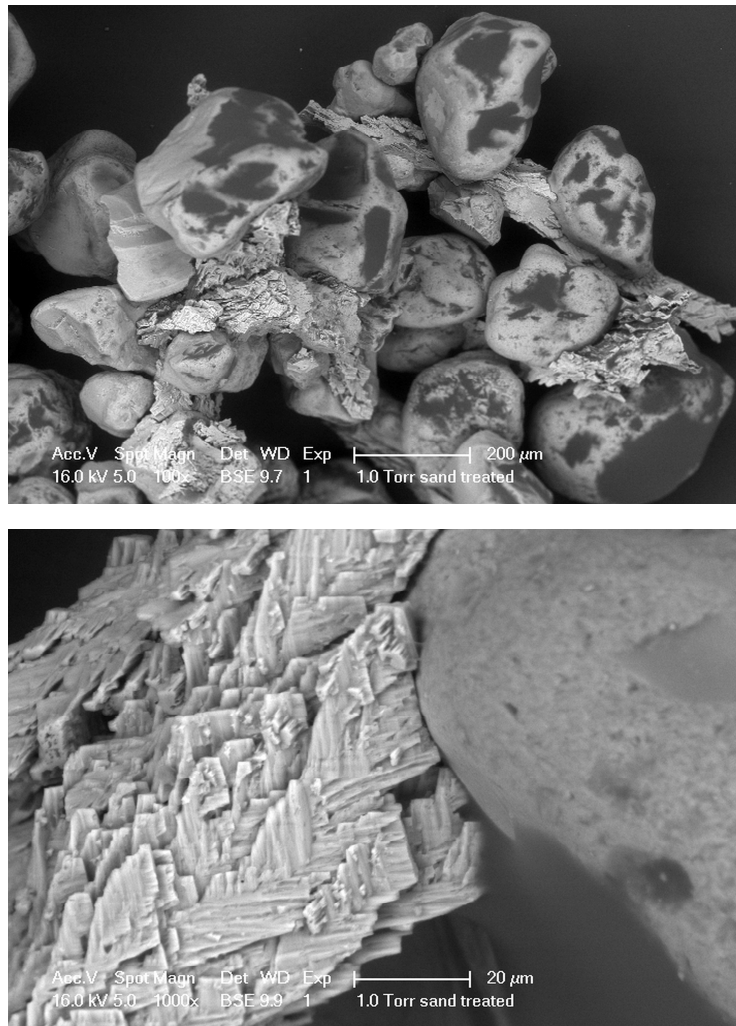


Figure 3-9. Presence of calcium carbonate in the sand treated with multiple substrate flushes at ambient pressure in ESEM images

The images produced by X-ray CT scanning (Figure 3-7) show that the gas produced during the experiment led to the development of cracks and open voids, which remained present after the column was flushed with water. The constructed 3D image in Figure 3-7b shows that the air was mostly present in the pores in the gravel layers and in the voids, which were developed mostly in the top of the column by the air bubbles themselves. However, as the resolution of the CT-scan is limited to approximately 200 µm, small gas bubbles could not be visualized.

Calcium carbonate measurements showed an average CaCO_3 content of about 1.1%. However, as shown in Figure 3-8 the CaCO_3 was not homogeneously distributed throughout the column. The distribution of CaCO_3 is largest at the

bottom of the sand layer and decreased to the top. Both gravel layers at the top and the bottom and upper part of the column had a relatively low CaCO_3 content. The presence of calcium carbonate was also confirmed by ESEM analysis (Figure 3-9). The crystals showed a dendritic texture with a size up to 200 μm .

3.4. Discussion

In order to assess the relevance of these results for ground improvement applications, first we discuss the accuracy of the experiments by analyzing the mass balance and secondly, we evaluate the effects of different process variables and test conditions on the process performance.

3.4.1. Mass balance

Concentration measurements during and after the reaction in each of the experiments are used to evaluate the mass balance of the different nitrogen compounds. Figure 3-3 and Figure 3-4 show the measured concentration of the different nitrogen compounds. The nitrogen gas concentration is calculated using the ideal gas law assuming ambient pressure (1 atm) and temperature (298K), and assuming that nitrogen gas was the only gas produced and all inorganic carbon either precipitated or remained in solution due to the relatively high solubility at neutral to high pH. Following these assumptions the sum of all nitrogen compounds (N-total) should be constant and equal to the initial nitrate concentration. Nevertheless, during the liquid batch experiments the sum of nitrogen compounds ranged between 40 and 70 mM, whereas the initial nitrate concentration was 55 mM in each of the experiments, which results corresponds to a deficiency in the mass balance of plus or minus 25%.

Table 3-3. Nitrogen balance for the triaxial tests

		300-350 kPa	345-350 kPa	50-100 kPa
Initial [mmol-N]	NO_3^- in the suspension	4.85	5.11	5.03
Final [mmol-N]	NO_3^- in cell water	n.d.	0.55	0.36
	NO_2^- in cell water	n.d.	0.54	0.57
	NO_3^- in [flushed+expelled] water	0.6	0	0.1
	NO_2^- in [flushed+expelled] water	0.01	0	0
	N_{2g}	2.14	2.13	5.18
	N_{2aq}	0.51	0.57	0.19
	Total	3.26	3.78	6.40
N-gap [mmol]		1.59	1.33	-1.37
N- gap [%]		33%	26%	-25%

For the triaxial tests, the total amounts of NO_3^- and NO_2^- were calculated by multiplying the measured concentration in each of the liquid fractions with the liquid volume. The total amount of nitrogen gas was calculated using the ideal gas law assuming that the volume of nitrogen gas is equal to the maximum volume change in the back pressure controller and that the partial pressure of nitrogen gas is equal to the back pressure. Assuming the gas phase is in equilibrium with the dissolved N_2 , its concentration was calculated using Henry's law. The resulting nitrogen balance in the triaxial test is shown in Table 3-3.

The mass balance calculations in Table 3 show that for the two experiments under high-pressure conditions, 26 and 33% of the nitrogen compounds in the nitrate added are unaccounted for and therefore lost, while for the experiment at (near) ambient pressure, the final nitrogen level is 25% higher than initially added. Further investigation is required to validate the assumptions and explain the observed discrepancies in the mass balance.

3.4.2. *The effect of substrate composition on process efficiency*

The results of the liquid batch experiments show that the substrate composition significantly affects the process performance. When denitrification is combined with MICP the pH is buffered at values which are slightly lower than the optimal range for denitrification reported in literature (Knowles, 1982, Wang et al., 1995). A similar pH buffering effect by MICP has been observed by Burbank et al. (2011). In their field experiments in which they stimulated MICP by a combination of urea hydrolysis and denitrification they observed that the pH remained around neutral. The results of this study are partly in agreement with the observations of (Glass and Silverstein, 1998), showing that a high pH - which occurs when sodium based media are used - favors the reduction of nitrate to nitrite, but can cause nitrite to accumulate. On the other hand the solutions containing calcium showed complete reduction of nitrate, with limited accumulation of nitrite even though the pH was buffered at a value below 7. This is contradicting the observations by (Glass and Silverstein, 1998), which found that nitrate reduction at pH 7 and below is completely inhibited. Still the observed pH values are within the range at which active denitrification has been reported by others and far from the lower limit that could cause N_2O accumulation (Knowles, 1982). Hence, the combined process of nitrate reduction and calcium carbonate precipitation promotes efficient conversion of nitrate to nitrogen gas and prevents the accumulation of toxic intermediates and potential greenhouse gases.

Also the C/N ratio in the growth medium significantly affects the conversion efficiency. Similar to the observations by (Chung and Chung, 2000), we found that high C/N ratios favor the complete conversion of nitrate and limit nitrite accumulation but lead to an excess of acetate and calcium at the end of the experiment. A low C/N ratio on the other hand, leads to full acetate consumption, but at the end of the experiment significant concentrations of residual nitrate and

accumulated nitrite remain. In our experiments the optimum Ac/N ratio appears to be around 0.8 which is slightly lower than the optimum ratio found by Chung and Chung (2000), but significantly lower than the ratio at maximum growth according to Rect. 2-2.

3.4.3. The effect of pressure conditions on gas formation and distribution

When stimulating MICP by denitrification in sand the pressure conditions significantly affect the formation and distribution of gas in the pore space. For a given amount of substrate the volume of gas is much lower at high pore pressures than at low pore pressures. This is as expected considering firstly that according to the ideal gas law the volume and pressure of gas are inversely proportional. Secondly, according to Henry's law the gas solubility is higher at high pressures. Thirdly, the higher gas solubility leads to higher dissolved gas concentrations which may lead to larger diffusive fluxes to surrounding water as observed in the case of 300-350 kPa and 345-350 kPa in Figure 3-5.

The total gas volume in the pore space significantly influences the geotechnical properties of sand, including strength, permeability and stiffness (Dejong et al., 2013). After a specific amount of gas is produced single gas bubbles will coagulate into gas pockets or form a continuous gas phase, which tends to migrate upwards in irregular patterns (Paassen et al., 2010, Haines, 1930)(Van Paassen, 2010; Haines, 1930). Also the confinement pressure influences the potential of MICP by denitrification for ground reinforcement applications. At low confinement conditions (shallow depth) the gas may form cracks and disturb the sand structure and reduce the stabilizing effect of the calcium carbonate minerals as shown in Figure 3-7.

3.4.4. The relationship between the distribution of gas and calcium carbonate

The average CaCO₃ content in the sand column which was flushed 9 times with substrate solution reached 1.1%. Although this amount of calcium carbonate is relatively low compared with other studies on MICP based on hydrolysis of urea such as (Van Paassen et al., 2010), it may still be sufficient to significantly increase cyclic shear resistance to mitigate liquefaction of loose sandy soils (DeJong et al., 2014, Kavazanjian et al., 2015). The relationship between strength and CaCO₃ content depends on many factors, including the density, mineral type and grain size distribution of the treated sand (Van Paassen et al., 2010, Cheng et al., 2013) and substrate concentrations, reaction rate and environmental conditions of the treatment process (Paassen, 2009a, Qabany et al., 2012, Mortensen et al., 2011).

Gas production can have a positive effect on the strength gain due to MICP. (Cheng et al., 2013) showed that columns which were treated under partially saturated conditions required lower amounts of CaCO₃ to obtain a similar increase in strength for fully saturated conditions. They considered that in partially

saturated conditions substrate solutions preferably filled the pore throats due to suction effects, resulting in a more efficient distribution of cementing calcium carbonate minerals. Similarly (Kavazanjian et al., 2015) showed that MICP by denitrification resulted in more efficient cementation than MICP by urea hydrolysis. Our study showed that within the sand column treated at ambient pressure CaCO₃ was predominantly formed at the bottom of the column, while gas was predominantly formed at the top. This seems obvious because there is less substrate available to react when gas displaces the substrate solution. As a result the potential improvement in the cementation efficiency due to desaturation is counteracted by a lower conversion efficiency. Secondly the cracks which were formed at low confining pressure disturb the sand stabilizing effect of the calcium carbonate minerals. The low number, large size and dendritic structure of the CaCO₃ crystals can be due to the fact that the crystals have grown in multiple phases at a relatively low reaction rate (Paassen, 2009b).

3.4.5. Conversion

The overall reaction rate of denitrification and precipitation is an important process parameter, which depends on many factors, including the amount and type of denitrifying organisms, substrate and product concentrations and environmental effects, such as temperature, pH, salinity and the presence of other catalyzing or inhibiting compounds (Paassen, 2009a). Reported NO₃⁻ consumption rates range from a few mmol/L/day up to 170 mmol/L/day (Ine's M. Soares et al., 1991, Glass and Silverstein, 1998, Paassen et al., 2010, Martin et al., 2013). This study showed that the reaction rate in the triaxial cell was about 10 to 15 mmol/L/day NO₃⁻. The liquid batch experiments in which the same substrate concentrations and inoculum size were used showed a rate which was with 1-2 mmol/L/day NO₃⁻ which was about 5 to 8 times lower than the triaxial cell. The average reaction rate in the sand column at ambient pressure was about 6 mmol/L/day NO₃⁻. However, the remaining substrates in the final flushes indicated that the reaction rate in the unsaturated top part of the column was lower than in the saturated bottom part. Considering at least a few mass% of CaCO₃ needs to be formed it is expected that under based on the current results it still requires several weeks to several months of treatment in order to obtain sufficient strength improvement using MICP through denitrification. Further investigation is required to explain the observed differences in reaction rate.

3.5. Conclusions

This study showed that the combined process of biological denitrification and microbial induced carbonate precipitation leads to a more efficient conversion than denitrification without precipitation. The precipitation of CaCO₃ buffers the pH and prevents the accumulation of toxic intermediates. The optimum acetate to nitrate ratio, at which all substrates are consumed most efficiently, is about 0.8 (which corresponds to a C:N ratio of 1.6). Lower Ac/N ratios lead to the

3. Applying MICP by denitrification in soils: a process analysis

accumulation of toxic intermediate nitrogen compounds, while higher ratios leave significant amounts of residual calcium and acetate. Sand column experiments confirmed that the volume and distribution of the gas phase strongly depend on the pressure conditions. The produced gas volume is inversely related to the pore pressure and can be reasonably predicted using a generic thermodynamic approach, which solves the mass and charge balance to determine the stoichiometry of the metabolic reaction, and making some simplifying assumptions to determine the distribution of gas over the dissolved and gas phase. Further investigation is required to explain the observed deficiency between measured and expected values. Under high pore pressure conditions in the triaxial cell the produced gas initially expels the liquid phase, but later on seemed to dissipate from the sand sample, probably by diffusion through the latex membrane. At low pore pressures the produced gas was higher than gas storage capacity of the sand column and escaped to the back pressure controller column while expelling part of the liquid phase. In the sand column which was treated with multiple batches of substrate solution, the conversion rate and cumulative amount of calcium carbonate appeared to be inversely related to the gas distribution. Due to the low confinement cracks were induced, which may negatively influence the sand stabilizing effect of the calcium carbonate minerals.

4.

Biogenic gas formation by denitrification-based MICP in sandy soils

Biogenic gas formation by denitrification is being considered as a potential ground improvement method. In this chapter a simplified calculation method is proposed to estimate the produced gas volume from denitrification and its results of gas saturation in the treated soil. Experiments using a modified triaxial test set-up were performed to validate the calculation and also to study the gas formation in the sand. Experimental results showed that average grain sizes and pressure conditions have significant influence on the gas dissolution rate. After a single treatment, the gas production reached the percolation threshold of the soil samples and vented out, resulting in a discrepancy in the predicted gas saturation results and the measurement. When the produced gas volume was below the percolation threshold or in a very fine sand, the induced gas phase had the most stability and remarkably reduced the hydraulic conductivity values. The results indicate that it is possible to control the gas production and its stability for applications, but requires further investigation.

4.1. Introduction

Biogenic gas formation is being considered as a potential ground improvement method (Rebata-Landa and Santamarina, 2011, He and Chu, 2014, Kavazanjian et al., 2015). Trapped gas bubbles in the pore space can dampen pore pressure changes due to cyclic loading (Yegian et al., 2007). In order to use biogenic gas production for geotechnical engineering applications, it is necessary to be able to predict the amount of produced gas and evaluate its remaining state in the soil. In this chapter a simplified calculation method is proposed to estimate the gas volume to be produced and its consequence for the gas saturation in the treated soil. To validate the calculation and also to study the gas formation in the sand, experiments using a modified triaxial test set-up were performed in which the average grain size and pressure conditions were varied. The effect of the produced gas on the mechanical behaviour was evaluated. In the discussion the calculations are compared with the experimental results. Output of this chapter allows to roughly evaluate the gas distribution and its stability in the tested soil and provide recommendations for future work on this topic.

4.2. Simplified calculation method to predict the gas saturation in porous media generated by denitrification.

To estimate the amount of gas production by the denitrification-based MICP process and its effect on the degree of saturation in sandy soils, a simplified calculation method is proposed using the following assumptions:

- (1) N_2 is the only gas component of the induced gas phase;
- (2) Pore gas pressure and pore water pressure in the soil are equal, effect of surface tension is neglected;
- (3) The soil is initially fully saturated.

Possible nitrogen containing components of the gas phase of denitrification besides N_2 can be NO and N_2O , but in general conditions these components can be neglected (see chapter 2), assuming NO_3^- is directly reduced to N_2 . Inorganic carbon produced from the microbial metabolism can also partially be transferred into the gas phase. However, because the pH remains close to neutral during the combined process of denitrification and precipitation, bicarbonate is the dominant solute species of dissolved inorganic carbon. Secondly, even under slightly acidic pH carbon dioxide is highly soluble (its Henry's coefficient is 28.53 atm.L.mol⁻¹) compared with N_2 gas, whose Henry's coefficient is 1542.6 atm.L.mol⁻¹. Hence for the purpose of simplification, CO_2 fraction in the gas phase is not considered and the produced gas is assumed to contain only N_2 gas.

In a closed system of liquid batch with known substrate consumption, and microbial metabolism represented by its specific growth rate μ , amount of N_2 to be produced can be calculated from its correspondent stoichiometric coefficients of N_2 and NO_3^- , Y_{N_2} and $Y_{NO_3^-}$.

$$c_{N_2tot} = \frac{Y_{N_2}}{Y_{NO_3^-}} \times c_{NO_3^-}^{consumed}$$

According to Henry's law, the distribution of N_2 between the gaseous and dissolved form depends on the partial pressure p_{N_2} is:

$$c_{N_2dissolved} = \frac{P_{N_2}}{k_{H_N_2}}$$

Where c_{N_2tot} [mol/L] is the concentration of N_2 to be produced from the substrate consumption with correspondent stoichiometry, $c_{N_2dissolved}$ [mol/L] is the concentration of dissolved N_2 in the system and $k_{H_N_2}$ is Henry's coefficient of N_2 ; $k_{H_N_2} = 1542.6$ (atm.L/moles), value taken from (Yaws, 2012).

When the gas phase is in equilibrium with the dissolved phase, the total amount of N_2 gas, $n_{N_2^g}$ in [mol], is determined using:

$$n_{N_2^g} = (c_{N_2tot} - c_{N_2dissolved}) \times V_L$$

Where V_L [L] is the liquid volume of the batch. Neglecting potential effects of surface tension which can occur in very small gas bubbles, the partial pressure, p_{N_2} , is assumed to be equal to the hydraulic pressure, u , in the pore fluid. In this case the volume of N_2 gas can be determined from the amount of gas (in moles) at the given pressure and temperature using the ideal gas law.

$$V_g = \frac{n_{N_2^g} \times R \times T}{p_{N_2}}$$

Where T is the temperature in the system in [K] and R is the universal gas constant, $R = 0.082056$ (atm.L/K/mol) or $8.31e-3$ (kJ/K/mol), value taken from (Kauzmann 2013).

When the reactions happen in the soil, assuming a soil is fully saturated before it is treated with denitrification-based MICP, the initial liquid volume V_L can be considered equal to the pore volume V_{pores} of the sample. When the gas is produced, the gas saturation is defined as the proportion in percentage of the gas volume over the total pore volume of the system and is calculated as following:

$$V_{pores} = V_L^{ini}$$

$$S_g = \frac{V_g}{V_{pores}} \times 100\%$$

Using the calculation method described above, the degree of saturation is calculated as a function of pore pressure (with corresponding water depth) for three different concentrations of nitrate and two extreme metabolic stoichiometry scenarios, of zero and maximal growth. Results are presented in Figure 4-1.

Figure 4-1 shows that the resulting gas saturation strongly depends on the amount of converted nitrate and pressure conditions in the soil and is less sensitive to the metabolic stoichiometry. When aiming to use the induced gas phase to decrease the pore fluid bulk stiffness and increase liquefaction resistance, increasing the gas saturation to about 5% showed to be sufficiently effective (He and Chu, 2014), while a high value of S_g could result in gas pressure building up and actually trigger liquefaction (Grozic et al., 1998) and should be avoided. To limit S_g to be lower than 10%, the results in Figure 4-1 suggests that one flush of substrates with a nitrate concentration of 20 mM NO_3^- or less, depending on the pressure conditions, is sufficient. When gas pressure is assumed to be equal to water pressure, this simplified calculation can give indications about the range of gas saturation to be expected at different pore water pressures corresponding to different depth below groundwater level.

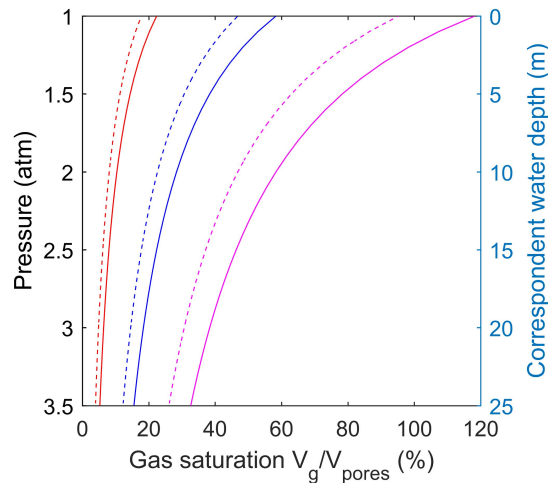


Figure 4-1. The gas saturation induced by denitrification as a function of pore pressure, calculated for the stoichiometry of maximal growth (dash lines) and pure maintenance or zero growth (continuous lines), for three different concentrations of consumed NO_3^- : 20 mM (—), 50 mM (—) and 100 mM (—).

4.3. Experimental method and materials

4.3.1. Experiment set-up and variables

To monitor the gas production by denitrification in the sand at different pressure conditions, a triaxial set-up as shown in Figure 4-2 was used for the experiments, similarly to the description in standard ISO/TS 17892-9:2004 (CEN, 2004). A third

controller was connected to the inlet of the sample and was placed at 1.5 m higher than the back pressure controller. The free head space of this controller was connected to that of the back pressure controller, which in turn were connected to the main pressure control, allowing flushing a sample at a defined back pressure under a constant head of 1.5m (150 kPa above the pressure in the system) to determine the hydraulic conductivity. Water tank of the back pressure controller and the third controller were put on balances to monitor change in the water mass while controlling pressure.

In the experiments, values of the pressure being mentioned with the triaxial test in kPa are the pressure added to ambient pressure.

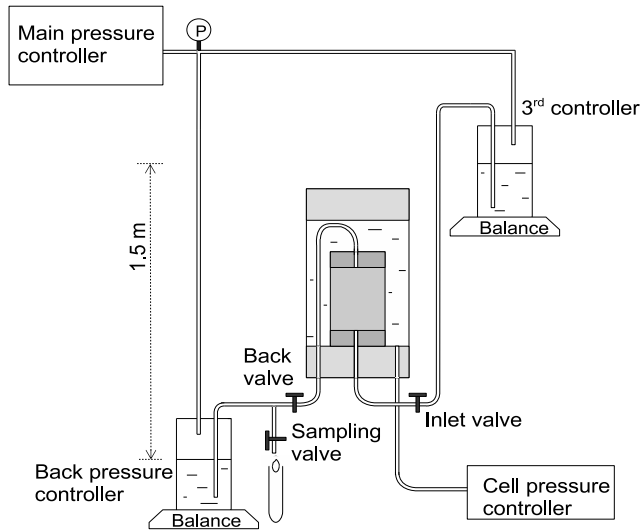


Figure 4-2. Triaxial test set-up

The procedure of the experiments was as followed:

(1) Sample preparation

Baskarp sand columns were prepared using a split mould with the rubber membrane mounted inside (inner diameter 65 mm, height 130 mm). 250 mL suspension was prepared containing the substrates together with the 40 mL/L bacteria suspension. The suspension and the sand were poured into the mould in turns so that the sand level was always below the liquid level. When the mould was nearly full, small amounts of liquid and sand were added so that they were filled slightly above the top of the mould. The top part of the mould was slightly tamped to densify the excess sand, the top surface was flattened to close the sample with porous stone and the top cap.

(2) Saturation and consolidation

The outer cell of the triaxial set-up was installed and filled with water. The sample was saturated to the conditions of 200 kPa cell pressure – 100 kPa pore pressure,

following the procedure presented in CEN (2004) ISO/TS 17892-9:2004. Then the back valve was opened for consolidation. Demineralized de-aired water was used in the back pressure controller.

(3) *Reaction phase*

During the Reaction phase, the back valve was opened so the expelled fluid would be collected in the back pressure controller. The amount of water expelled from the sample through the controller was continuously registered (through a balance).

(4) *Washing*

At the end of a reaction phase, the third controller containing demineralized de-aired water was connected to the bottom line of the sample to wash the sample from bottom to top. Hydraulic head during flushing was 1.5 m.

(5) *Shearing*

After flushing with demineralized water, the sample was loaded in compression under constant confinement of 200 kPa cell pressure and undrained conditions at a loading speed of 0.5 mm/s.

Table 4-1. Sandy soil information

Sand type	Treatment	Bulk density [g/cm ³]	Porosity [%]	Relative density [%]	Hydraulic Permeability × 10 ⁻⁶ [m/s] K _{ini}
d ₅₀ = 0.123 mm	Control	1.48±0.02 ⁽¹⁾	44.1±0.6	29.2±6	9.7±1.4
d ₅₀ = 0.100 mm	Control	1.45	45.4		9.2
d ₅₀ = 0.250 mm	Control	1.52	42.6		10.3
d ₅₀ = 0.123 mm	50-100 kPa	1.50	43.3	39.5	
d ₅₀ = 0.123 mm	50-150 kPa	1.51	42.9	43.1	
d ₅₀ = 0.123 mm	100-200 kPa	1.54	42.8	43.4	
d ₅₀ = 0.123 mm	250-300 kPa	1.52	42.6	45.6	
d ₅₀ = 0.100 mm	100-200 kPa	1.47	44.4	n.d.	
d ₅₀ = 0.250 mm	100-200 kPa	1.55	41.6	n.d.	

⁽¹⁾ The sample preparation method described above was performed several times on fine Baskarp sand to obtain the average value and standard deviation of bulk density.

The experiments were performed for variable average grain size and pressure conditions. Sandy soils with 3 different average grain sizes were tested at 100 kPa back pressure – 200 kPa cell pressure. The sand with an average grain size of 0.123 mm was chosen to test at different pressure conditions. Table 4-1 provides an overview of the different test conditions

4.3.2. *Bacteria cultivation and substrate concentrations*

This study used facultative denitrifying microorganisms, which were enriched from a sample of the top soil from the Botanic garden of Delft University of Technology. They were enriched through 6 sequential liquid batch transfers using

calcium salts of nitrate and acetate (30mM $\text{Ca}(\text{C}_2\text{H}_3\text{O}_2)_2$ - 25mM $\text{Ca}(\text{NO}_3)_2$), following the procedure presented by Pham et al. (2016b). In the 6th batch, it took about 3 weeks for the nitrate to be completely consumed and for the newly accumulated nitrite to be depleted. After that, the suspension containing microorganisms was transferred to a new bottle by decantation, leaving out any visible crystals. To increase the reactivity of the inoculum, the bacteria were separated from the liquid by centrifugation. From the bottle, the liquid was evenly divided into 100mL-test tubes, totally 4 tubes and centrifuged at 300 g (LKB 2610 Midispin centrifuge at 2000 rpm) in 1.5 hours. After centrifugation, the supernatant was removed, the pellet containing microorganisms was collected by rinsing the test tubes with 5 mL of demiwater. These cells were further incubated 3 more times in 30mM $\text{Ca}(\text{C}_2\text{H}_3\text{O}_2)_2$ - 25mM $\text{Ca}(\text{NO}_3)_2$ solution using the same procedure. At the end of the last incubation, after 1.5hr centrifugation the supernatant remained turbid, indicating that there was still significant amount of cells in it besides the isolated biomass pellet in the bottom of the tubes. This supernatant was brought into new test tubes and centrifuged again for total 3 hours until it became clear and all were present at the bottom. The precipitant after centrifuging was collected using solution of NaCl 0.9%. This is the stock inoculum for all the following experiments.

The experiments used substrate concentrations of 25 mM $\text{Ca}(\text{NO}_3)_2$ - 30 mM $\text{Ca}(\text{C}_2\text{H}_3\text{O}_2)_2$. Besides the main substrate components, substrate solution contained the following nutrients: 0.003 mM $(\text{NH}_4)_2\text{SO}_4$, 0.0024 mM MgSO_4 , 0.006 mM KH_2PO_4 , 0.014 mM K_2HPO_4 and 1 mL/L trace element solution SL12B (Overmann et al. 1992) to avoid nutrient limitation.

4.4. Experimental results

4.4.1. Water saturation and hydraulic conductivity changes

Changes of water saturation during the reaction period were calculated from the expelled liquid that had been continuously monitored. The results are presented in Figure 4-3 and Figure 4-4. All tests, except for the test performed at the highest pressure of 250 kPa back pressure - 300 kPa cell pressure, showed similar desaturation profiles: Over a period of 1 to 4 days the desaturation rate gradually increased until a threshold was reached after which the water saturation was hardly reduced any further. For the test performed at 250 kPa back pressure the threshold was not reached. End values of S_w at the end of the reaction period, i.e. before flushing, are presented in Table 4-2. Due to the gas production and possibly transportation and redistribution, pore and back pressure of the samples had spontaneous jumps and deviated from the controlled values. These results are presented in the supplemental data S1.

4. Biogenic gas formation by denitrification-based MICP in sandy soils

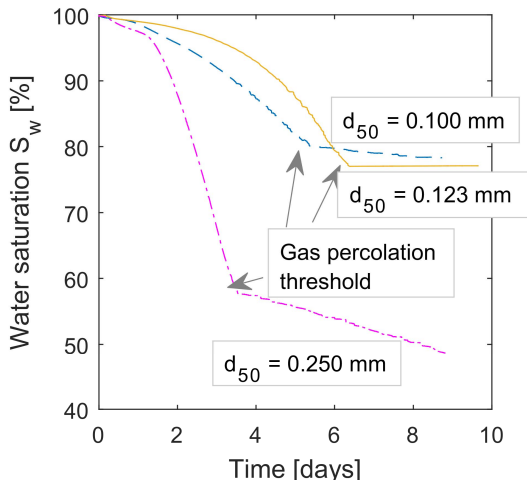


Figure 4-3. Results of different sandy soil treated at 100 kPa back pressure - 200 kPa cell pressure

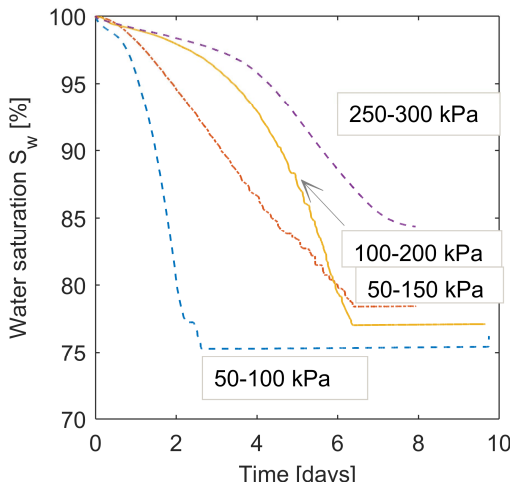


Figure 4-4. Results of fine sand ($d_{50} = 123\mu\text{m}$) treated at different pressure conditions, legend indicates controlled back pressure – cell pressure in kPa

By flushing with water at the end of the experiment, part of the gas phase was replaced again by water resulting in a regain of S_w . Proportion of the gas volume which had been replaced by flushing over the amount before flushing was calculated accordingly and presented also in Table 4-2, together with the changes of hydraulic conductivity. Hydraulic conductivity K of the treated sand was calculated with flow rates at the end of flushing, where the flow was stable and no further gas had been replaced.

The relative permeability which represents the loss of K , K_{end}/K_{ini} , due to the gas production was within one order of magnitude except the case of very fine sand $d_{50} = 0.1$ mm, where the flow was clogged and its K after treatment was 2.5 cm/d, which is 3% of its initial value. Flushing could replace almost all the gas in the case of fine sand ($d_{50} = 0.123$ mm) treated at 100-200 kPa, but could only replace about 5% of the gas when this sand was treated at 250-300 kPa.

Table 4-2. Changes of gas and water saturation, and hydraulic conductivity

Grain size d_{50} (mm)	Pore – Cell pressure (kPa)	After reaction		K_{end} (cm/d)	K_{end}/K_{ini} (-)	After flushing with water		Gas replacement by flushing (-)
		S_w (-)	S_g (-)			S_w (-)	S_g (-)	
0.100	100-200	0.78	0.21	2.5	3 %	0.84	0.16	26.5 %
0.123	100-200	0.77	0.22	45.5	54 %	0.98	0.02	89.2 %
0.250	100-200	0.49	0.51	63.3	71 %	0.80	0.20	61.2 %
0.123	250-300	0.84	0.16	36.9	44 %	0.85	0.15	5.7 %
0.123	50-150	0.78	0.22	62.1	74 %	0.92	0.08	63.8 %
0.123	50-100	0.76	0.24	52.9	70 %	0.82	0.18	26.4 %

4.4.2. Results of the sand behaviour under undrained monotonic loading

Typical behaviour of the treated sand under undrained monotonic loading is presented in Figure 4-5 and Figure 4-6. Thanks to the gas phase, the pore pressure change of the treated sand became insignificant compared to that of the non-treated sand, resulting in the overlap of its effective and total stress path. As the gas phase helped to dampen the pore pressure change, the dilatancy effect was significantly reduced as seen in the stress-strain behaviour. Considering the potential ground improvement applications of the biogenic gas, it shows not to be beneficial in term strength improvement at large deformation. On the other hand, its effect of reducing the pore pressure build-up and increasing the soil stiffness at small strain prove its potential in the applications such as liquefaction mitigation.

4. Biogenic gas formation by denitrification-based MICP in sandy soils

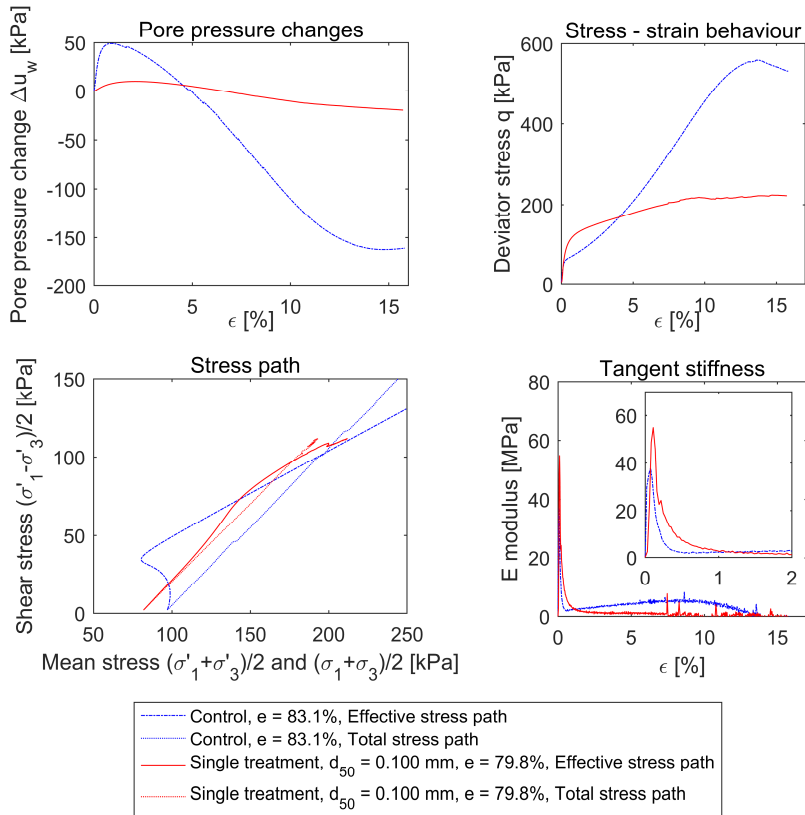


Figure 4-5. Behaviour of the very fine sand, $d_{50} = 0.100$ mm, after treatment under undrained monotonic loading

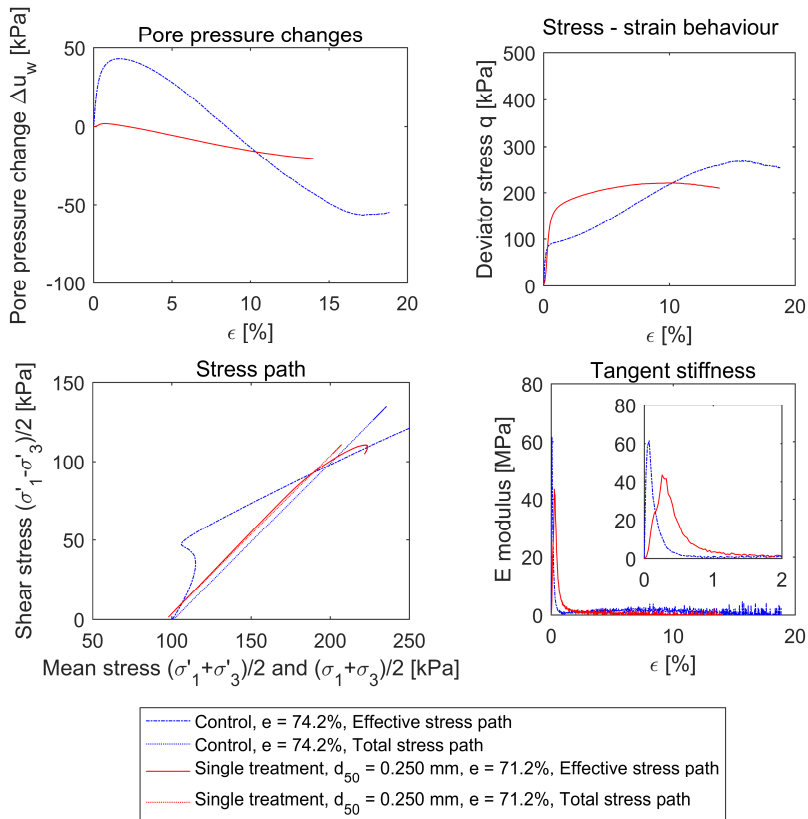


Figure 4-6. Behaviour of the medium sand, $d_{50} = 0.250$ mm, after treatment under undrained monotonic loading

4.5. Discussion

4.5.1. Comparing the simplified model with experimental results

The gas saturation from calculation in Figure 4-1 is plotted again in Figure 4-7 together with the experimental results. In all cases, except for the medium sand ($d_{50}=0.25$ mm), the volume of gas was equal or smaller than the predicted amount.

In the medium sand the gas production was about double the predicted amount. This discrepancy can be attributed to the incorrectness of the assumption that N_2 is the only gas component, and CO_2 might be significant in the gas phase. Besides, the assumptions that the expelled liquid is equal to the produced gas volume and that the total volume of the sample is constant may be invalid. In case the total volume was not constant due to some deformation during the reaction phase, compaction of the sample may cause additional liquid volume to be expelled. As a result, expelled liquid is not representative for the gas saturation in

the soil and the gas volume from the experiment may be overestimated. Reconsidering the experiment set-up as well as tracking the gas components are needed to improve the accuracy. However, the large difference between the calculation and measurement suggest that there are other physical mechanisms that have been missed.

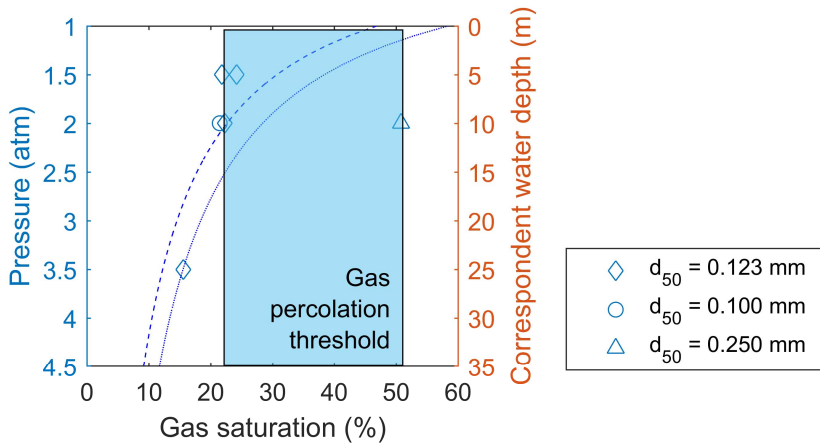


Figure 4-7. Induced gas saturation in sandy soil in correspondence with their boundaries. Range of gas saturation induced by denitrification between maximum growth (blue dash lines) and pure maintenance (blue dot lines); concentration of consumed NO₃- 50 mM.

In the proposed calculation, the pore gas pressure is assumed to be equal with the hydraulic pressure and capillary effects are neglected, but in a partially saturated soil, the gas and water pressure can be significantly different. When the gas phase is in direct contact with the atmosphere the pressure in the gas phase is equal to the atmospheric pressure. In this zone above the phreatic surface water can be held up by capillary suction, in which the suction in the water phase is related the elevation above the phreatic surface and the pore size. When the gas is not in contact with the atmosphere, the pressure in the gas phase can be significantly higher than the fluid pressure. The difference between its gas and water pressure is expressed by Young-Laplace equation (Blander and Katz, 1975):

$$p_{non-wet} - p_{wet} = \frac{2\gamma}{R}$$

Following this equation, the difference between gas and liquid pressure is determined by the surface tension of the liquid γ and the radius of curvature R of the liquid-gas interface. For water at 20°C, γ is 71.97 mN/m. For soil with average grain size radius of r , its average pore size can be estimated as (Roth, 2012):

$$r_c \approx 0.087 \times r$$

When bubbles occupy the pore space, assuming $R \approx r_c$ resulting in about 33 kPa pressure difference for the very fine sand $d_{50} = 0.1\text{mm}$ or 13 kPa for the medium sand $d_{50} = 0.25\text{ mm}$. Accordingly, the coarser the sand is the less pore gas pressure,

and following Henry's law results in a lower dissolved fraction and more N₂ and CO₂ going into the gas phase. In term of bubble nucleation, the threshold for nucleation can be lowered to different extent depending on gas pressure and the dissolved fraction (Lubetkin, 2003).

Besides the significant difference in the case of sand with d₅₀ of 0.25mm, experimental results show a gas percolation threshold above which the gas vented out of the sample, causing the difficulty in validating the calculation. In practice, gas clusters in seabed is also considered as potential cause of blowing-out in the soil and pose a threat to offshore installation (Hovland and Judd, 1988). Instead of mitigating liquefaction, the mobile gas phase can be the risk to trigger liquefaction (Grozic et al., 1998). Using biogenic gas for applications requires the guarantee that gas formation is crucially sufficient so that there is no risk of blowing-out, and the formed gas phase has to be sufficiently stable to carry the load instead of trigger liquefaction. Comparing the calculated and measured gas saturation in this study suggest that gas percolation threshold can be used as a criteria to determine the sufficiency limit. In the case of fine sand tested at 250 kPa – 300 kPa back-cell pressure, as the produced gas volume was below the soil's percolation threshold, there was no gas flow during the reacting phase so there was no risk of blowing-out. Under the hydraulic gradient of 1.5m, most of the gas was flushed away in all the cases except this case, indicating a strongly stable gas phase. The experiments need to be duplicated as well as tested at different conditions to validate this suggestion.

The experiments did not meet the objective of validating the gas calculation, but the overall results show that they are useful to predict the required substrate concentrations and working pressure conditions for the gas production not to exceed the percolation threshold of the soil.

4.5.2. *Effect of soil matrix and pressure conditions on gas formation and stability*

Experimental results show that the amount of gas in the sample is determined by the produced gas volume and the percolation threshold of the soil. The produced gas volume is determined by the amount of reacted substrate and the pore pressure, while the gas percolation threshold is related to the air entry value of the soil and is determine by state of the porous network of the soil (Broadbent and Hammersley, 1957). At micro scale, the solid matrix can act as a nucleation site for gas bubble formation as well as entrapment for gas bubble agglomeration and transportation (Rebata-Landa and Santamarina, 2011, Brooks and Corey, 1964), and determine the amount, size, shape and connectivity of the gas bubbles (Gauglitz and Radke, 1989, Lee et al., 2004, Mosdorf and Wyszowski, 2013). Theoretically the gas production can completely replace the pore water when the pore pressure is relatively low or the amount of produced gas is large as seen in the case of 100 mM NO₃⁻ consumption in Figure 4-1. In practice this is unlikely to

occur in granular soils as the gas will tend to migrate upwards, unless the granular soils are covered by soil layers with low permeability, such as clay or salt. In order to migrate upwards, the pressure in the gas phase has to exceed the air entry value of the coarsest pore throats it is connected to (Haines, 1930, Brooks and Corey, 1964). Once this happens, the gas pressure drops, while the gas volume expands. This irregular migration events of gas bubbles are often referred to as Haines jumps (Haines, 1930, Armstrong et al., 2015). Once the N_2 gas forms a network of connected air pockets it can rapidly accumulate forming air filled pockets in the soil and find or create pathways venting upwards (Istok et al., 2007, Ine's M. Soares et al., 1988). This is when the gas percolation threshold is reached, resulting in a threshold of gas content that could stay in the soil.

Regarding the gas percolation threshold all the tests on fine grained and very fine grained sand showed a threshold between 21 to 24%. When the produced gas volume reaches this threshold, it is believed that the gas bubbles have agglomerated to form channels, lenses and pockets, which form continuous pathways to allow the excess gas volume to vent out of the sample. This process can be described as growth of isolated gas clusters in a manner similar to the invasion percolation process (Yortsos and Parlar, 1989, Li and Yortsos, 1995, Dominguez et al., 2000). In this approach, the gas production develops a global percolation pattern with capillarity to be the control factor, and the percolation threshold depend crucially on the nucleation characteristics of the porous medium, and for the case of medium sand ($d_{50}=0.25\text{mm}$) it could be the layered strata. In this sand it showed a significantly higher gas threshold of 43%. Besides the influences of capillarity, a significantly high value of the gas percolation threshold can occur in layered strata, where the gas is captured in the coarse grain zones, and the fine grain zones with higher air entry value work as the gas barriers. In this case, the porous stone of the set-up might play the role of the fine grain zone.

Influence of capillarity and pore pressure on gas formation can be used to explain the difference in gas formation rates in Figure 4-3 and Figure 4-4. The Young-Laplace equation shows that the coarser sand has a lower capillary effect, and hence it has less dissolved fraction and consequently lower threshold of gas nucleation (Lubetkin, 2003). This is consistent with the results in Figure 4-3 as the gas dissolution rate, which is the overall process of bubble nucleation and growth and reflected by the reduction rate of water saturation, was the fastest in the medium sand ($d_{50} = 0.25\text{mm}$), indicating a significantly lower threshold of phase transition. With the fine sand ($d_{50} = 0.123\text{mm}$) at different pressure conditions in Figure 4-4, lower pore water pressure resulting in less dissolved fraction and lower phase transition threshold, so the fastest gas dissolution rate was seen with the cases at 50 kPa back pressure and the slowest rate at 250 kPa back pressure. The difference rates between the fine sand at 50 kPa – 100 kPa and 50 kPa – 150 kPa back – cell pressure is attributed to the confinement effect of the experiment

which can influence the mass transfer inside the pores when the gas dissolution rate is high (Li and Yortsos, 1995).

In terms of gas stability, using the results of gas replacement by flushing in Table 4-2 shows the most stability corresponds with the case of fine sand treated at 250 kPa – 300 kPa back – cell pressure, in which the gas production did not exceed the percolation threshold. It is believe in this case that because the global percolation pattern was not completely developed, the gas was well distributed as discrete small bubbles and stayed stably in the soil pores. In the cases of very fine sand tested at 100 kPa – 200 kPa back – cell pressure and fine sand tested at 50 kpa – 100 kPa back – cell pressure, about a quarter of the gas phase in both the cases was flushed away but influence on hydraulic conductivity was in contrast. The case of very fine sand ($d_{50} = 0.1\text{mm}$) was the only one whose the gas phase blogged the hydraulic flow and reduced the permeability by a factor of ten. This is also counted on the gas stability and average grain size is also a controlling factor.

Gas stability is considered to be important when aiming to mitigate liquefaction by partial desaturation. This study shows that a stable gas phase can be obtained when the produced gas volume is within the storage capacity or when the pore size is small enough to prevent gas accumulation. Besides average grain size, grain size distribution and relative density are the important soil matrix parameters that influence the gas formation and stability. For a poorly graded sand, the average grain size can be used as a direct parameter to estimate bubbles size and related gas stability. For well graded sand, a pore size distribution should be determined using analytical or theoretical approaches to investigate the gas phase distribution and stability. This analysis is recommended for further evaluation.

4.6. Conclusion

This study showed that a simplified model can be used to calculate the amount of nitrogen gas and desaturation consequence in soils. Although the model was not completely validated due to the results that the gas production exceeded the soil's percolation threshold and vented out, the model is useful to estimate the required conditions to avoid this situation if it is needed. Experiments show that when the gas production did not exceed the percolation threshold, the gas phase was the most stable among all the tested cases. Soil matrix and pressure conditions are the controlling factors on the gas formation and stability. Even when the gas production exceed the percolation threshold, the induced gas phase can still be very stable in a very fine sandy soil and lead to clogging. Further study on this subject requires to cooperate knowledge and experimental technics of multiphase transport in porous media so gas formation, distribution and stability can be controlled for practical applications in the soil.

4. Biogenic gas formation by denitrification-based MICP in sandy soils

5.

Evaluating strategies to improve process efficiency of denitrification based MICP

Microbially induced carbonate precipitation (MICP) through denitrification can potentially be applied as a bio-based ground improvement technique. In this chapter, multiple batch treatments in a modified triaxial test set-up were used to study the process efficiency of denitrification based MICP. All treatments aim to achieve 1 w% of precipitated calcium carbonate and differ in number of flushes, hydraulic residence time and substrate concentrations. In the experiment with few flushes at a high concentrations the microbial process was inhibited, only 0.28 w% CaCO₃ was measured in the sand after 5 weeks of treatment. The regime with many flushes at low concentrations was favorable to microbial growth resulting in 0.65 w% CaCO₃ over the same time. Biomass growth and nitrogen gas production were stable throughout the experiment at low concentration, reducing the hydraulic conductivity of the sand which eventually led to clogging. Precipitation rates up to 0.26 w%/day CaCO₃ were observed. Applying a suitable substrate regime and resident time is important to limit inhibition and maintain the cell activity, allow for an efficient conversion and generate a good precipitation rate.

This chapter has been submitted as Pham, V.P., van Paassen, L.A., van der Star, W.R.L., and Heimovaara, T.J. & (2017) " Evaluating strategies to improve process efficiency of denitrification based MICP". Journal of Geotechnical and Geoenvironmental Engineering.

5.1. Introduction

Microbially induced carbonate precipitation (MICP) is a potential method to improve soil characteristics and behavior for geotechnical and environmental applications. Various bacteria are capable to induce carbonate precipitation by producing dissolved inorganic carbon (DIC) through their metabolism in an environment which has available nucleation sites, suitable pH as well as sufficient supply of dissolved calcium. Dissimilatory nitrate reduction to dinitrogen gas, or denitrification, is one of these MICP processes, and has the potential advantages of using waste streams for substrates, producing no by-products requiring removal and making use of indigenous species of denitrifying bacteria (Van der Star et al., 2009). Denitrification consists of four sequential reduction steps from nitrate to (di)nitrogen gas: $\text{NO}_3^- \rightarrow \text{NO}_2^- \rightarrow \text{NO} \rightarrow \text{N}_2\text{O} \rightarrow \text{N}_2$, where each step in the metabolic pathway is carried out by a different enzyme (van Spanning et al., 2007). Denitrifying bacteria generally have strategy to limit accumulation of the toxic intermediates (Ferguson, 1994, Zumft, 1997, van Spanning et al., 2007), so the measured concentrations of NO and N_2O are often far less than NO_2^- (Betlach and Tiedje, 1981), making nitrite NO_2^- the only intermediate considered in studies monitoring denitrification.

One of the challenges of denitrification-based MICP is the low reaction rate compared to MICP via urea hydrolysis. MICP based on urea hydrolysis has been most widely studied and has been successfully demonstrated at large scale (Van Paassen et al., 2010, DeJong et al., 2009). It has shown to generate up to 6 w% calcium carbonate within several treatment days (Whiffin et al., 2007, Burbank et al., 2011, Chu et al., 2012), whereas denitrification based MICP needed several months up to a year to obtain an average 1-3 w% (Paassen et al., 2010, O'Donnell, 2016).

In wastewater treatment systems nitrate with concentrations ranging from several mM (Matějů et al., 1992) to above 100 mM are treated and nitrate removal rates of up to 31 mmol per litre per day (Pinar et al., 1997) have been reported. If nitrate is assumed to be directly reduced to dinitrogen without accumulating the intermediates and all carbonate produced is used for CaCO_3 , the precipitation rate can be calculated accordingly. The yield of DIC production over NO_3^- consumption (Y_{DIC}/Y_N), ranged from 1.25 to 1.45 (Pham et al., 2016b). If calcium is in excess and all DIC is converted to CaCO_3 , the amount of precipitated CaCO_3 per kilogram of soil with given dry density (ρ , [kg/L]) and porosity (ϕ , [-]) is:

$$w_{\text{CaCO}_3} = \frac{m_{\text{CaCO}_3}}{m_{\text{soil}}} = \frac{\frac{Y_{DIC}}{Y_N} \times R_{\text{NO}_3^-} \times M_{\text{CaCO}_3}}{1000 \times \rho_{\text{dry}} \phi}$$

Where w_{CaCO_3} is the weight fraction of CaCO_3 precipitated, $R_{\text{NO}_3^-}$ is the NO_3^- consumption rate [mol/L/day] and M_{CaCO_3} is 100 [g/mol]. So the nitrate removal

rate of 31 mM/day can theoretically result in a precipitation rate between 0.06 and 0.13 w%/day depending on the reaction stoichiometry and the initial density and porosity of the sand. As several studies showed that 0.5-3 w% of precipitated CaCO_3 can already help to increase the soil strength, especially at small strain (Montoya and DeJong, 2015, Lin et al., 2016), denitrification-based MICP may have potential as ground improvement method or subsurface remediation (Martin et al., 2013) within a limited timeframe. The nitrogen gas, which is considered a side-product of denitrification based MICP, has an effect on the distribution and transport of the soluble substrates and as a consequence limits the available substrates for denitrification and carbonate precipitation. On the other hand, the induced gas phase may be a target on itself considering that it decreases water saturation, which can help to enhance the soil resistance to dynamic loading and e.g. mitigate liquefaction (He et al., 2013, He and Chu, 2014, Rebata-Landa and Santamarina, 2011). Due to the low solubility of nitrogen gas, only very small amounts of gas need to be produced to improve the resistance to cyclic loading. The method can be considered as a two-stage process for liquefaction mitigation and has given promising results (Kavazanjian et al., 2015). According to this concept, first the induced gas dampens pore pressures and secondly the calcium carbonate minerals provide more durable strengthening.

The treatment protocol for denitrification based MICP needs to consider several variables, among which there are substrate concentrations and flushing frequency. Applying high substrate concentrations has the advantage that less frequent substrate supplies are required to reach the target amount of desired product. Nevertheless, for denitrification based MICP high substrate concentration may result in temporary or permanent nitrite accumulation, which leads to inhibition of further denitrification (Almeida et al., 1995, Glass and Silverstein, 1998, Dhamole et al., 2007). In this study, effect of the regime with which substrates are supplied regime on the efficiency of denitrification-based MICP is evaluated experimentally in sand columns under confined pressure conditions using a modified triaxial test set-up. Two treatment protocols are evaluated, which both aimed to produce 1 w% calcium carbonate in about one month. One using a low number of 3 flushes with relatively high substrate concentrations (50 mM calcium nitrate – 60 mM calcium acetate) and a long hydraulic residence time of 10 to 12 days. The other using a high number of 15 flushes with low substrate concentration (10 mM calcium nitrate – 12 mM calcium acetate) and a short hydraulic residence time of 2 to 3 days. The efficiency of the treatment is evaluated based on reaction rates, amount of precipitated CaCO_3 , the conversion of substrates, impact on the sand permeability and drained response under monotonic loading.

5.2. Materials and methods

5.2.1. Bacteria cultivation

(The experiments used the same bacterial inoculum which had been cultivated as described in section 4.3.2)

This study used denitrifying microorganisms, which were enriched from a sample of the top soil from the Botanic garden of Delft University of Technology. They were enriched through 6 sequential liquid batch transfers using calcium salts of nitrate and acetate (30mM $\text{Ca}(\text{C}_2\text{H}_3\text{O}_2)_2$ – 25mM $\text{Ca}(\text{NO}_3)_2$), following the procedure presented by Pham et al. (2016b). In the 6th batch, it took about 3 weeks for the nitrate to be completely consumed and for the newly accumulated nitrite to be depleted. After that, the suspension containing microorganisms was transferred to a new bottle by decantation, leaving out any visible crystals. To increase the reactivity of the inoculum, the bacteria were separated from the liquid by centrifugation. From the bottle, the liquid was evenly divided into 100 mL-test tubes, totally 4 tubes and centrifuged at 300 g (LKB 2610 Midispin centrifuge at 2000 rpm) during 1.5 hours.) After centrifugation, the supernatant was removed, and the pellet containing microorganisms was collected by rinsing the test tubes with 5 mL of demi water. These cells were further incubated 3 more times in 30mM $\text{Ca}(\text{C}_2\text{H}_3\text{O}_2)_2$ – 25mM $\text{Ca}(\text{NO}_3)_2$ solution using the same procedure. At the end of the last incubation, after 1.5hr centrifugation the supernatant remained turbid, indicating that there was still significant amount of suspended cells in the liquid besides the isolated biomass pellet in the bottom of the tubes. This supernatant was brought into new test tubes and centrifuged again for total 3 hours until it became clear and all cells were at the bottom. The remaining pellets after centrifuging were resuspended in a solution of 9 g/L NaCl, which was the stock inoculum for all the following experiments.

5.2.2. Sand types

Baskarp sand was used in the experiments, its properties are presented in Table 5-1.

Table 5-1. Soil properties

Sand type	d_{10} [mm]	d_{50} [mm]	$C_u, d_{60}/d_{10}$	C_c	e_{\max}	e_{\min}
Baskarp	0.083	0.123	1.6	1.05	0.91	0.54

5.2.3. Substrate concentrations, resident duration and number of flush

Substrate solutions were prepared using demineralised water. The experiments used two regimes of substrate concentrations, in which the proportions of the two main substrates were kept equal but their concentrations varied:

- A high concentration regime – using substrate concentrations of 50 mM calcium nitrate, $\text{Ca}(\text{NO}_3)_2$, and 60 mM calcium acetate, $\text{Ca}(\text{C}_2\text{H}_3\text{O}_2)_2$;

- A low concentration regime – using substrate concentrations of 10 mM calcium nitrate, $\text{Ca}(\text{NO}_3)_2$, and 12mM calcium acetate, $\text{Ca}(\text{C}_2\text{H}_3\text{O}_2)_2$;

Next to the main components the solutions contained the following nutrients: 0.003 mM $(\text{NH}_4)_2\text{SO}_4$, 0.0024 mM MgSO_4 , 0.006 mM KH_2PO_4 , 0.014 mM K_2HPO_4 and 1 mL/L trace element solution SL12B (Overmann et al. 1992) to avoid nutrient limitation during bacterial growth. The amount of substrate required to obtain 1 w% of calcium carbonate in the sand samples can be calculated with an estimate of sample size, density and porosity and assuming the denitrification and precipitation reactions were complete following the stoichiometry of maximum growth according to Pham et al. (2016b). Accordingly, the high concentration regime required 3 flushes of substrate solution to reach the target amount of calcium carbonate and the low concentration regime required 15 flushes.

The residence time, which is the duration between two flushes supplying fresh substrates, was determined based on conversion rates observed in earlier experiments (Pham et al., 2016b). They are 10 days and 2 to 3 days for the high and low concentration regimes respectively. To take into account a possible lag phase of bacterial growth to allow the population to adapt to the change of the substrate concentrations and the environment (from liquid to porous media), the first residence time was extended by 6 days and 3 days for the high and low concentration regimes respectively.

5.2.4. *Equipment*

A triaxial set-up as shown in Figure 1 was used for the experiments which is similar to the one described in the ISO/TS 17892-9:2004 standard (CEN, 2004). An additional third controller was connected to the inlet at the bottom of the sample and was placed at 1.5 m above the back pressure controller. Both the back pressure and inlet controllers were partly filled with liquid and the head space of both controllers was connected to the main pressure control, which allowed flushing the sand column from bottom to top at a defined back pressure under a constant head difference of 1.5m (15 kPa above the pressure in the system). The back and inlet pressure controllers were put on balances to monitor change in the water mass while controlling pressure. In this way, the flow rate could be determined during flushing, in order to determine the hydraulic conductivity similar to a constant head test.

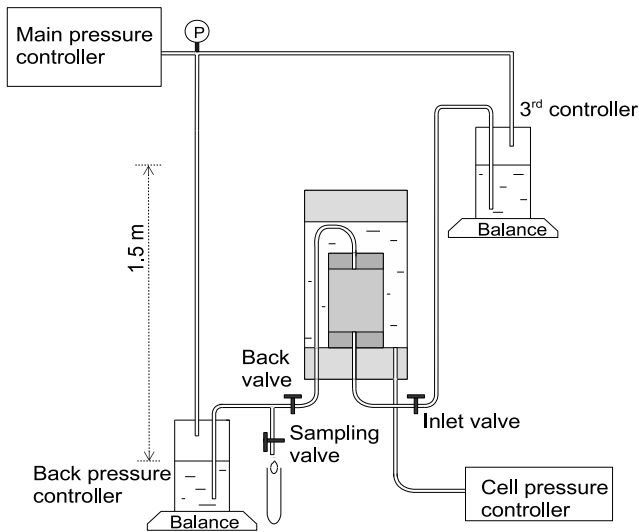


Figure 5-1. Modified triaxial test set-up used in the experiments

5.2.5. Experimental procedure

The experiments were carried out according to the following procedure:

(1) Sample preparation

Sand columns were prepared using a split mould with the rubber membrane mounted inside (inner diameter 65 mm, height 130 mm). A 250 mL suspension was prepared containing the substrates together with 40 mL/L inoculum with the suspended bacteria. The suspension and the sand were poured into the mould in turns so that the sand level was always below the liquid level in order to avoid air entrapment. When the mould was nearly full, small amounts of liquid and sand were added until they filled up slightly above the top of the mould. The top part of the mould was slightly tamped to densify the excess sand and then, the top surface was flattened in order to close the sample with a porous stone and the top cap. The resulting dry density of the samples was 1.48 ± 0.01 g/cm³, the porosity 0.44 ± 0.003 and the pore volume of the sample was approximately 0.2 L.

(2) Saturation and consolidation

The outer cell of the triaxial set-up was installed and filled with water. The sample was pressurized to 200 kPa cell pressure – 100 kPa pore pressure using the procedure described in CEN (2004) ISO/TS 17892-9:2004. Then the back valve was opened for consolidation. Demineralized de-aired water was used in the back pressure controller.

(3) Reaction phase

During the reaction phase, the back valve was opened in order to collect any expelled fluid in the back pressure controller. The amount of water expelled from the sample to the controller was continuously registered using a balance. The volume of expelled liquid during the reaction phase is assumed to be equal to the volume of gas formed inside the sample. Subsequently, the change in saturation was calculated assuming the porosity remained constant throughout the test and the sample was initially fully saturated with water.

(4) Flushing

At the end of a reaction phase, the inlet controller was connected to the bottom line of the sample. This controller contained the new substrate solution, so when the inlet and back valves were opened, the sand column was flushed with fresh substrate from bottom to top with a 1.5m water head gradient across the sample. In the experiment under the low concentration regime the sample clogged during the 10th flush which was removed by temporarily increasing the hydraulic gradient across the sample to 2.5 m by lowering the back pressure. Residual liquid in the sample was flushed to the back pressure controller and replaced by the fresh substrate solution. When the pore volume of the sample was completely replaced by the fresh solution, the inlet controller was disconnected by closing the inlet valve and the sample was left standing for the new reaction phase. The difference between injected and expelled liquid volumes was used to calculate the change in saturation. The pore pressure coefficient (or B-factor), which is the ratio of the change in pore pressure over the change in cell pressure and which is related to the degree of water saturation of the sample (Skempton, 1954), was determined before and after flushing. The mass changes in the controllers measured by the balances were used to interpret the inflow and outflow rates. The inflow rate at the start and end of a flushing phase were used to determine the hydraulic conductivity at the constant hydraulic head.

The electrical conductivity (EC) of the effluent was monitored as an indicator for substrate conversion. During flushing, samples of the outflow were taken at regular time intervals for manual determination of EC and ion concentration. When taking the samples, the inlet and back valves were closed to temporarily stop flushing, the sampling valve was opened to let the first 1 mL liquid run through and collect the next 3 ml for sampling. After this the sampling valve was closed and the other two valves were reopened to continue flushing. Flushing continued until the EC of the outflow reached the value of the fresh substrate solution. EC was measured using a SK10B electrode (Consort) and recorded using a C3010 data logger (Consort). Nitrate, nitrite, calcium concentrations were determined using a spectrophotometer (Lasa 100, Hach Lange) with standard test kits LCK339, LCK341 and LCK327 respectively). Acetate was determined using organic acid test kit LCK365, as it was the only soluble source of organic carbon present in the samples.

In order to reach 1 w% precipitated CaCO₃ in the sand, 3 times of substrate supply were required for the high concentration. The first supply was together with the inoculum when preparing the sample in the mould. From the second supply onward, fresh substrate was flushed through the sample. After flushing two times with fresh substrates, it was flushed the last time with de-aired de-mineralized water. The same approach was applied for the low concentration regime except that the pore volume was flushed 14 times and then rinsed with de-aired de-mineralized water.

(5) *Shearing*

After rinsing the columns as described above, the samples were sheared in compression under a constant confining pressure and drained conditions at a loading speed of 0.5 mm/s.

(6) *Post-treatment analysis*

After shearing, the sample was removed from the set-up, cut into 6 slices, which were dried overnight at 105°C. After drying, the dried sand lumps were collected for micro-CT scanning and ESEM analysis (Philips ESEM XL30). The CaCO₃ content was measured using a larger but similar set-up to that of Whiffin et al. (2007). From each slice about 100 gr of the dried sample was placed in a closed bottle to which 60 mL of a 100 g/kg hydrogen chloride (HCl) solution was added, allowing the CaCO₃ to dissolve. The produced CO₂ was collected into an inverted 250 mL graduated cylinder placed in a water bath. When the reaction of CaCO₃ and HCl was finished, the cylinder height was adjusted to bring the gas pressure inside the cylinder back to ambient condition. The difference in gas volume inside the cylinder before and after the experiment corresponds to the volume of the produced CO₂, V_{CO₂} [mL]. The set-up was calibrated using known amounts of CaCO₃.

5.3. Results

5.3.1. *Substrate consumption of the stock inoculum in liquid batch*

It took 7 days for all nitrate to be consumed from an incubation of 15 mL stock inoculum in 380 mL of a suspension containing 26mM Ca(NO₃)₂ - 36mM Ca(C₂H₃O₂)₂ (corresponding inoculum concentration of 40 mL/L) (Figure 5-2). The NO₂⁻ concentration was below the detection level of 0.016 mM throughout this period. After all NO₃⁻ was consumed the residual acetate and calcium levels were around 40% of the initial values. A consumption of 42 mM of acetate required 52 mM nitrate consumption, consequently the ratio between consumed acetate over nitrate was 0.8, similar to the ratio observed by Pham et al. (2016b). The substrate consumption rate was 7.5 mM/day for nitrate and 6.0 mM/day for acetate.

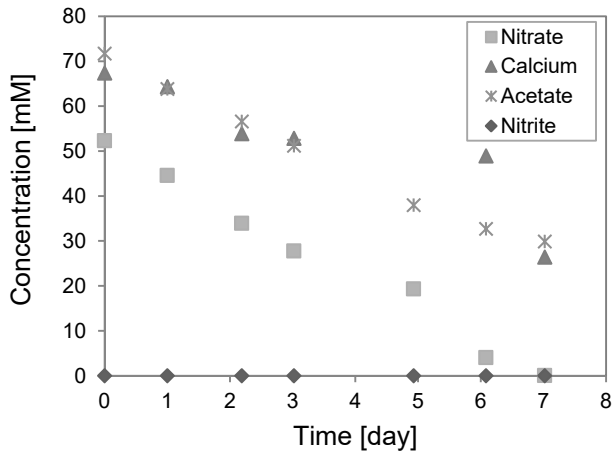


Figure 5-2. Substrate consumptions of the stock inoculum in

5.3.2. *Water saturation changes and permeability reduction of the sand samples in the triaxial tests*

Gas production in the set-up resulted in a reduction of water saturation up to 75-80% of the pore volume in both the regimes for each reaction phase (Figure 3). During the flushing with fresh substrate, it was not possible to remove all gas from pore space, the remaining gas phase stayed in the range of 10-15% after flushing (water saturation ranged from 85 to 90%). The unsaturated condition was also reflected in the B-factor, which was below 10% throughout the experiments.

Gas production and the stability of the produced gas phase in the pore space had significant impact on the hydraulic conductivity of the sand. However, a difference was observed between the two regimes. In the high concentration regime, gas production during the first period resulted in a reduction of more than two thirds of hydraulic conductivity, half of which was regained after flushing, similar results were found for the subsequent flushes. In the low concentration regime, hydraulic conductivity was also partly regained after each flush, but the subsequent treatments gradually led to clogging. At the 10th flush the hydraulic conductivity had reduced by a factor of 200 compared to the initial conductivity. The resulting increase in water head from 1.5 m to 2.5 m in the 11th and 13th (and the last flush to rinse the liquid through the sample) interrupted the flow to the back pressure controller. Therefore monitoring the water balance was stopped from the 11th flush and the water saturation was not further calculated (expelled liquid during the resident periods were still continuously monitored). The final value of the hydraulic conductivity of the treated sand in this regime was 5.8 cm/d, which was 15 times lower than the initial value.

5. Evaluating strategies to improve process efficiency of denitrification based MICP

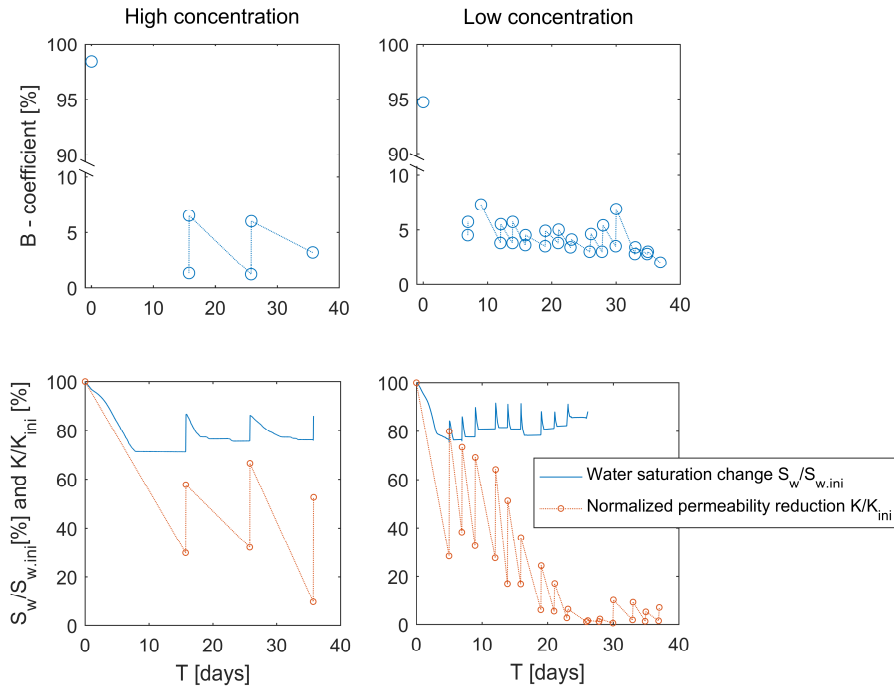


Figure 5-3. B-coefficient variation (top row), and changes of water saturation during the treatment periods and the effective pore area at the end of each treatments (bottom row)

5.3.3. Flow rates during flushing after each treatments

Flow rates during flushing for the high and low concentration regime are presented in Figure 5-5 and Figure 5-4, respectively. All the profiles show that the inflow started slowly, and outflow did not appear at the beginning of most of the flushes, but only occurred several seconds to minutes after the start of the flush. After this lag phase the outflow rates increased to a level comparable with the inflow. In this period, treatments with the low concentration regime resulted in steady flows while the flow rate in the treatments with the high concentration regime appeared to be irregular. Finally, for the high concentration regime the final flow rate did not seem to be significantly affected, while for the low concentration regime the maximum flow rate during flushing gradually decreased resulting in the decrease in hydraulic conductivity (as shown in Figure 5-3)

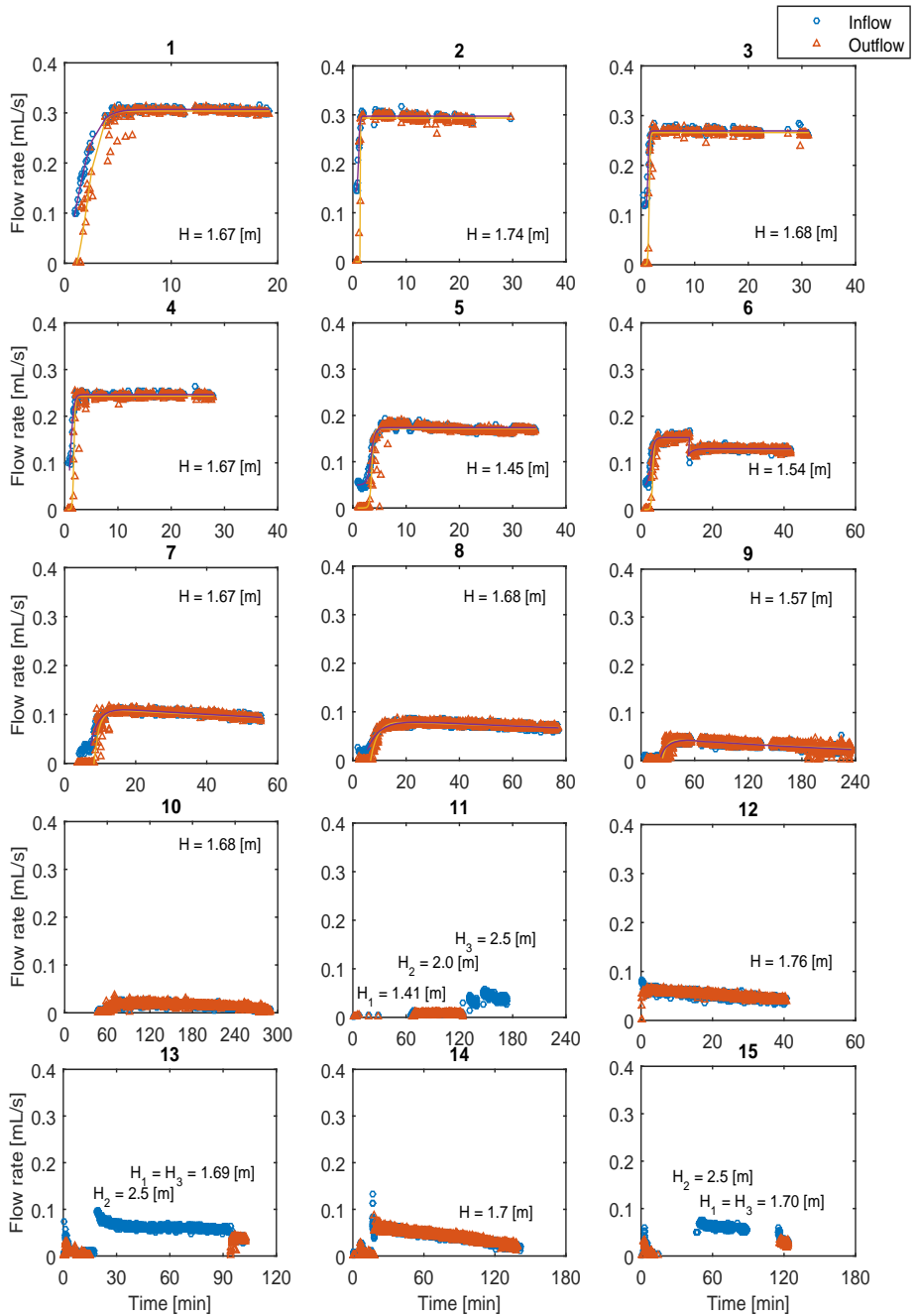


Figure 5-4. Flow rates after each treatments in low concentration regime

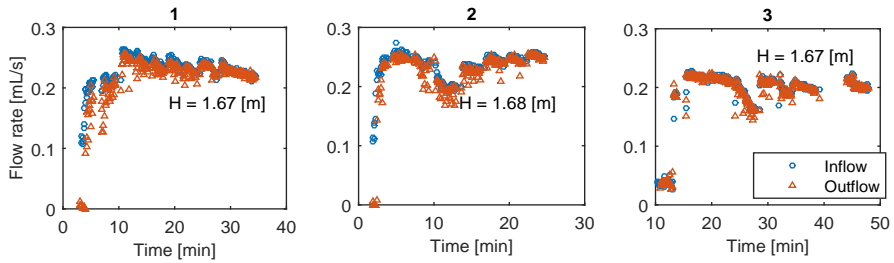


Figure 5-5. Flow rates during flushing after each treatment in high concentration regime

5.3.4. Substrate consumption and production rate in the sand columns throughout the treatments

There was a clear difference in the substrate consumption efficiency between the two regimes, as presented in Figure 5-6. In the high concentration regime, all acetate and most of the nitrate was consumed with small amounts of nitrite (<2 mM) remaining in the first reaction phase, but this conversion efficiency was absent in the subsequent reaction phases, resulting in significant amounts of residual solute substances in the set-up and in the expelled liquid. In the second batch almost 70% of nitrate was consumed, but about half of that was not fully converted to dinitrogen gas and remained in the liquid as nitrite. The conversion in third batch showed an even lower conversion as only about 40% of nitrate was consumed and the major part remained as nitrite in solution. The low conversion efficiency was visible not only through substrate conversion, but also in the ratio consumed acetate over nitrate ratio A/N, which reduced from the range that favours growth to the range where maintenance is dominant over growth (0.5 ± 0.05). At the end of the experiment, the average consumed acetate was around 15%, and the consumed nitrate NO_3^- was about 40% of the injected concentrations, but a large fraction of it remained as the nitrite (about 50% and above).

The substrate consumption efficiency in the low concentration regime was retained throughout the experiment. With the initial supplied concentration of 20 mM (5 mmol of nitrate in correspondence with the sample size), the remaining nitrate levels after 2 days were insignificant, and there was no detectable nitrite accumulation. The acetate to nitrate ratio shifted slightly from 0.8-0.9 to 1.1-1.3, approaching a ratio that corresponds to the theoretical stoichiometry of maximum growth.

Using the measured substrate consumption ratios and amounts of left over nitrite, the corresponding stoichiometry of the denitrification reaction can be calculated using the thermodynamic approach described by (Heijnen and Kleerebezem 2010), assuming that nitrite is the only accumulating intermediate. Assuming the expelled volume of liquid during the reaction phase resulting in the water saturation reduction shown in Figure 5-3 is equal to the volume of produced

nitrogen gas, the gas production rate can be calculated from the flow rate at which the liquid is expelled during the reaction phase using the ideal gas law. Accordingly, by deriving the stoichiometric coefficients from the observed substrate consumption ratio, the nitrate consumption and total dissolved inorganic carbon production can be calculated from the nitrogen gas production. Once the gas content in the samples reaches its threshold and the gas production could not be monitored anymore, it is assumed that the nitrate consumption continues at a rate which is linearly extrapolated until the remaining nitrate concentrations reach zero. The results of calculated nitrate consumption and cumulative DIC production are presented in Figure 5-7. This extrapolation suggests that substrate conversions in the low concentration regime were all completed before newly substrates were supplied.

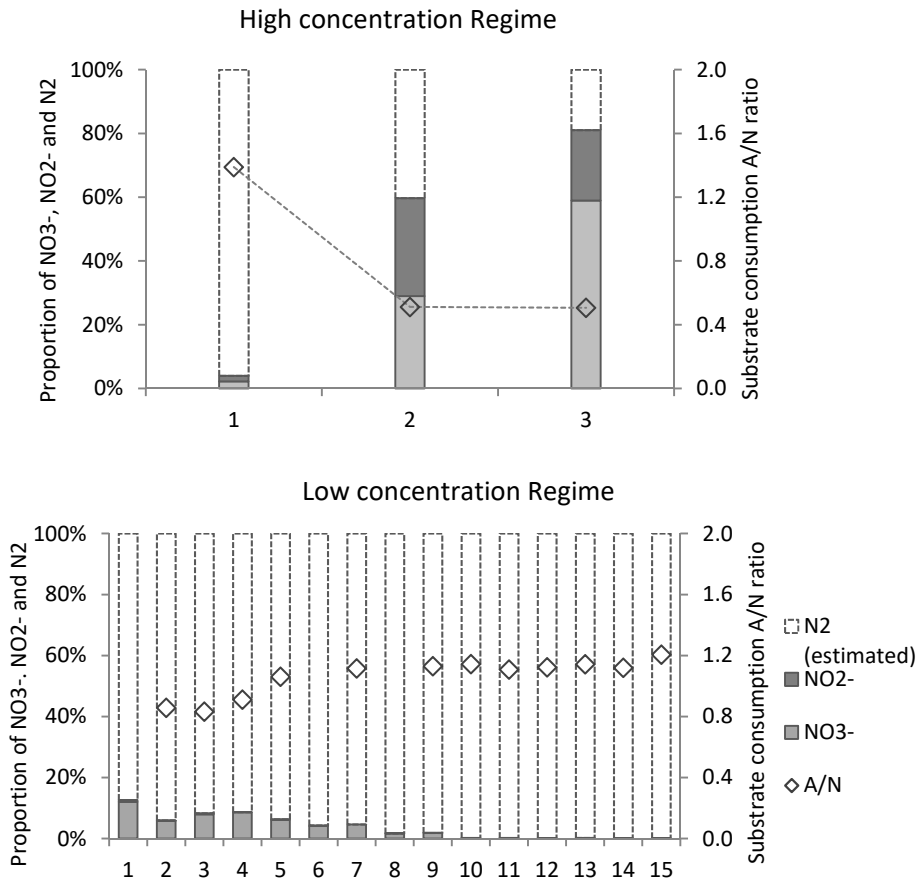


Figure 5-6. Nitrogen components and substrate consumption ratio after each treatments

5. Evaluating strategies to improve process efficiency of denitrification based MICP

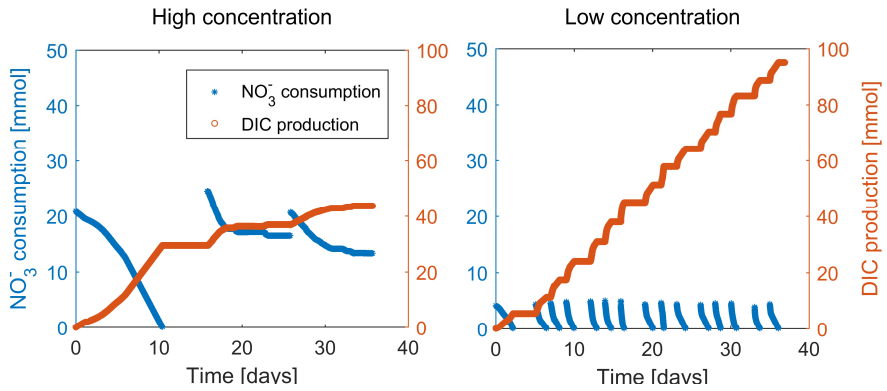


Figure 5-7. Calculated NO_3^- consumption and DIC production from measured stoichiometric coefficients

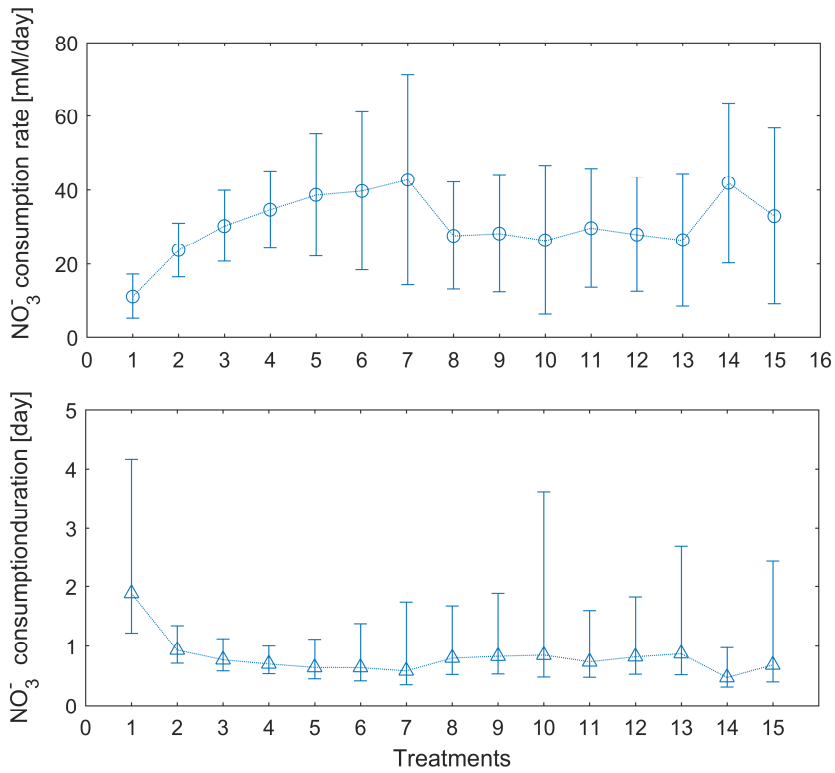


Figure 5-8. Substrate consumption durations of the treatments in the low concentration regime

The average NO_3^- consumption rates in a 1 hour time interval and its standard deviation were calculated for each treatment period (the extrapolated values are not included). From this calculated consumption rate, the consumption duration, which is the time that the reactions take place in the period after flushing, are calculated by dividing the supplied nitrate by the average consumption rate. The upper boundary was calculated with the lowest NO_3^- rate which corresponds with the measured rate when the gas production approached the gas content threshold, and lower boundary was calculated with fastest NO_3^- possible rates corresponding with the measured rates in the beginning of the resident period. These results are presented in Figure 5-8. This analysis shows that NO_3^- consumption rates gradually increased in the first 7 treatments, reaching the average value of 42.7mM/day corresponding with an average CaCO_3 precipitation rate of 0.17 w%/day. The fastest gas production rate was recorded in also the 7th treatment, and it corresponds with the maximum nitrate conversion rate of 65 mM/day and a precipitation rate of 0.26 w%/day.

5.3.5. Amount of precipitated CaCO_3

The total amount of precipitated calcium carbonate was estimated to be 30.0 mmol for the high concentration regime, and 71.5 mmol for the low concentration regime using the calcium measurements before and after each flush. In this calculation we assume mass conservation for calcium. The post treatment analysis using 10% hydrogen chloride solution, presented in Figure 5-9, showed that the average CaCO_3 content for the high concentration regime was about 0.28 w%, which is 19.4 mmol CaCO_3 . The distribution along the column did not show a clear trend. For the low concentration regime, the measured CaCO_3 content showed an uneven distribution along the column, ranging from 0.77 w% close to the inlet at the bottom to 0.53 w% top close to the outlet at the top of the column. The average value was about 0.65 w% which is 44.1 mmol CaCO_3 . The difference between calculated and measured CaCO_3 content may be due to some precipitation in other parts of the set-up (tubing, pressure controllers). Considering the target of 1w% precipitated CaCO_3 in the sand, the low concentration regime has better results than the high concentration regime.

The difference in the amount of precipitated CaCO_3 between the two regimes was also seen in the dried sand lumps of the experiments. Figure 5-10 presents the lumps taken from the dried slices of the sand columns in the sequence of slices from top (left of the figure) to bottom (right of the figure). The high concentration regime resulted in small lumps with maximum diameter of about 1 cm. The lumps were very loose and the sand particles easily fell out of the lumps by very slight handling pressure. The low concentration regime resulted in significantly larger and more stable lumps, whose average diameter was about 2 cm.

5. Evaluating strategies to improve process efficiency of denitrification based MICP

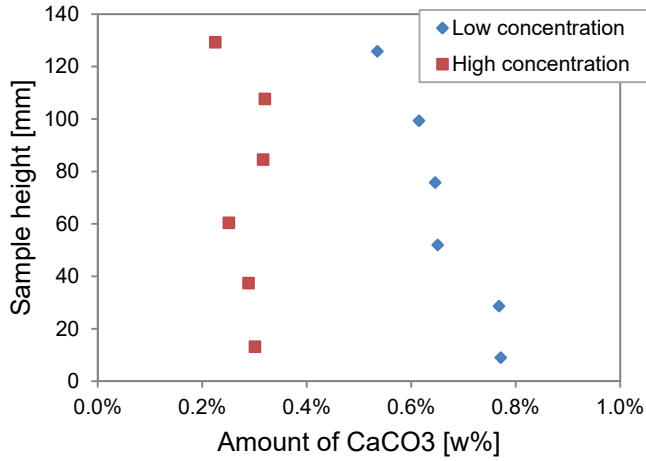


Figure 5-9. Amount of CaCO₃ w% along the sand sample



Figure 5-10. Dried cemented sand - (upper) after the treatment with high concentration; (lower) after the treatment with low concentration.

5.3.6. Soil behaviour under monotonic loading

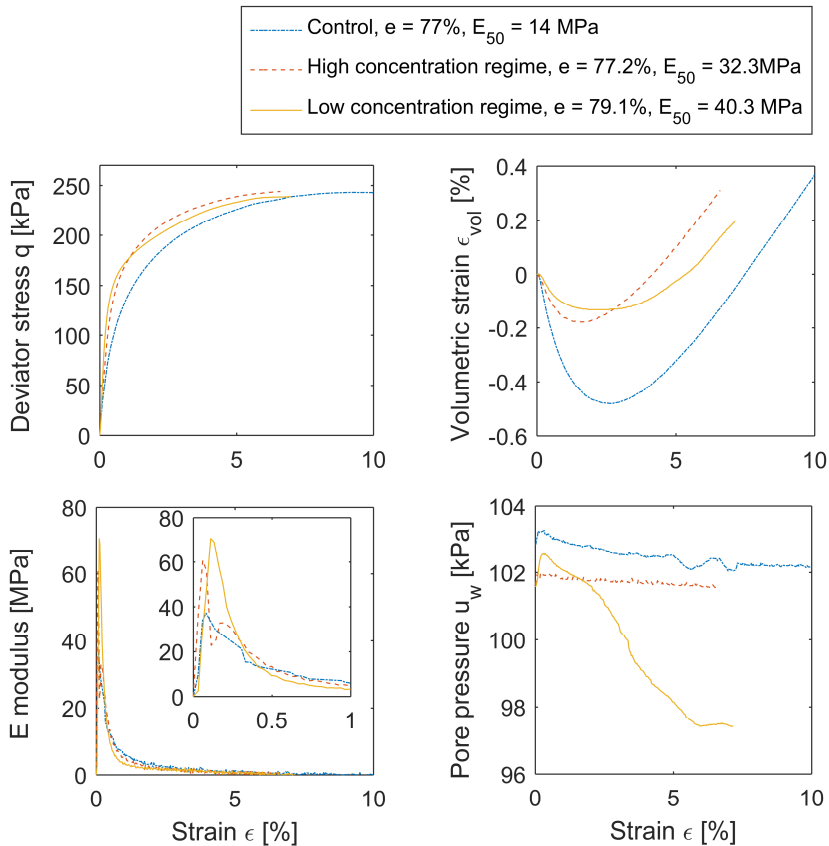


Figure 5-11. Shearing results

Results of the drained triaxial compression tests are shown in Figure 5-11. The treatment did not significantly increase the peak shear strength, but a clear increase was observed in small strain stiffness. The initial tangent modulus E of the treated sand in both the regimes was more than doubled compared to the non-treated control column. Impact of the gas phase was observed in the volumetric strain profile, (ϵ_{vol}), as the gas phase dampened the volumetric strain measured by the pore liquid changes of the samples. In the low concentration regime, the pore pressure profile dropped by several kPa as soon as the sample started to dilate, which may be the result of the reduced hydraulic conductivity preventing water from filling up the dilating pore space.

5.3.7. ESEM images of a sand lump

ESEM analysis on a dried lump of sand from the third slice of the low concentration regime showed that a relatively low amount of large calcium carbonate crystals (up to 150 μm in diameter) was formed between the sand particles. Calcium carbonate crystals could be distinguished from sand particles by 1) the lighter grey value indicating a slightly higher particle density, 2) their position between the other grains, being grown around the existing sand grains and 3) their rougher surface texture, probably indicating these crystals are calcite which is grown in multiple phases. EDX analysis on the crystals confirmed their main components to be calcium, carbon and oxygen. XRD analysis should be performed to confirm the crystals are indeed calcite.

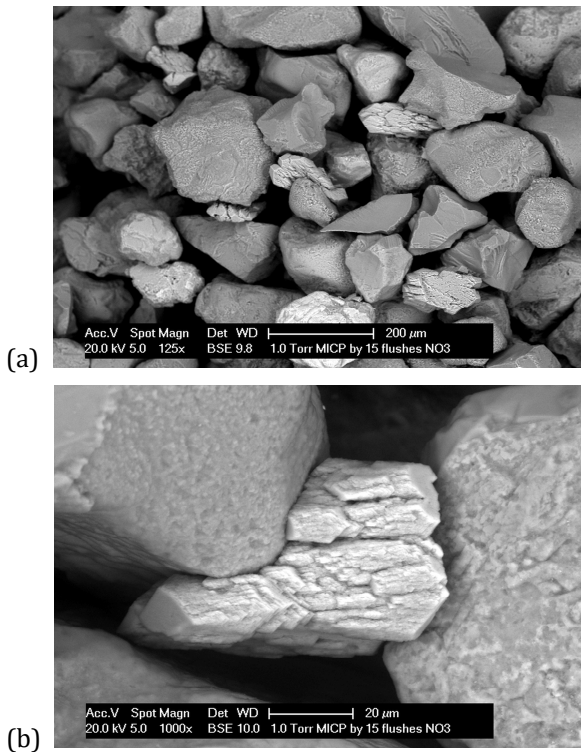


Figure 5-12. ESEM image of a lump from Regime 2 of low substrate concentrations. CaCO_3 precipitation happened discretely resulting in large few crystals.

5.4. Discussion

5.4.1. Effect of initial concentrations on the conversion rate and yield

The experiments clearly show an effect of substrate concentration on the substrate consumption ratio and the overall conversion rate and efficiency. Although the two tested regimes started with the same inoculum of bacteria and the same ratio of the supplied substrates, which was meant to stimulate microbial growth, the

substrate consumption in the different concentration regimes was completely different.

Microbial growth was successfully stimulated in the low substrate concentration regime, which resulted in a high conversion rate and efficiency. With average conversion rates of up to 40 mM/day, the nitrate consumption rate was significantly higher than the 7.5 mM nitrate per day observed in the liquid batch incubation. Within 4 treatments, the consumed substrate ratio (A/N) shifted from 0.8 for the liquid batch incubation towards 1.2, which is close to the stoichiometry related to maximum growth. Another possible indication of active microbial growth was the significant reduction in hydraulic conductivity. Both regimes showed similar values of gas saturation ranging from 20-25% after the reaction phase to 10-15% after a flushing phase, which showed that part of the reduction in hydraulic conductivity was reversible. The gradually increasing irreversible reduction in hydraulic conductivity during the low concentration regime which eventually resulted in clogging indicates that there must have been another material to fill the pores in addition to the induced gas phase. Microbial growth has been widely reported to significantly influence hydrodynamics of porous media, and can reduce sand permeability by up to three orders of magnitude (Thullner et al., 2002, Gerlach and Cunningham, 2010, Baveye et al., 1998). Considering the permeability reduction of the sand in the low concentration regime, biomass growth and accumulation can contribute to the irreversible part of the reduced hydraulic conductivity, besides the possibility that less gas to be produced in the low concentration regime could result in smaller and homogeneously distributed bubbles leading to a higher blocking effect on the water flow.

The high levels of nitrite, low A/N ratio, limited conversion rates and efficiency observed in the high concentration regime are indications of strong inhibition or toxicity and consequently, lack of biomass growth. In this case, the gas phase is hypothesized to be unstable because there was no grown biomass to support its stability, which resulted in a nearly completely reversible reduction in hydraulic conductivity. The difference in the end results of the two regimes confirms that a high substrate concentration is strongly related to loss of microbial activity, nitrite accumulation and inhibition. This relation has been observed in other studies (Almeida et al., 1995, Sijbesma et al., 1996, Glass and Silverstein, 1998, Dhamole et al., 2007). The nitrite reduction rate can initially be slower than the rate of nitrate reduction (Almeida et al., 1995), therefore when the microbial activity is not sufficient, a high dose of nitrate may cause nitrite to accumulate to an amount that in turn inhibits both cell growth and activity. Wang et al. (1995) showed with their experiments that after an initial proportional correlation up to 0.6 mM NO_3^- , the net specific growth rates of a pure denitrifying culture decrease with increasing nitrate concentration. In the high concentration experiment of this current study, the negative effect of high substrate concentration was not evident in the first batch reaction period. However, for the subsequent second and third

batch the bacteria in the high concentration regime had higher stress than those in the low concentration regime. Another reason for the observed inhibition in the second flush and third flush could be the long waiting time between first and second batch. Complete consumption in the first batch caused a longer lag phase with low microbial activity, which according to Pirt (1975) can also be the cause of nitrite accumulation and loss of microbial activity when the bacteria were suddenly exposed to a high nitrate concentration.

Minimizing the length of the lag phase and its consequences can be achieved by matching the hydraulic residence time to the substrate concentration and microbial activity. Another way to avoid a lag phase is by continuous supply of fresh substrates, as illustrated by the experiments of (Paassen et al., 2010). They continuously flushed a 2 m sand column with a recycled solution initially containing 100 mM calcium acetate and 120 mM calcium nitrate and found that all substrates were consumed within 10 days, which corresponds to nitrate consumption rate of 24 mM/day, without any detectable accumulation of nitrite. Besides, using an enriched inoculum with a high concentration of bacteria is also useful to increase its ability dealing with the stress of the lag phase (Pirt, 1975) and therefore to limit nitrite accumulation. Erşan et al. (2015) also found that in the case of complete nitrate consumption, the measured nitrite concentration was inversely proportional to the cell concentration. They also found that less leftover nitrite corresponds with the increase of CaCO₃ precipitation rate when the cell concentration was increased.

5.4.2. Effect of other process conditions on conversion rate and yield

The presence of calcium has an important impact on the metabolism of denitrifying organisms. Calcium carbonate precipitation is not only the chemical consequence of an alkalinity producing bacterial metabolism in presence of sufficient dissolved calcium, but it also provides a positive feedback on the metabolism. In the absence of precipitation, denitrification can cause the pH to increase to the upper limit of microbial denitrification, at which permanent nitrite accumulation occurs. Carbonate precipitation buffers the pH slightly below neutral and limits nitrite accumulation (Pham et al., 2016b). Carbonate precipitation in the micro-environment of the bacterial cell could facilitate the cellular proton fluxes through the cell membrane and chemically favor the bacterial metabolism (Hammes and Verstraete, 2002), similarly to root calcification of plants (McConnaughey and Whelan, 1997). The interaction between carbonate precipitation and a robust microbial metabolism is also apparent in this current study. Although there was no analysis to verify the environmental conditions at micro-scale, results of complete substrate uptake, higher CaCO₃ precipitation yield and indication of high cell concentration in the low concentration regime suggest precipitation in itself can boost the overall performance through the positive feedback mechanism.

When comparing the liquid batch incubations with the sand column experiments, it shows that when the metabolism takes place in the sand, higher conversion rates and different substrate consumption ratios can be obtained. The positive effect on the performance of the denitrifying organisms is particularly evident for the low concentration regime, where average nitrate consumption rate of 42 mM and maximum values of 65 mM/day (as compared to 7.5 mM/day for the liquid batch incubation) and substrate consumption ratios corresponding to conditions of maximum growth were observed. Whether this is due to the applied substrate ratio or concentration, difference in anaerobic conditions or due to availability of granular surface which may create favorable micro-environments for the denitrifying organisms to grow or allow formation of biofilms as suggested by Van Paassen et al (2010), cannot be concluded from these experiments.

The production of nitrogen gas also has an impact on the conversion. When pores are filled with nitrogen gas, liquid is expelled and the amount of available substrates is reduced. This may not affect the conversion rate, but will influence the yield per volume of treated sand as observed by Pham et al. (2016b), in which the parts of the columns which showed a higher gas saturation contained a lower calcium carbonate content. As the amount of produced gas is proportional to the consumed substrate, supplying high substrate concentrations in batch mode could cause the gas production to exceed its percolation threshold and lead to completely gas-filled zones or channels, disturbing homogeneous substrate supply.

Finally, the presence of other oxidizing agents, such as oxygen, ferric iron or sulfate, may also affect the denitrifying metabolism. For example, when substrates are supplied to the sand by surface percolation, the air or oxygen present in the unsaturated zone may inhibit the denitrifying microbial activity or allow aerobic micro-organisms to compete with denitrifying organisms for the available carbon source. The inhibiting effect of oxygen on the denitrification metabolism is well known (Ferguson, 1994), and may be an alternative explanation for the loss in microbial activity during the second and third flush of the high concentration regime. During the first flush, the A/N ratio of the supplied substrates was 1.5, which is higher than the theoretical maximum A/N ratio corresponding to the stoichiometry for the denitrification metabolism at maximum growth. Still all acetate appeared to be consumed when analyzing the expelled and flushed out liquid. Besides potential measuring inaccuracies, the high acetate consumption may either indicate diffusion of substrates across the membrane or it may indicate the presence of an alternative electron acceptor, which could be dissolved oxygen in the cell water or pressure controllers. Verifying these suggested explanations requires additional research, in which potential adjustments to the triaxial set-up need to be considered, such as the type of water used in the cell and the controllers or the diffusivity of the membrane.

5.4.3. *Gas production and its stability in the sand*

From the water saturation profiles of the treated sand columns, the produced gas created a gas saturation of about 20-30% regardless of the consumed substrate amount. This is seen most clearly in the first treatment of the two regimes where all nitrate was consumed and only a little amount of nitrite had accumulated. As the consumed nitrate at the high concentration regime was 5 times higher than that at the low concentration regime, the amount of nitrogen gas produced was also expected to be 5 times higher. However, the difference in expelled liquid volume resulting in a gas saturation of 29% and 25% for the high and low concentration regimes respectively, which was insignificant compared to the expected gas volume. The sand appeared to have a limited gas storage capacity, and excess produced gas probably had vented from the sample to the back pressure controller. Similarly, transportation of excess nitrogen gas was also experimentally captured by Istok et al. (2007), who could obtain also only 23% gas saturation, which was significantly less than predicted based on their supplied amount of substrates. This discrepancy confirms that – under the conditions tested – the volume of produced gas was higher than the measure amount of gas in the sample and excess gas had vented from the system. In order to leave the sample the gas first needs to reach its percolation threshold and force an exit. Individual bubbles or isolated zones of gas either need to connect and form continuous gas-filled channels or the pressure in these isolated gas zones needs to exceed the air entry pressure of the narrow pore throats they need to squeeze through in order to migrate upward. A similar process is required in order to allow the gas to flow through the tubing towards the back pressure controller.

The cyclic process of a decrease in water saturation by gas production followed by an increase in saturation by flushing shows a similar behavior as seen during drying and wetting cycles in soils. As described by Fredlund et al. (2012), this process results in hysteresis of both the water content and hydraulic conductivity, which is attributed to the entrapped air that stays after the first drying-wetting cycle. For the tested soil of this study, the permanently entrapped air was about 10-15% of the pore volume in both the substrate regimes. Nevertheless, the flow rate patterns of the two regimes (Figure 4 and 5) were significantly different inferring a difference in the stability of this entrapped gas. The steady flow rates for the low concentration regime indicate that after flushing distribution of the residual gas was not significantly influenced. The entrapped air of this regime is therefore considered to be significantly more persistent under the tested hydraulic flow, possibly due to a more homogeneous distribution throughout the pore space. In contrast, the irregular flows in the high concentration regime indicate regular venting of gas to the back pressure controller implying that the gas could be less stable and was redistributed by flushing. The significant difference in the amount of gas produced between the two

regimes during the first treatment contributed to the different connectivity and persistence of the trapped gas.

The persistence of the trapped gas in the low concentration regime was also reflected by the pore pressure response during undrained loading and can be partly attributed to the formation of biofilms and microbial aggregations (Guelon et al., 2011). Whereas the presence of biomass in the pore space increases the resistance for both hydraulic and gas transport, the gas which is entrapped by the biomass is more stable and will lower the hydraulic conductivity even further.

5.4.4. *Impact of the reaction products on the sand*

The amount of precipitated CaCO_3 obtained during both the regimes were not sufficient to significantly increase the peak strength under monotonic drained compressive loading. Nevertheless, the small amount of precipitated CaCO_3 did help to increase the soil stiffness and dilatancy, particularly at small strain corresponding with a significant increase in tangent Young's modulus which agrees with other results of MICP treatment on sandy soils (Feng and Montoya, 2016, Lin et al., 2016), The limited response may be related to the size and distribution of the calcite crystals. As shown in the ESEM analysis, the low concentration regime resulted in large but isolated crystals, loosely fitting between some but not all particle contacts. It seems such crystals do not provide significant cohesive strength to the sand, but do increase dilatancy, corresponding to observations by Van Paassen et al. (2012) or O'Donnell (2016). Still, after drying the lumps of the treated sand from the low concentration regime showed significant cohesive strength when compared with the lumps of high concentrated regime. Part of the cohesive strength of the dried sample may be attributed to the biomass, as dried biofilms could bear some strength (Guelon et al., 2011).

The role of the induced gas phase is clearly seen in the dampening effect on volumetric strain of the samples from both the regimes (Figure 5-11). This behavior can be compared with the effect of reducing the pore pressure build up under undrained monotonic loading by the induced gas phase (He and Chu, 2014). In the pore pressure profile, the result of sand column in the low concentration regime showed a pressure decrease by 4 kPa under drained shearing. This drop is believed to be related to the decreased hydraulic conductivity caused by the residual induced gas phase and the biomass aggregation. With the support of overgrown biomass and microorganisms, the gas phase in the low concentration regime was able to stay in the pores while shearing, preventing water movement and generating such pore pressure response.

Overall, all the reaction products, which are solid CaCO_3 minerals, gas phase and biofilms, can clearly alter the geotechnical engineering behaviour of the sand. The challenge is to optimize the ratio between the different products toward the desired behaviour and to scale up the results from sample scale.

5.4.5. *Implications for practical application of denitrification-based MICP*

The presented results show that it is possible to optimize substrate concentration and acetate to nitrate ratio in order to stimulate microbial growth and improve the conversion rate and efficiency which results in increased cell concentration and microbial activity. However, favoring microbial growth can lead to clogging before the target amount of calcium carbonate is reached. This would require extra effort to force the liquid into the clogged areas. Clogging can be prevented by limiting microbial growth by controlling the overall substrate supply. If a large amount of CaCO_3 precipitation is the target, then the design needs to take into account the risk of clogging through microbial growth. First the aim should be to stimulate the microbial growth until cell concentration and activity are sufficient. Subsequently, the aim should be to limit a further growth of the microbial population by changing the substrate concentration and acetate to nitrate ratio so that the system moves from one favoring growth towards one based on maintenance of the existing population only. This can be done by either increasing the nitrate concentration or lowering the acetate concentration, or increasing both the substrate concentrations ensuring that the A/N ratio is less than 1.2 to increase the precipitation yield. The end results of the high concentration regime also showed that inhibition and nitrite accumulation can occur when the acetate to nitrate ratio is applied at the stoichiometry of the catabolic reaction. Therefore the optimized A/N ratio for CaCO_3 precipitation should be between the ratio of maximum growth and pure maintenance, which are 1.2 and 0.6 respectively. Results of the batch liquid incubation and sand column experiments at the A/N ratio of 0.8 by (Paassen et al., 2010) and (Pham et al., 2016b) showed that at this ratio it is also possible to maintain a robust metabolism with complete substrate consumption and limited accumulation of nitrite.

The observed precipitation rates for the low concentration regime are high compared with other reported rates in literature (Paassen et al., 2010, Kavazanjian et al., 2015). The low concentration regime achieved the result of 0.65 w% in 5 weeks of treatments. However, all substrates were completely consumed during each step and based on rate of expelled volume of liquid and, within the reaction period, fastest precipitation rates up to 0.26w% per day were observed. These high rates would improve the applicability of the process for soil reinforcement purposes.

Differences between the end results of the two regimes showed that stimulating microbial activity and minimizing the lag phase in the beginning of experiments is important for process performance, and as a result precipitation rate could therefore be improved. Supplying the substrates at low concentrations dosages showed to be effective for this target but it means more frequent flushing and increases the clogging potential. Consequently, it requires more work for contractors in the field. A high precipitation yield can practically be achieved with

high dosage of substrate supply only after a phase in which microbial growth is stimulated using dosage of substrate at low concentrations.

An additional benefit of the method is the induced gas-phase and biofilm aggregation to alter the geotechnical properties of sand. This study and others (Montoya and DeJong, 2015, Lin et al., 2016) show that around 1.0 w% of precipitated CaCO_3 supported by stably induced gas phase and biofilm can be sufficient for soil stabilization, particularly in situations that do not require high peak strength, e.g. road or slope construction. Using the induced partially saturated state for liquefaction mitigation was demonstrated to be feasible, (He and Chu, 2014, He et al., 2013, Kavazanjian et al., 2015), and this desaturation state is proved to be stable under a 1,5 m hydraulic gradient when it has the support from precipitate CaCO_3 and biomass aggregation. Persistence of biomass leading to clogging (Kim and Fogler, 2000, Castegnier et al., 2006) is a drawback of the method which limits supply of substrates for precipitation, but on the other hand it could be a potential approach to create waste containment or seepage barriers (James et al., 2000) or mitigate issues of piping and leakage in an aquifer (Mitchell and Santamarina, 2005, Ivanov and Chu, 2008, Dejong et al., 2013). The possibility for selectively forming one of the three reactions products (CaCO_3 , N_2 gas and biomass) by applying a suitable substrate supply regime allows tailoring of the method to specific geotechnical applications. This option is a unique advantage of this method compared to many other traditional geotechnical applications.

5.5. Conclusion

In this study, different strategies for applying denitrification to stimulate the precipitation of calcium carbonate to improve the mechanical properties of sand have been evaluated. Selecting the appropriate substrate concentrations, inoculum and environmental conditions are important to obtain fast reactions, high yield and efficient use of resources. Appropriate choices make it possible to avoid accumulation of inhibiting intermediate products and to achieve the optimum final mechanical properties. Application of low substrate concentrations results in higher calcium carbonate content and higher cohesive strength. The tests showed that at high substrate concentrations, intermediate nitrogen compounds can accumulate, causing inhibition and reducing the microbial activity. Providing an inoculum of denitrifying bacteria (bio-augmentation) helps to kick-off microbial activity at the start of experiments, to obtain a high initial conversion rate and minimize risks of inhibition during the process.

The obtained maximum precipitation rates of 0.26 w%/day in this study may already be sufficient for practical ground improvement applications of denitrification based MICP. The results of drained monotonic loading showed a significant increase in small strain stiffness at the obtained calcium carbonate contents of 0.28% and 0.65%. Besides the strengthening effect from the precipitation, the produced nitrogen gas may also prove useful. Considering a

5. Evaluating strategies to improve process efficiency of denitrification based MICP

significant fraction of gas appeared to be stable throughout the experiments, it may mitigate liquefaction by damping pore pressure build up during undrained loading. Excessive biomass growth can cause clogging and may limit the substrate supply but it also has potential to be employed for applications as it has shown to enhance the stability of the gas phase and provide cohesive strength under dried conditions. All the reaction products interact in changing the soil properties and can support or counteract each other in applications.

6.

Model of two-step denitrification-based MICP

Denitrification has been demonstrated to be feasible for ground improvement applications with negligible amount of accumulated nitrite, but full control to limit the accumulation is not yet available. In this chapter, a theoretical two-step denitrification model is proposed, which studies the growth kinetic of denitrification in couple with calcium carbonate precipitation. Denitrification is considered to consist of two reduction step: nitrate to nitrite and nitrite to (di)nitrogen gas, and results of batch incubation experiments in Chapter 3 was used to validate the model. Stoichiometry of the two-step denitrification indicates that the substrate consumption ratio corresponding with no nitrite accumulation is in range of 0.9 – 1.25, and supplying carbon source in excess in an option to limit nitrite accumulation. The output of the model shows that simulation results of NO_3^- , TC and Ca^{2+} fit well with experimental data regardless the selected model approaches. However, to simulate the kinetic of NO_2^- accumulation, it is important to consider the dependence of reaction stoichiometry on metabolic state and growth rates. Not simulating the NO_2^- accumulation accurately can influence the CaCO_3 and N_2 output of the model. The theoretical calculation indicates that NO_2^- accumulation should not only be minimized to avoid toxicity issues but also to maximize CaCO_3 and nitrogen gas production. The current model structure could fit the experimental data but still with a high uncertainty, indicating that the current model structure is mechanistically not yet complete and is of interest for further investigation.

6.1. Introduction

Nitrite accumulation can occur when employing denitrification for MICP, which is seen in experimental results under high substrate ratios, low carbon to nitrogen ratio, or low amounts of active denitrifying bacteria conditions. Accumulation of nitrite should be prevented as it inhibits the denitrification reaction and may result in emission of toxic greenhouse gases N_2O and NO . In this chapter, a theoretical modelling approach is proposed to simulate the process of denitrification-based MICP, while taking the accumulation of nitrite and its associated inhibiting effect into account. In this model, denitrification is considered to consist of two reduction steps: nitrate (NO_3^-) to nitrite (NO_2^-) and nitrite to (di)nitrogen gas (N_2). Each reduction step is treated separately and consists of a catabolic and anabolic reaction. The stoichiometry of each step is determined using the bioenergetics approach suggested by Heijnen and Kleerebezem (2010). Similar to the results in chapter 2, the stoichiometry of the metabolic reaction of each reduction step in the two-step approach is expected to be dependent on the specific growth rate, ranging from maximum growth to full maintenance. However, the specific growth rates of each reduction step are considered to be two independent variables. The growth rate of the second reduction step relative to the first step, determines the stoichiometry of the overall reaction and the amount of NO_2^- accumulation. Using a fixed stoichiometry for the simulation of biological conversions, which involve growth of micro-organisms often gives reasonable results when compared with experimental investigations, particularly when the biological system under study is in steady state (Matějů et al., 1992, Kaelin et al., 2009). However, for the 2-step denitrification whereby the overall stoichiometry is determined by two independent growth rates, it is worthy to investigate whether it is necessary to apply a rate-dependent stoichiometry into the model. This issue will be examined and the model performance will be evaluated using a modelling toolbox developed by (van Turnhout et al., 2016). Using this toolbox, two approaches in which the stoichiometry is either fixed or rate-dependent will be tested. Each approach will be considered in the cases of substrate limitation with and without substrate inhibition.

6.2. Theory

6.2.1. Kinetic growth and inhibition mechanisms

Denitrification is a rate-dependent process, in which biomass concentration C_X is the driving parameter of the system defining the specific rates of substrate uptake q_S , growth μ and production q_P associated with microbial growth kinetic. When a substrate is not limited and the inhibition of the metabolism is negligible, the biomass is able to consume the substrate at a rate which is close to the maximum specific substrate uptake rate, q_S^{max} , and the substrate consumption is tightly coupled to microbial growth. Its specific growth rate at this state is also close to the maximum value μ^{max} . The total inhibition factor I , ranging from 0 to 1, is used to

cover the effect of substrate limitations and inhibitions on the microbial metabolism:

$$\begin{aligned}\mu &= \mu^{\max} \cdot I \\ q_s &= \mu^{\max} \cdot Y_{SX} \cdot I\end{aligned}$$

Stoichiometric coefficient of substrate S over biomass X , Y_{SX} , represents the ratio between the consumed substrate over the newly produced biomass:

$$Y_{SX} = \frac{dC_s}{dC_X} = \frac{q_s}{\mu}$$

q_s , μ and q_p are defined as:

$$\begin{aligned}q_s &= \frac{1}{C_X} \frac{dC_s}{dt} \\ \mu &= \frac{1}{C_X} \frac{dC_X}{dt} \\ q_p &= \frac{1}{C_X} \frac{dC_p}{dt}\end{aligned}$$

Other inhibition factor such as pH, temperature, cross inhibition of NO_3^- to the NO_2^- reduction and NO_2^- to the NO_3^- reduction can also be added into this total inhibition factor (Soto et al., 2007, Wang et al., 1995)

In this model, the half-saturation equation (Monod, 1949) is applied for substrate limitation kinetics, and the inhibition equation by Andrews (1968) is applied for the NO_3^- and NO_2^- inhibitions. NO_3^- is reported to show inhibition at concentration of 0.2M (Glass and Silverstein, 1998), so this value is considered to be the theoretical value of $K_{I-\text{NO}_3}$. Theoretical value of $K_{I-\text{NO}_2}$ is 0.0007 following Wang et al. (1995). These mechanisms will be applied on each reactions of the two-step denitrification. Overall substrate limitations on these reactions are:

Eq. 14.

$$\begin{aligned}I_1 &= \frac{C_{\text{Acetate}}}{C_{\text{Acetate}} + K_{\text{Acetate}}} \times \frac{C_{\text{NO}_3^-}}{C_{\text{NO}_3^-} + K_{\text{NO}_3^-}} \\ I_2 &= \frac{C_{\text{Acetate}}}{C_{\text{Acetate}} + K_{\text{Acetate}}} \times \frac{C_{\text{NO}_2^-}}{C_{\text{NO}_2^-} + K_{\text{NO}_2^-}}\end{aligned}$$

When substrate inhibition is considered, the following equation is used:

Eq. 15.

$$I_1 = \frac{C_{Acetate}}{C_{Acetate} + K_{Acetate}} \times \frac{C_{NO_3^-}}{C_{NO_3^-} + K_{NO_3^-} + \frac{(C_{NO_3^-})^2}{K_{I_NO_3^-}}}$$

$$I_2 = \frac{C_{Acetate}}{C_{Acetate} + K_{Acetate}} \times \frac{C_{NO_2^-}}{C_{NO_2^-} + K_{NO_2^-} + \frac{(C_{NO_2^-})^2}{K_{I_NO_2^-}}}$$

Specific growth rates of the two reduction reactions are calculated correspondently:

Eq. 16

$$\mu_1 = \mu_{max}^{(1)} \times I_1$$

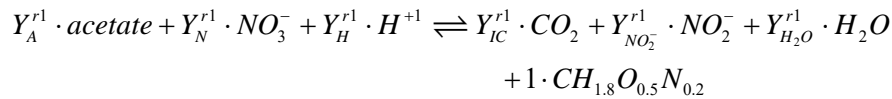
$$\mu_2 = \mu_{max}^{(2)} \times I_2$$

whereby $\mu^{max(1)}$ and $\mu^{max(2)}$ are calculated to be 0.446 and 0.853 (h⁻¹) respectively

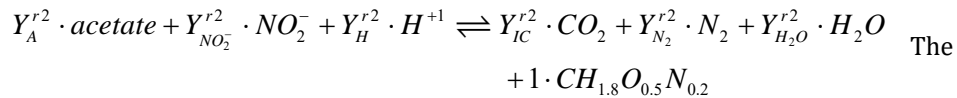
6.2.2. Stoichiometry of two2-step denitrification and the overall reaction

The metabolism of denitrification is studied using acetate (C₂H₃O₂⁻) as carbon source and electron donor, and nitrate as nitrogen source and electron acceptor. It is considered to consist of two separate metabolic reactions corresponding with the two reduction steps: NO₃⁻ to NO₂⁻ and NO₂⁻ to N₂. Taking CH_{1.8}O_{0.5}N_{0.2} as the representative molecular formula for bacterial biomass, the stoichiometry for both reactions producing 1 C-mol of biomass is written as:

Rect. 6-1.

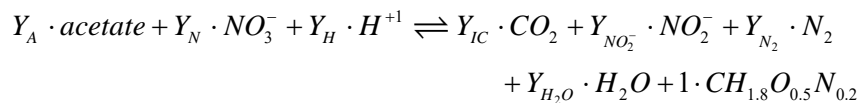


Rect. 6-2.



overall metabolic reaction of the two-step denitrification is in the form as:

Rect. 6-3.



In which Y is the stoichiometric coefficient for each compound per mol of biomass.

It is assumed that only one microorganism is responsible for both the metabolic reactions, which can either grow on nitrate or nitrite. C_x is the biomass

concentration. The stoichiometry of the overall reaction is the sum of the reactions above with their correspondent rates, which is:

$$\text{Rect. 6-3} = \mu_1 \times C_X \times \text{Rect. 6-1} + \mu_2 \times C_X \times \text{Rect. 6-2}$$

The total biomass production in the overall reaction is accordingly:

$$\mu_{\text{overall}} \times C_X = \mu_1 \times C_X + \mu_2 \times C_X$$

Consequently, Rect. 6-3 is shortened and the overall specific growth rate of the system is:

$$\text{Rect. 6-3} = \mu_1 \times \text{Rect. 6-1} + \mu_2 \times \text{Rect. 6-2}$$

Eq. 17 $\mu_{\text{OVERALL}} = \mu_1 + \mu_2$

f_{NO_2} is defined as the nitrite accumulation proportion, which is the ratio of the NO_2^- in the overall reaction Rect. 6-3 over the NO_2^- to be produced in the nitrate reduction step in Rect. 6-1:

Eq. 18.
$$f_{NO_2} = \frac{\mu_1 \cdot Y_{NO_2^-}^{r1} + \mu_2 \cdot Y_{NO_2^-}^{r2}}{\mu_1 \cdot Y_{NO_2^-}^{r1}}$$

When f_{NO_2} is equal to 1, nitrate reduction stops at the first step of $NO_3^- \rightarrow NO_2^-$ and nitrite stays permanently in the solution, Y_{N_2} in Rect. 6-3 is 0. When f_{NO_2} is equal to 0, all the nitrite is consumed and nitrate is completely reduced to N_2 , and $Y_{NO_2^-}$ in Rect. 6-3 is 0.

6.2.3. Dependence of the stoichiometry on the specific growth rate of the metabolism

Stoichiometry of each reduction steps is calculated similarly to the procedure performed for the complete denitrification reaction in chapter 2 following the bioenergetics approach suggested by Heijnen and his colleagues (Heijnen and Kleerebezem, 2010, Heijnen et al., 1992). In their model, microbial catabolism is divided into anabolism and catabolism with the proportion represented by f_{cat} :

$$\text{Metabolism} = \text{Anabolism} + f_{cat} \cdot \text{Catabolism}$$

Gibbs energy of the overall growth, Y_G^{gr} , consists of the Gibbs energy from the anabolism, Y_G^{an} , and catabolism Y_G^{cat} :

$$Y_G^{gr} = Y_G^{an} + f_{cat} \cdot Y_G^{cat} \quad \text{(Eq. 4, chapter 2)}$$

The Gibbs energy of catabolism and anabolism are calculated from their correspondent stoichiometry according to Eq. 5 and corrected to the environment concentration by **Eq. 6** as presented in chapter 2. The Gibbs energy of the overall growth depends on the specific growth rate μ of the microorganism:

$$Y_G^{gr} = Y_G^{\max} + \frac{m_G}{\mu} \quad \text{(Eq. 7, chapter 2)}$$

where Y_G^{\max} is the needed Gibbs energy to make 1 C-mol biomass (kJ/C-molX), and m_G is the Gibbs energy needed for biomass maintenance (kJ/C-molX/h).

Stoichiometry of the catabolic and anabolic reactions of the two reduction steps, the calculated correspondent Gibbs energy and the maximal specific growth rate are presented in Table 6-1. The metabolism stoichiometry of the two reduction steps Rect. 6-1 and Rect. 6-2 and overall denitrification Rect. 6-3 can be calculated with a range of specific growth rate from maintenance only to maximum growth. Therefore, from the bioenergetics perspective, stoichiometry of the overall denitrification metabolism in particular, and microbial metabolism in general, is dependent on their specific growth rate.

6.2.4. Equilibrium calculation

Concentration of the dissociated species under equilibrium is calculated by the OCHESTRA program using the MINTQA2 V4.0 thermodynamic database (Meeussen, 2003). The equilibrium calculation includes dissociations of acetate and inorganic carbon, phase equilibrium of N_2 and CO_2 , and possible derived species of calcium including $CaCO_3$ at the correspondent pH level. Equilibrium between the gas and the liquid phase is calculated using Henry's law.

6.3. Model implementation

6.3.1. Model structure

The calculation procedure of the two-step denitrification model is elaborated in Figure 6-1. Substrate consumption rates q_s and production rates q_p are calculated using the initial concentrations, assumed stoichiometric coefficients and specific growth rates. q_s and q_p are used to obtain the total concentrations of all the species in the first time step. Concentration of the dissociated species under the new equilibrium are then calculated and the dissociated substrates (CH_3COO^- , NO_3^- , NO_2^-) are used to update the specific growth rates μ in each reaction for the next time step calculation. Using a rate-dependent stoichiometry approach, the updated μ is used to recalculate the stoichiometric coefficients of the both reactions for the next time step.

6. Model of two-step denitrification-based MICP

Table 6-1. Gibbs energy Y_{Gibbs} , μ_{max} , and stoichiometric coefficients of the reactions

Reactions	Y_{Gibbs}	μ^{max}	$C_2H_3O_2$	NO_3^-	NO_2^-	N_2	H_2O	CO_2	H^+	$CH_{1.8}O_{0.5}N_{0.2}$
Rect. 6-1:		0.446	Y_{Ar^1}	Y_{Nr^1}	$Y_{NO_2r^1}$	0	$Y_{H_2Or^1}$	Y_{ICr^1}	Y_{Hr^1}	1
Catabolic	-501.8		-1	-4	4	0	2	2	-1	0
Anabolic	-65.1		-0.725	-0.2	0	0	0.65	0.45	-0.925	1
Rect. 6-2:		0.853	Y_{Ar^2}	0	$Y_{NO_2r^2}$	$Y_{N_2r^2}$	$Y_{H_2Or^2}$	Y_{ICr^2}	Y_{Hr^2}	1
Catabolic	-970.9		-1	0	$-\frac{8}{3}$	$\frac{4}{3}$	$\frac{10}{3}$	2	$-\frac{11}{3}$	0
Anabolic	-38.61		-0.675	0	-0.2	0	0.55	0.35	-0.875	1
Rect. 6-3			Y_A	Y_N	Y_{NO_2}	Y_{N_2}	Y_{H_2O}	Y_{IC}	Y_H	$\mu_1 + \mu_2$

Minus sign (-) indicates stoichiometric coefficients of the consumed substances.

Table 6-2. Model parameters and investigation ranges of calibration

Case	Ac/N	$K_{S-Ace}^{(1)}$	$K_{S-Ace}^{(2)}$	K_{S-NO_3}	K_{S-NO_2}	K_{I-NO_3}	K_{I-NO_2}	$\mu_{max}^{(1)}$	$\mu_{max}^{(2)}$	C_X
I	0.6									
	0.8	0.002	0.002	0.0001	0.0001	(-)	(-)	[10 ⁻³ -10]	[10 ⁻³ -10]	[10 ⁻⁵ -1]
	1.2									
II-1	0.8	0.002	0.002	0.0001	0.0001	0.2	0.0007	[10 ⁻³ -10]	[10 ⁻³ -10]	[10 ⁻⁵ -1]
II-2	0.8	[10 ⁻⁵ -1]	[10 ⁻³ -10]	[10 ⁻³ -10]	[10 ⁻¹ -1]					

6. Model of two-step denitrification-based MICP

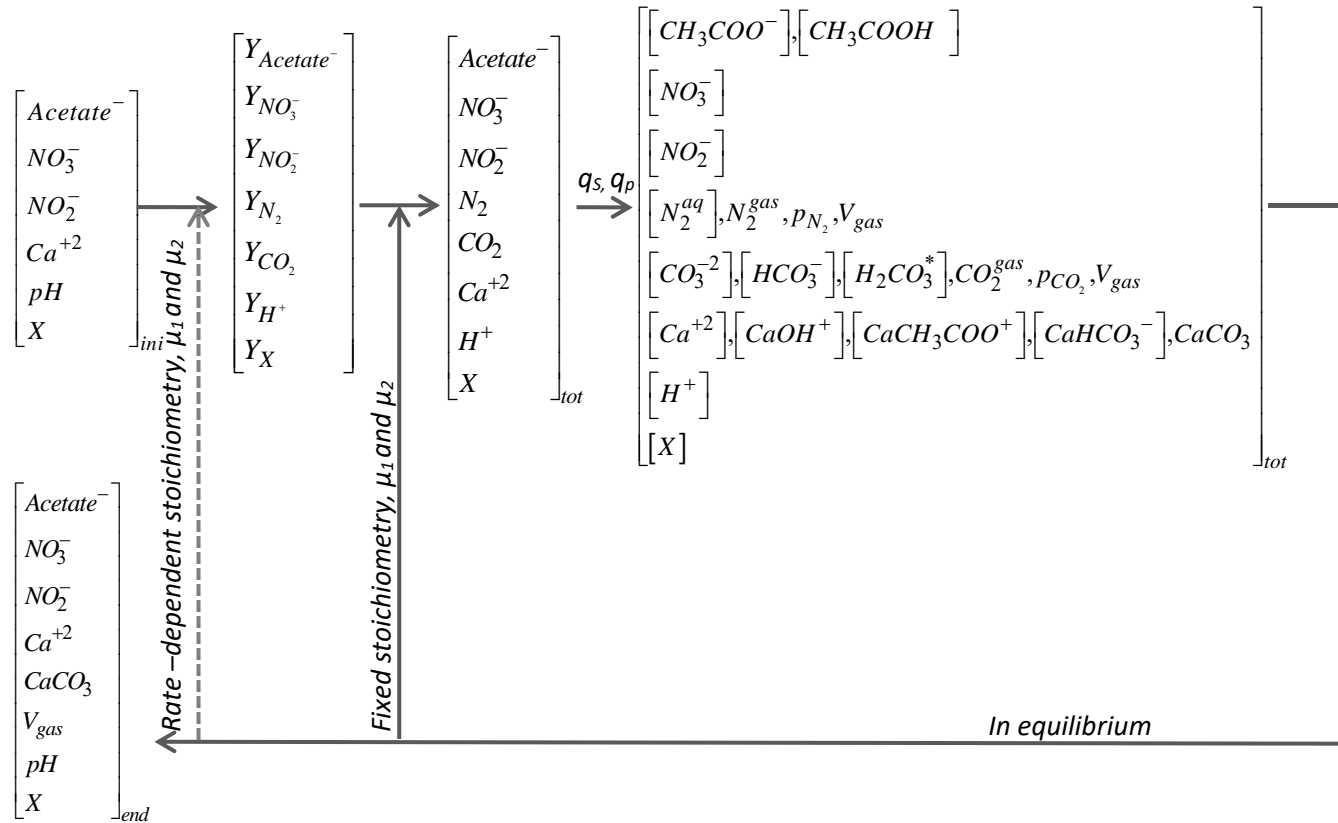


Figure 6-1. Overview of the biological-chemical network of two-step denitrification based MICP

6.3.2. Testing cases and model variables

The model considers two cases:

- (I) In the first case, substrate limitation is the only factor limiting the growth rate in the model structure (Eq. 14), in which the K_s values of the substrates are fixed, and inhibition is not considered. μ_1 , μ_2 , and the initial biomass concentration C_x are used to calibrate the model by fitting the simulation results with the experimental results of all the three A/N cases;
- (II) In the second case both substrate limitation and inhibition are considered as rate limiting factors in the model structure (Eq. 15). The K_s and K_i values are either fixed (case II-1) or also used as the parameters for model calibration (case II-2). The outcomes are evaluated by comparison to the data of the liquid batch experiment using the A/N ratio of 0.8 only;

The investigation ranges of the model variables, its parameters and the initial concentrations are presented in

Table 6-2 Table 6-3.

For both cases, the stoichiometry of the metabolic reactions is calculated using two approaches:

- The first approach considers a fixed stoichiometry for the two metabolic reactions. The stoichiometry of the two reduction reactions are shown in Table 6-4. This stoichiometry was calculated assuming an overall A/N ratio of 0.8 without nitrite accumulation, which was the final substrate consumption ratio observed in the liquid batch experiments.
- For the second approach a rate-dependent stoichiometry is considered for both metabolic reactions. The stoichiometry of the two reduction reactions is updated in each time step when the specific growth rates of the two reactions are updated by the growth kinetic calculation.

Table 6-3. Initial concentrations

Ac/N	CH ₃ COO ⁻ [Mol/L]	H ₂ CO ₃ [Mol/L]	NO ₃ ⁻ [Mol/L]	Dissolved N ₂ [Mol/L]	pH	Ca ²⁺ [Mol/L]	NO ₂ ⁻ [Mol/L]
0.6	0.034	0.00	0.049	0.65.10 ⁻³	7	0.045	0.00
0.8	0.042	0.00	0.051	0.65.10 ⁻³	7	0.045	0.00
1.2	0.063	0.00	0.052	0.65.10 ⁻³	7	0.057	0.00

Table 6-4. Fixed stoichiometry scenario

Reactions	C ₂ H ₃ O ₂ ⁻	NO ₃ ⁻	NO ₂ ⁻	N ₂	H ₂ O	H ₂ CO ₂	H ⁺	CH _{1.8} O _{0.5} N _{0.2}
NO ₃ ⁻ →NO ₂ ⁻	-3.25	-10.3	10.1	0	0.2	5.5	-3.45	1
NO ₂ ⁻ →N ₂	-2.01	0	-3.75	1.78	1.98	3.01	-5.76	1

6.3.3. Evaluate performance of the model by the 'grey modelling' toolbox

To evaluate the performance of the model, the simulation results are compared with the experimental results of the liquid batch incubation experiments described in chapter 3 using a 'grey modelling' toolbox developed by Turnhout et al. (2016). The model allows to build a biogeochemical reaction network which includes kinetic reactions, phase's equilibrium reactions and environmental inhibitions in a multi-phase system.

This toolbox aims to find the optimal model structure that can best fit with experimental data with minimal mechanistic uncertainty by applying Bayesian inference, which is a statistical inference to examine a possible ranges of model parameters and find results that can satisfy statistical criteria. To find the best fit for a measured dataset, the toolbox starts with values of the model variables in the investigation ranges that can possibly fit the experimental data. Then it evaluates the model performance by plotting the model results with the measured data, calculating the standard deviations of total error (σ) and check the required statistical criteria whether the model describes the measured data with sufficient accuracy. If it is not sufficiently accurate, the reaction network is updated in the next iteration and is evaluated until an optimal set of model variables is found.

To evaluate the performance of the model structure, the toolbox uses several quantitative criteria in which standard deviations of total error σ for each subset of data are included. Narrow ranges of σ in combination with a small bandwidth of the calibrated parameter within a 95% confidence interval indicates a result with low uncertainty. If a calibrated parameter besides satisfying that condition and corresponds closely with its theoretical value then the model structure is considered mechanistically correct. In contrast, a large deviation of the calibrated parameters from their theoretical values indicates that there are other mechanisms that are not yet accounted for in the model structure.

6.4. Results and discussion

6.4.1. Result of the 2-step denitrification stoichiometry analysis

By varying the range of the possible specific growth rates of the two reduction steps separately, the stoichiometry of the overall two-step denitrification reaction can be evaluated. Figure 6-2 illustrates the overall results. Nitrite accumulation occurs when the nitrite consumption rate in the second reduction step is not able to accommodate the nitrate reduction rate, as seen in Figure 6-2a. In this panel, $f_{NO_2^-}$ is the highest approaching the maximum value of 1 when the overall growth completely based on nitrate and the second reduction step is completely inhibited. Complete conversion of nitrate to nitrogen gas without nitrite accumulation ($f_{NO_2^-} = 0$) can only occur when μ_1 is lower than μ_2 and the overall growth rate, $\mu_1 + \mu_2$, is higher than 10^{-2} h^{-1} . Overall growth rates lower than 10^{-2} h^{-1} always result in some nitrite accumulation.

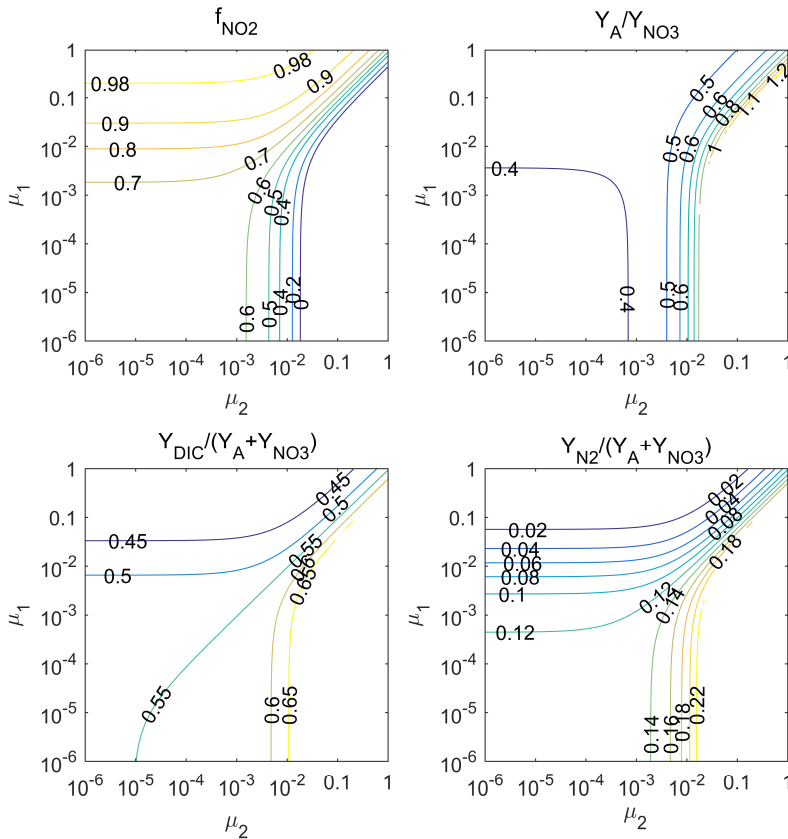


Figure 6-2. Stoichiometry of 2-step denitrification

The effect of the growth rates on the substrate consumption ratio (Y_A/Y_N) does not show the same patterns as for $f_{NO_2^-}$, but its boundaries overlap the boundaries of $f_{NO_2^-}$. In other words maximum Y_A/Y_N of 1.25 corresponds with a complete denitrification without nitrite accumulation. When the growth on nitrate is inhibited and bacteria still grow using nitrite at a maximum growth rate of 10^{-2} (h^{-1}), the substrate consumption ratio Y_A/Y_N is reduced to 0.9. In Chapter 2 when denitrification is considered as a single reaction, with Y_A/Y_N to be reduced further to the value corresponding with maintenance, there is still possibly no nitrite accumulation. Nevertheless, considering the nitrite accumulation kinetic in the two-step denitrification suggest that nitrite likely accumulates at limited growth. At lower growth rates, significant nitrite accumulation occurs and the substrate consumption ratio drops even further. At nitrite accumulation of 60% ($f_{NO_2^-} = 0.6$) and above, Y_A/Y_N is always below 0.6. In Figure 6-3, the Y_A/Y_N range corresponding with $f_{NO_2^-} = 0$ for the two-step denitrification is only within 0.9 – 1.25, and the $\mu_{overall}$ is above 0.01, instead of the wider Y_A/Y_N range of 0.62 – 1.25 covering the whole range of $\mu_{overall}$ in the single denitrification reaction. This evaluation suggests that

supplying carbon source in excess ensuring that Y_A/Y_N is always above 0.9 is one option to minimize the nitrite accumulation risk.

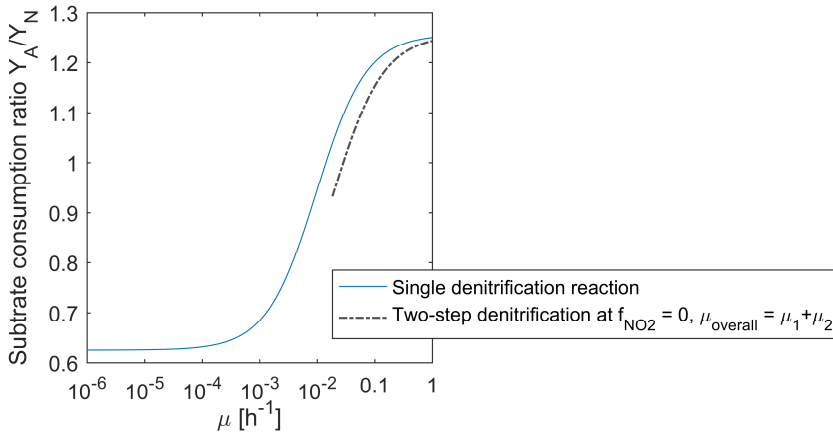


Figure 6-3. Substrate consumption ratio Y_A/Y_N when there is no nitrite accumulation

Figure 6-2c shows that the total amount of inorganic carbon is also reduced under nitrite accumulating conditions. Nitrogen gas production shows a similar trend, but it is much more sensitive to nitrite accumulation as less nitrite is reduced to form nitrogen gas.

6.4.2. Case I – Considering substrate limitation with fixed kinetic constants

The simulation results that showed the best fit to the experimental data in which only substrate limitation with fixed half-saturation constants is considered are presented in Figure 6-4. The visual fitting results for Ca^{2+} , NO_3^- , and total carbon (TC) are reasonable for both the fixed or rate-dependent stoichiometry. However, the NO_2^- profiles significantly differed depending on the selected modelling approach. In the experiment with an A/N ratio of 0.8, the fixed stoichiometry approach seemed to provide the best fit. Alternatively, in the other two experiments, the fixed stoichiometry failed to simulate any nitrate accumulation.

Results of calibrated model parameters and the standard deviations of the total error are presented in Table 6-5 and Table 6-6. Table 6-6 show that standard deviation of total errors for most of the data do not differ very much, except that of NO_2^- for the A/N ratios of 0.6 and 1.2. In these two substrate ratio cases, the fixed stoichiometry resulted in a significantly larger range of σ_{NO_2} . Also, broad bandwidths of C_X and $\mu_{max}^{(2)}$ imply a strong uncertainty in the model results. These results indicate that the chosen fixed stoichiometry is not suitable to simulate nitrite accumulation appropriately for the A/N ratios of 0.6 and 1.2. Therefore it is necessary to update the two-step denitrification stoichiometry and evaluate alternative approaches.

Table 6-5. The range of calibrated model parameters for Case I

Ac/N	Stoichiometry	C_x [Mol/L]	$\mu_{\max}^{(1)}$ [h ⁻¹]	$\mu_{\max}^{(2)}$ [h ⁻¹]
0.6	Fixed	0.0052 - 0.323	0.001 - 0.038	0.512 - 9.428
	Rate-dependent	0.0022 - 0.086	0.0014 - 0.14	0.017 - 0.25
0.8	Fixed	0.0028 - 0.048	0.009 - 0.695	0.022 - 0.172
	Rate-dependent	0.099 - 0.119	0.001 - 0.0013	0.017 - 0.021
1.2	Fixed	0.068 - 0.262	0.001 - 0.004	0.702 - 9.639
	Rate-dependent	0.044 - 0.072	0.001 - 0.006	0.014 - 0.022

Table 6-6. The standard deviations of the total error for Case I

Ac/N	Stoichiometry	σ_{Ca+2} (x10 ⁻³)	σ_{NO_3} (x10 ⁻³)	σ_{NO_2} (x10 ⁻³)	σ_{TC} (x10 ⁻³)
0.6	Fixed	2.6 - 4.5	3.1 - 6.1	6.7 - 11.3	4.8 - 11.4
	Rate-dependent	2.6 - 6.2	3.1 - 6.9	0.8 - 2.9	5.1 - 13.6
0.8	Fixed	4.0 - 8.4	4.1 - 5.5	1.2 - 3.1	6.6 - 12.0
	Rate-dependent	4.5 - 8.5	4.1 - 5.6	1.3 - 2.9	6.4 - 9.4
1.2	Fixed	2.8 - 4.0	3.4 - 4.3	6.6 - 13.4	5.8 - 11.1
	Rate-dependent	2.9 - 5.4	3.4 - 5.4	2.2 - 5.4	6.6 - 12.8

For the A/N ratio of 0.8, using a fixed stoichiometry approach gave a good fit and the ranges of the standard deviation σ were comparable with the results of the rate-dependent stoichiometry. Nevertheless, the rate-dependent stoichiometry gave remarkably better converged values, illustrated by smaller bandwidths of the calibrated model parameters in Table 6-5. These results indicate a lower uncertainty as compared with the results of the fixed stoichiometry. Additionally, although the fixed stoichiometry can give a good fit, the wide bandwidths of the calibrated parameters could not give any clear suggestion on how to improve the model performance. For the rate-dependent stoichiometry results, very small values of $\mu_{\max}^{(1)}$ and $\mu_{\max}^{(2)}$ were observed compared with their theoretical values. It indicates that they had to cover other inhibiting mechanisms that were acting on the process but not yet counted. The total inhibition factors $I_{1,2}$ in both the reactions, as shown in Eq. 16, were calculated only with the substrate limitation mechanisms while their 'realistic' values should be less due to the inhibition effect. As a result to give a reasonable μ to fit the measured data, the model reduced $\mu_{\max}^{(1),(2)}$ values to cover the inhibition effect.

6. Model of two-step denitrification-based MICP

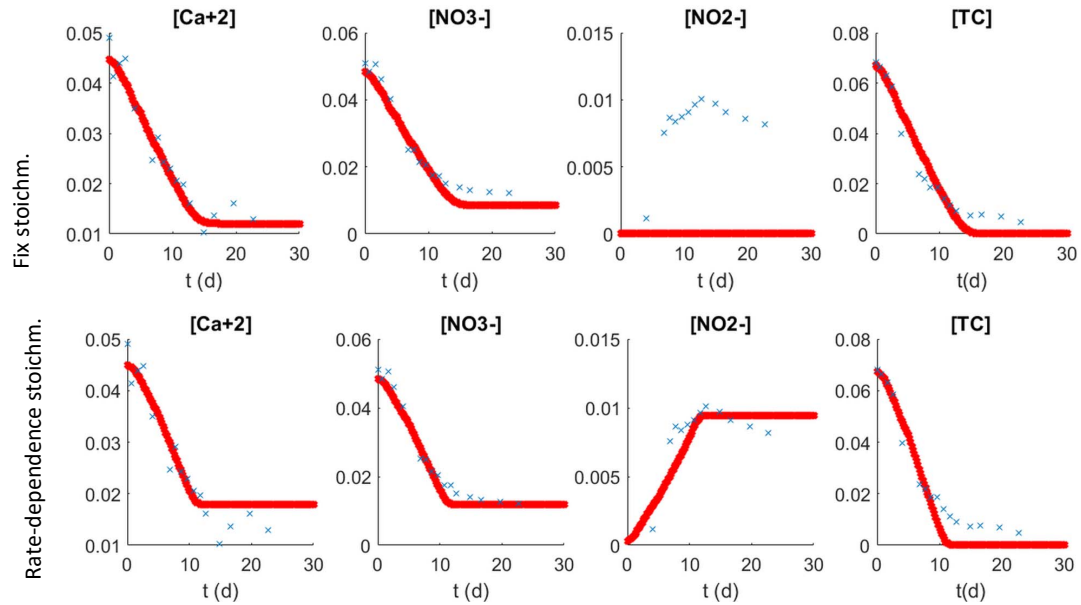


Figure 6-4a. Fitting results for Case I, $A/N = 0.6$

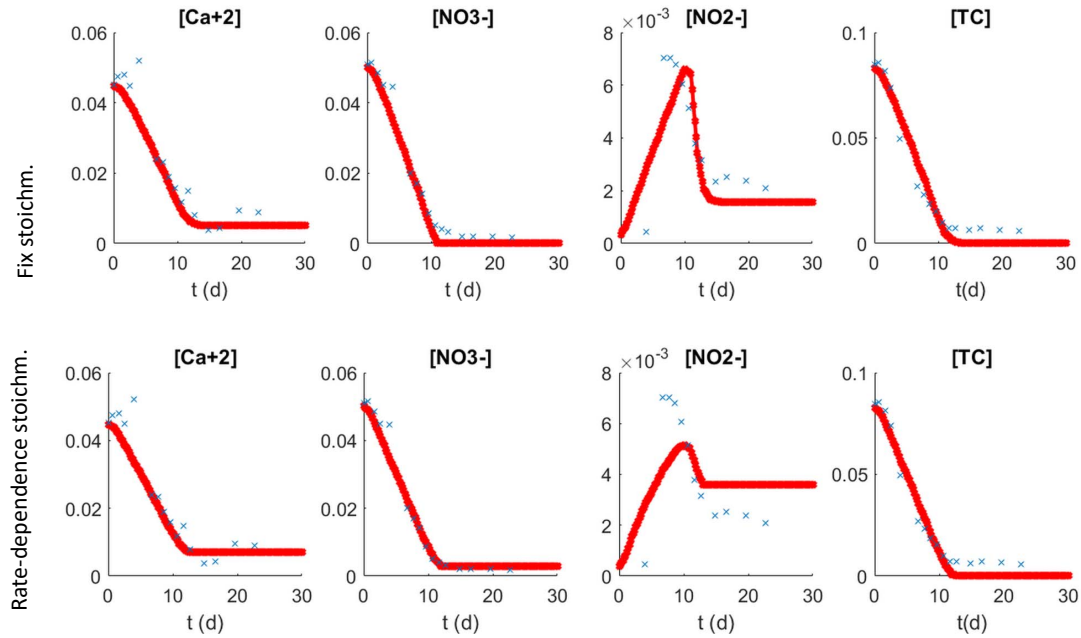


Figure 6-4b. Fitting results for Case I, $A/N = 0.8$

6. Model of two-step denitrification-based MICP

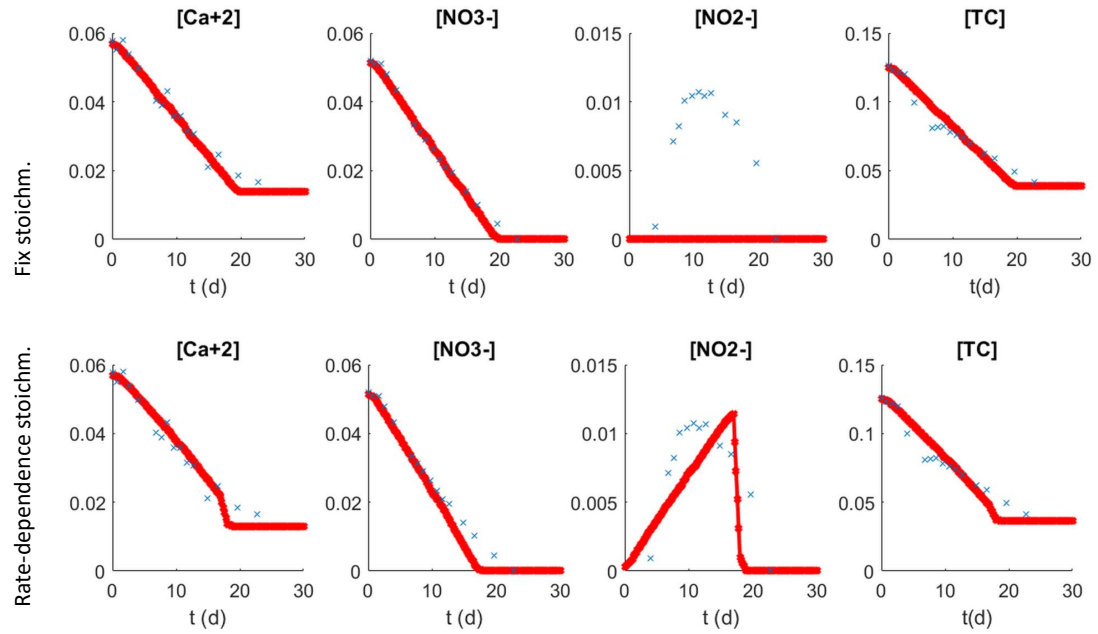


Figure 6-4c. Fitting results for Case I, $A/N = 1.2$

6.4.3. Case II –Considering substrate limitations and inhibitions with fixed and calibrated parameters

When considering both the substrate limitations and inhibitions in the model structure, the model was tested using either fixed values for the constants (case II-1) or by using these constants together with C_X , $\mu_{max}^{(1)}$, $\mu_{max}^{(2)}$ as calibration parameters (case II-2). The models were calibrated using the data from the experiments with the A/N ratio of 0.8, and the results are presented in Figure 6-5 and Table 6-7 to Table 6-9. Similar to Case I, in Case II all approaches considering both substrate limitation and inhibition provided a reasonable fit with the experimental data for Ca^{2+} , NO_3^- and TC, while NO_2^- showed significant differences.

The results of Case II show that adding substrate inhibition helps to improve the fit, but only if the kinetic constants are included in the parameter calibration. The results in Figure 6-5a suggest that using fixed values for the constants does not provide a good match with the measured NO_2^- concentrations. For case II-2, in which the rate constants were calibrated the simulated results fit significantly better for both the fixed and the rate-dependent stoichiometry. In both these sub-cases, the bandwidths of the calibrated parameters as well as the ranges of the standard deviation of total errors were significantly larger when the model used the fixed stoichiometry than for the rate-dependent stoichiometry, as presented in Table 6-8 and Table 6-9. These results indicate that taking the rate-dependent stoichiometry into account in the model structure reduces the model uncertainty. However, adding the kinetic constants in the model calibration, also increased the degrees of freedom of the model. As a result the convergence of C_X , $\mu_{max}^{(1)}$ and $\mu_{max}^{(2)}$ was lost even with the rate-dependent stoichiometry. The substrate inhibition mechanism used in Eq. 16 seemed not to be sufficient to properly simulate the process and obtain a unique solution.

6. Model of two-step denitrification-based MICP

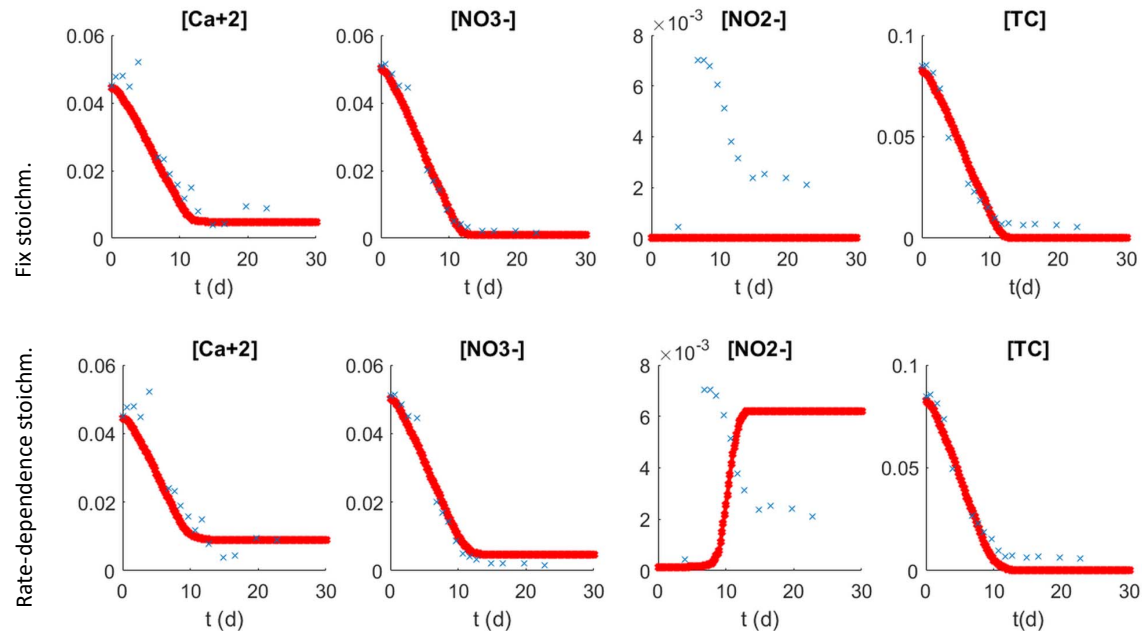


Figure 6-5a. Fitting results for Case II, $A/N = 0.8$, using fixed substrate limitation and inhibition constants in the case II-1

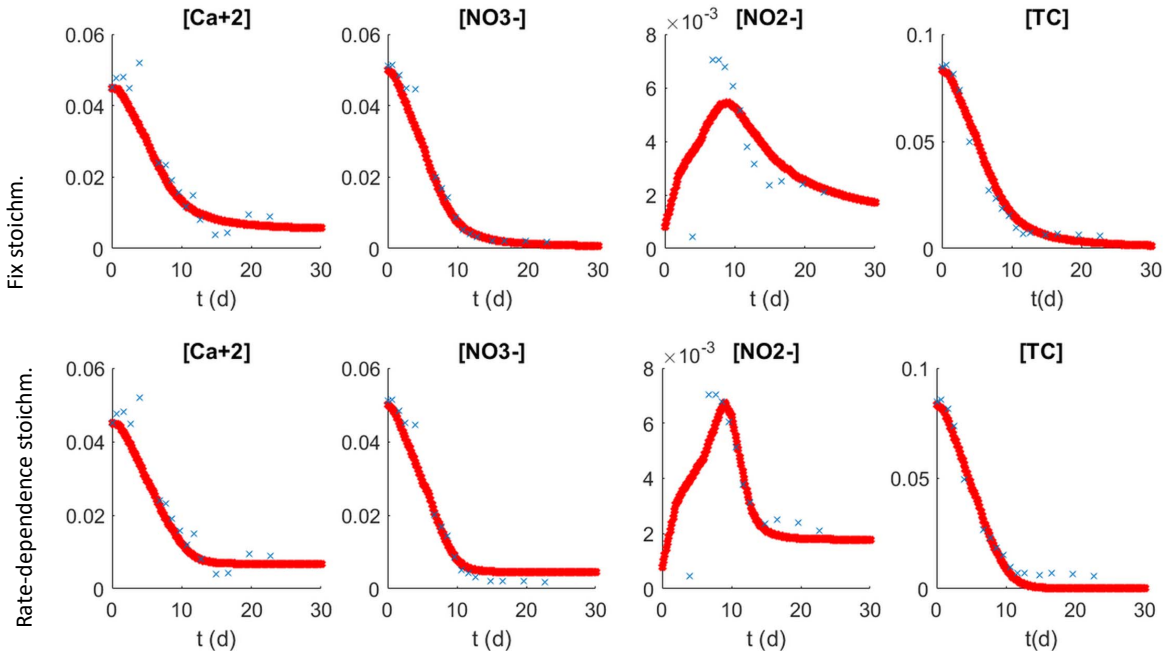


Figure 6-5b. Fitting results for Case II, Ac/N = 0.8, using calibrated substrate limitation and inhibition constants in the case II-2

6. Model of two-step denitrification-based MICP

Table 6-7. Fixed values and bandwidth of calibrated kinetic constants model parameters for Case II

Case	Stoichiometry	$K_{S-Ac(1)}$ [Mol/L]	$K_{S-Ac(2)}$ [Mol/L]	K_{S-NO3} [Mol/L]	K_{S-NO2} [Mol/L]	K_{I-NO3} [Mol/L]	K_{I-NO2} [Mol/L]
II-1	Fixed	0.002	0.002	0.0001	0.0001	0.2	0.0007
	Rate-dependent	0.002	0.002	0.0001	0.0001	0.2	0.0007
II-2	Fixed	0.0113	0.0203	0.0116	0.1576	0.0003	0.0966
		-0.971	-0.802	-0.614	-0.985	-0.1522	-0.945
	Rate-dependent	0.0013	0.026	0.092	0.0038	0.0006	0.063
		-0.9564	-0.826	-0.970	±0.818	-0.882	-0.970

Table 6-8. Bandwidths of calibrated model parameters for Case II

Case	Stoichiometry	C_x [Mol/L]	$\mu_{max}^{(1)}$ [h ⁻¹]	$\mu_{max}^{(2)}$ [h ⁻¹]
II-1	Fixed	0.0345-0.438	0.0012-8.269	0.6757-9.1357
	Rate-dependence	0.0634-0.1034	0.0012-0.0071	0.0442-0.0764
II-2	Fixed	0.076-0.9034	0.0297-0.81	1.218-9.63
	Rate-dependence	0.047-0.108	0.044-9.018	0.631-9.693

Table 6-9. Ranges of the standard deviations of total error for Case II

Case	Stoichiometry	σ_{Ca+2} (x10 ⁻³)	σ_{NO3} (x10 ⁻³)	σ_{NO2} (x10 ⁻³)	σ_{TC} (x10 ⁻³)
II-1	Fixed	4.9-18.0	4.2-34.6	3.3-9.4	6.5-29.7
	Rate-dependence	4.9-10.1	4.2-7.5	3.1-7.9	6.4-9.9
II-2	Fixed	4.5-9.4	4.1-9.7	1.2-3.6	6.4-12.3
	Rate-dependence	4.1-8.0	4.1-6.7	1.2-3.6	6.4-9.8

6.4.4. Predicting results of calcite and pH

Figure 6-6 shows the results of the different simulation approaches for the calcite concentration and pH. All simulations result in a similar pattern for the calculated pH results, but they are slightly more acidic than the experimental values.

Table 6-10. Proportion of calculated calcite over the correspondent total consumed substrates

		A/N = 0.6		A/N = 0.8		A/N = 1.2	
End NO ₂ ⁻		8.2 [mM]		2.0 [mM]		0.0 [mM]	
	Case	Fixed stoic.	Rate-dependent	Fixed stoic.	Rate-dependent	Fixed stoic.	Rate-dependent
Y_{CaCO_3}	I	0.35	0.29	0.45	0.43	0.61	0.62
$(Y_A + Y_N)$	II-1			0.45	0.41		
	II-2			0.44	0.43		

The calculated calcium carbonate concentrations are also similar between the different simulation conditions. The largest deviation between the simulations was shown at the final concentration, which seemed to be inversely proportional to the remaining NO₂⁻. The overall yield of calcite over the sum of consumed substrates (acetate and nitrate) was calculated and presented in Table 6-10. For the A/N ratio of 1.2, there was more temporary NO₂⁻ than for A/N of 0.8, but all NO₂⁻ was depleted at the end of the experiment, which results in a higher calcite production in the model results. For the A/N ratio of 0.6 the fixed-stoichiometry model did not show any NO₂⁻ accumulation, which resulted in a higher calcite production than for the rate-dependent stoichiometry approach, where a significant amount of NO₂⁻ was left at the end of the reaction.

6.4.5. Utilization of results

The stoichiometry analysis and kinetic simulations using the different 'greybox' modelling approaches indicate that direct reduction of nitrate to nitrogen gas without nitrite accumulation is required not only to avoid accumulation of toxic intermediates but it also appears to be to enhance DIC and nitrogen gas production. In chapter 2 the model considering a single denitrification reaction suggested that staying in the maintenance mode is beneficial for CaCO₃ precipitation, considering that more carbon source is converted to inorganic carbon and less to biomass as presented in Figure 2-2. Similarly it is seen in Figure 6-2c that DIC production is reversely proportional to μ_1 . On the other hand, DIC production is proportional to μ_2 and it reaches the upper boundary when there is no NO₂⁻ accumulation. Therefore, complete denitrification without NO₂⁻ accumulation is wanted not only to avoid the toxicity of nitrite but also for the interest of precipitating CaCO₃ or producing nitrogen gas.

6. Model of two-step denitrification-based MICP

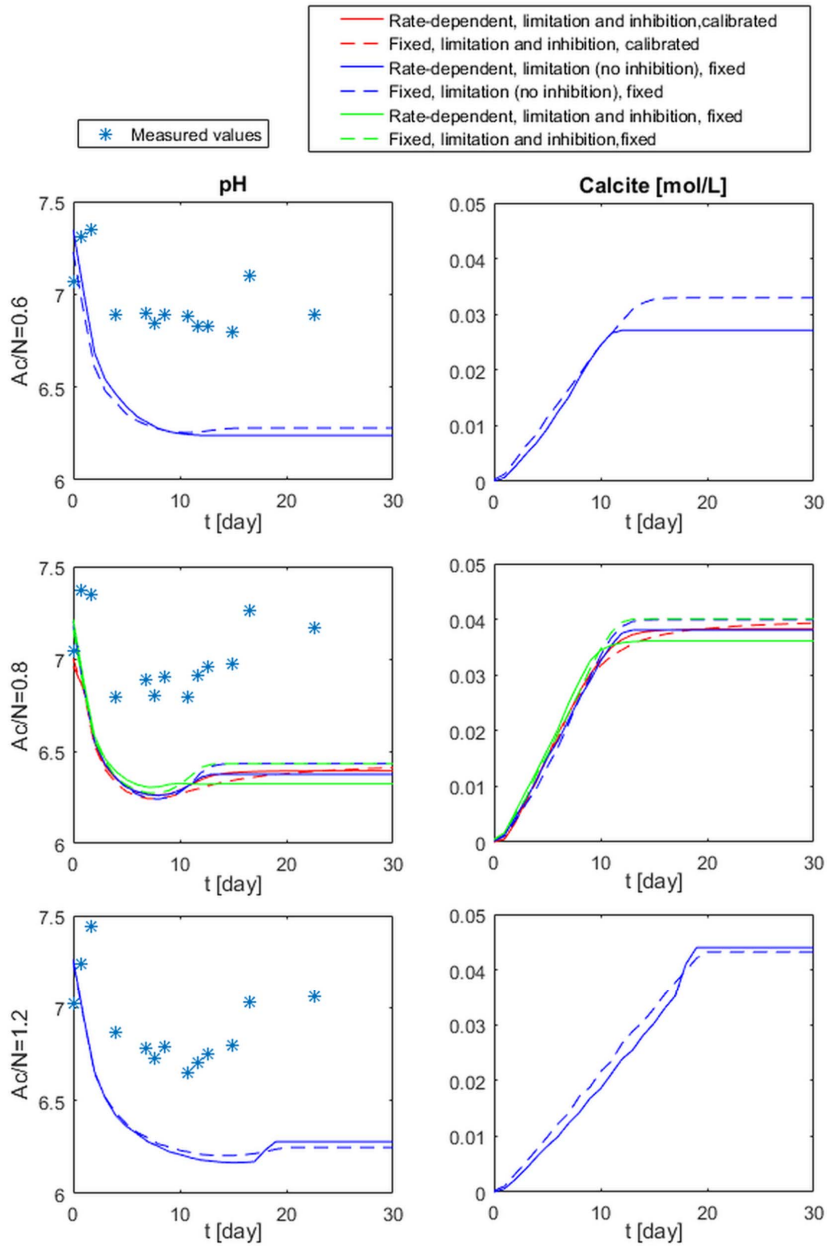


Figure 6-6. Calculated results of pH and calcite. Legend indicates the conditions of [stoichiometry, considered mechanisms, corresponding constants]

To ensure that there is no NO_2^- accumulation in the 2-step denitrification, the results in Figure 6-2a shows that the second reduction step, NO_2^- to N_2 , must be fast enough to be able to consume the NO_2^- produced from the first reaction. In chapter 2 when complete denitrification was considered as a single reaction nitrite did not accumulate by definition at any specific growth rate ranging from pure maintenance to maximal growth. However, considering denitrification as a 2-step process in this chapter indicates that the second reduction step must be performed at a specific growth rate that is higher than 0.0184 h^{-1} . If the metabolism of the $\text{NO}_2^- - \text{N}_2$ reduction reaction falls toward maintenance resulting in the overall metabolism to lean forward maintenance mode, NO_2^- is very likely to occur. The Y_A/Y_N result also gives an indication, which can be considered as a condition, of complete denitrification without nitrite accumulation is to have the carbon source in excess favouring microbial growth. Considering Figure 6-2a-b, when Y_A/Y_N is in the range of 0.6 – 0.8, f_{NO_2} is around the range of 0.2 - 0.5.

6.4.6. Model limitations and recommendations for future work

The main limitation of this model is the assumption that denitrification consists of 2 separate metabolic reactions with 2 different specific growth rates for each reduction step, whereas in the actual microbial metabolism the bacteria do not distinguish which sources of catabolism that supply the energy for their growth and maintenance on NO_3^- and NO_2^- .

In the metabolism model of microorganism, energy from catabolic reaction is carried by the carriers namely ATP and ADP for the cells to function and grow (Haynie, 2008, Heijnen and Kleerebezem, 2010). According to Heijnen and Kleerebezem (2010) the electron transfer through these carriers is restricted to a maximum value of 3 e-mol/X-mol/h at 298K, due to potential kinetic bottlenecks in microbial metabolism. In the 2-step denitrification approach, the two reduction reactions happen simultaneously resulting in a total of 5 e-mol/X-mol/h in the electron donor flux. So if the maximal electron restriction is applied into the 2-step denitrification, its μ_{overall} must be reduced by a factor of 5/3. Yet the μ_{overall} calculation of the 2-step denitrification is still debatable.

An alternative to the selected modelling approach would be to separate the anabolic and catabolic reactions. In principle energy from both the catabolic reactions can be used in the microbial growth on either nitrate or nitrite or both the nitrogen sources simultaneously, and the priority is based on the energy level. Although growth on nitrite has been experimentally identified (Almeida et al., 1995, Kornaros et al., 1996), denitrifying bacteria can grow on only nitrate when using the energy generated from both the $\text{NO}_3^- - \text{NO}_2^-$ and $\text{NO}_2^- - \text{N}_2$ reduction. Recent works of modelling nitrite accumulation in waste water treatment plants have used different approach of denitrification metabolism and mathematical structure of the growth rate expression, but the underlying mechanism is still yet unclear (Sin et al., 2008). Building a complete metabolic model was outside the scope of this thesis work, but it can overcome this issue by separating the catabolic and anabolic reactions in the model structure. So instead of consisting of 2

complete metabolic reactions, the model structure can consist of 2 catabolic reactions together with either 1 or 2 anabolic reactions and compute their relative rates to determine the overall metabolic reaction that best fits with the experimental data with the lowest uncertainty.

Secondly the current kinetic model takes only a limited number of substrate limitation and inhibition mechanisms into account. Other substrate inhibition mechanisms have been proposed by different authors in literature (Luong, 1987, Edwards, 1970) that have been investigated for nitrite inhibition (Carrera et al., 2004, Puyol et al., 2014). Besides, the cross inhibition of NO_2^- on the NO_3^- reduction and pH inhibition can also be significant in the system (Wang et al., 1995). In principle the model structure can be further expanded and examined with different inhibition mechanisms for future study. Complexity of the model can become accordingly intensive, therefore the ability of the 'grey toolbox' to evaluate uncertainty of the model structure is a helpful aspect to judge the necessity of this complexity. For future work, this model structure can help investigating the uncertainty of different substrate inhibition mechanisms.

6.5. Conclusions

In this chapter a model has been proposed which can be used to simulate the coupled process of denitrification-based MIDP, which considers a two-step reduction of NO_3^- to NO_2^- and NO_2^- to N_2 . Several approaches to describe the kinetics of the metabolic reactions have been evaluated. The output of the model shows that simulation results of NO_3^- , TC and Ca^{2+} fit well with experimental data regardless the selected model approaches. However, to simulate the kinetic of NO_2^- accumulation, it is important to assume that the stoichiometry of the two metabolic reactions are dependent on the reaction rates. Besides, the theoretical calculation indicates that NO_2^- accumulation should not only be minimized to avoid toxicity issues but also to maximize CaCO_3 and nitrogen gas production. Not simulating the NO_2^- accumulation accurately can influence the CaCO_3 and N_2 output of the model. The current model structure could fit the experimental data but still with a high uncertainty, indicating that the current model structure is mechanistically not yet complete. There are other inhibition mechanisms that have been studied for NO_2^- inhibition, which are of interest to expand this two-step denitrification-based MICP model. By evaluating uncertainty, the appropriate model structure with reasonable complexity can be found.

7.

Conclusion

In this thesis, the potential of using denitrification-based microbially induced desaturation and (carbonate) precipitation, denitrification based MICP or MIDP, as ground improvement method has been confirmed. To prepare the method for practical applications, several challenges had to be overcome, including the risk of nitrite accumulation, the low rate of precipitation and the uncertainty in employing the produced gas phase. From both the theoretical and experimental studies that have been performed in this thesis, those issues have been tackled and the following conclusions are drawn.

Denitrification based MICP is considered to be a coupled process, in which both the denitrification and calcium carbonate precipitation processes influence and are beneficial for each other. Calcium carbonate precipitation is a direct consequence of denitrification in a solution containing dissolved calcium ions, through the production of inorganic carbon and alkalinity in the denitrification reaction. In exchange, the precipitation reaction provides a positive feedback as it neutralizes the alkaline tendency of denitrification. Result of this interaction is a reduced amount of temporarily accumulated nitrite, as shown in chapter 3. In other applications, such as nitrogen removal from waste water, which require buffering the pH to lower the risk of nitrite accumulation and inhibition, coupling denitrification with calcium carbonate precipitation by using calcium based substrates may prove beneficial.

Selecting the appropriate ratio of substrate concentrations is one of the factors affecting process efficiency which has been addressed in this thesis. The theoretical range of the acetate over nitrate consumption ratio assuming complete denitrification without accumulation of intermediate nitrogen compounds, is between 0.6 and 1.25. These ratios correspond with biomass growth rates, ranging from zero to maximum growth respectively, as calculated in chapter 2. Examining this range in batch liquid experiments of chapter 3 showed that at the lower boundary, acetate was limited resulting in remaining nitrate and permanent nitrite accumulation while the upper boundary left acetate in excess. Substrate was consumed most efficiently in liquid environment when the acetate over nitrate ratio A/N was 0.8. In sand column experiments in chapter 5 the observed A/N consumption ratio varied between the two extremes. At conditions which favour

7. Conclusion

microbial growth A/N ratio of 1.25 was observed, whereas during conditions of incomplete denitrification in which nitrite accumulation was observed and growth was inhibited the ratio shifted towards 0.6.

Not only the substrate ratio but also the concentration to be used is important to minimize nitrite accumulation. Results of the triaxial tests on sandy soils described in chapter 5 indicated that applying low substrate concentrations with short residence time allows to maintain a high activity of the denitrifying bacteria and results in denitrification without nitrite accumulation. The obtained maximum conversion rates during this experiment correspond to a precipitation rate of 0.25 w%/day, which is higher than observed so far in literature and improves the potential of using this process for ground improvement applications. Apparently, limiting nitrite accumulation not only improves the conversion rate, but also increases the precipitation yield.

In order to study the kinetics of denitrification including the effect of nitrite accumulation, evaluate the product yield for different metabolic growth rates and identify the main inhibiting mechanism, a theoretical model is proposed in chapter 6 which assumes the denitrification process to be a two-step reaction and includes nitrite as an intermediate product. Simulations using this model confirmed that an A/N ratio of 0.6 is not suitable to generate complete denitrification and will result in nitrite accumulation. The A/N ratio which can generate complete denitrification was calculated to be between 0.9 and 1.25. The model also confirmed preventing the accumulation of nitrite improves the conversion rate and increases the inorganic carbon production over total consumed acetate and nitrate. Overall, to improve yield and rate of denitrification-based MICP, it is important to consider and put the effort in minimizing nitrite accumulation and maintaining a high microbial activity.

Biogenic formation of nitrogen gas, which was initially considered a by-product of MIDP, appeared also to have potential for ground improvement applications as shown by laboratory experiments presented in chapter 4. Using a bio-augmentation approach in which the sand is inoculated with a concentrated suspension of active denitrifying bacteria, showed that applying a single flush of low concentrated substrates, sufficient gas was produced within 1 or 2 days to desaturate the sand to the gas percolation threshold, ranging from 21 to 50% depending on pore size. The results presented in chapter 4 and 5 showed that part of the gas formed in the sand in one reaction period is mobile and can be removed by flushing, but a significant part remains after flushing. The persistent gas saturation is about 10 to 15% throughout the experiments.

Employing the nitrogen gas production for applications requires engineering tools to monitor and control the gas distribution and persistence in the soil. Experimental results on sand samples indicate that those properties are dependent on the produced gas volume and the gas storage capacity or gas

percolation threshold of the soil. The produced gas volume is function of the amount of supplied substrates, the stoichiometry of the reaction and the pressure conditions, while the gas storage capacity of the soil is function of pore size distribution and confining pressure. These parameters need to be considered to design applications using the gas phase.

Results of monotonic loading on the treated sand in chapter 4 and 5 showed that carbonate precipitation increases soil stiffness and dilatancy, and biogenic gas formation decreases hydraulic conductivity, and dampens pore pressure response in undrained loading. This results confirm the potential of using denitrification-based MICP, or MIDP, in applications such as liquefaction mitigation. The resulting response to mechanical loading is attributed to the combination of the precipitation, the gas formation and biomass accumulation when microbial growth is favourable. To a certain extent the process can be directed towards one of the three products by selecting the right treatment regime, in order to obtain the desired properties for specific applications.

Overall in this thesis, MIDP has shown its capability to alter hydro-mechanical behaviour of sandy soils at laboratory scale. Both the precipitation of calcium carbonate and the biogenic formation of nitrogen gas may be applied for a wide range of ground improvement applications. For these applications, substrate concentrations and supplying regimes have to be appropriately selected to maintain a good microbial activity with negligible accumulation of toxic intermediate nitrogen compounds and obtain a high conversion rate and product yield. The formation, distribution and persistence of the gas phase, is also affected by substrate regime and environmental pressure conditions and grain size distribution of the soil. With the proposed models and simplified calculation methods presented in this thesis, these controlling factors can be studied to design the treatment procedure. Upscaling the investigation and optimizing it toward different specific applications are required for future work.

List of figures

Figure 1-1. Calcium carbonate precipitation induced by denitrification and its potential impact on a unit volume of soil.	17
Figure 1-2. Denitrification in the nitrogen cycle, figure reproduced from (Payne, 1981) and (op den Camp et al., 2006).....	18
Figure 2-1. Comparison of nitrate reduction through different pathways, reproduced from (Payne, 1981)	25
Figure 2-2. Stoichiometry of complete denitrification at different growth rate μ	32
Figure 3-1. Liquid batch incubation testing.....	35
Figure 3-2. Set-up of the sand column with multiple substrate flushes at ambient pressure	38
Figure 3-3. Comparison of changes in chemical composition during denitrification in the presence (left column) and absence (right column) of calcium ions during the 5th incubation. Legends indicate chemical compounds (TC is total dissolved carbon).....	40
Figure 3-4. Comparison of changes in chemical composition during denitrification in the presence of calcium at 3 different acetate:nitrate ratios in the 6th incubation. Left column: Ca:A:N = 55:60:50, A/N = 1.2; middle column: Ca:A:N = 45:40:50, A/N = 0.8 and right column: Ca:A:N = 40:30:50, A/N = 0.6. Legends indicate chemical compounds (TOC is total organic carbon).....	41
Figure 3-5. Volume changes in the triaxial tests at cell pressure – back pressure values of : (a) 350 kPa – 300 kPa; (b) 350 kPa – 345 kPa; (c) 100 – 50 kPa. The total volume change is the difference between the measured volume changes in the pressure cells.....	42
Figure 3-6. Measured values of (a) EC, (b) pH, (c) $[\text{NO}_3^-]$, (d) $[\text{NO}_2^-]$, (e) $[\text{Ca}^{+2}]$ and (f) Hydraulic conductivity for the sand column experiment at ambient pressure.	45
Figure 3-7. Result of the gas distribution in the sand column treated at ambient pressure with multiple substrate flushes: (a) the X-ray CT scanned images and (b) the constructed 3D image.....	46
Figure 3-8. CaCO_3 distribution in the sand column treated at ambient pressure.....	46
Figure 3-9. Presence of calcium carbonate in the sand treated with multiple substrate flushes at ambient pressure in ESEM images.....	47
Figure 4-1. The gas saturation induced by denitrification as a function of pore pressure, calculated for the stoichiometry of maximal growth (dash lines) and pure maintenance or zero growth (continuous lines), for three different concentrations of consumed NO_3^- : 20 mM (—), 50 mM (—) and 100 mM (—).....	56
Figure 4-2. Triaxial test set-up.....	57

Figure 4-3. Results of different sandy soil treated at 100 kPa back pressure - 200 kPa cell pressure	60
Figure 4-4. Results of fine sand ($d_{50} = 123\mu\text{m}$) treated at different pressure conditions, legend indicates controlled back pressure - cell pressure in kPa	60
Figure 4-5. Behaviour of the very fine sand, $d_{50} = 0.100$ mm, after treatment under undrained monotonic loading	62
Figure 4-6. Behaviour of the medium sand, $d_{50} = 0.250$ mm, after treatment under undrained monotonic loading	63
Figure 4-7. Induced gas saturation in sandy soil in correspondence with their boundaries. Range of gas saturation induced by denitrification between maximum growth (blue dash lines) and pure maintenance (blue dot lines); concentration of consumed NO_3^- 50 mM.	64
Figure 5-1. Modified triaxial test set-up used in the experiments.....	74
Figure 5-2. Substrate consumptions of the stock inoculum in	77
Figure 5-3. B-coefficient variation (top row), and changes of water saturation during the treatment periods and the effective pore area at the end of each treatments (bottom row).....	78
Figure 5-4. Flow rates after each treatments in low concentration regime	79
Figure 5-5. Flow rates during flushing after each treatment in high concentration regime	80
Figure 5-6. Nitrogen components and substrate consumption ratio after each treatments.....	81
Figure 5-7. Calculated NO_3^- consumption and DIC production from measured stoichiometric coefficients.....	82
Figure 5-8. Substrate consumption durations of the treatments in the low concentration regime	82
Figure 5-9. Amount of CaCO_3 w% along the sand sample	84
Figure 5-10. Dried cemented sand - (upper) after the treatment with high concentration; (lower) after the treatment with low concentration.....	84
Figure 5-11. Shearing results	85
Figure 5-12. ESEM image of a lump from Regime 2 of low substrate concentrations. CaCO_3 precipitation happened discretely resulting in large few crystals.....	86
Figure 6-1. Overview of the biological-chemical network of two-step denitrification based MICP	102
Figure 6-2. Stoichiometry of 2-step denitrification	105
Figure 6-3. Substrate consumption ratio Y_A/Y_N when there is no nitrite accumulation.....	106
Figure 6-4a. Fitting results for Case I, $A/N = 0.6$	108

List of figures

Figure 6-5a. Fitting results for Case II, $A/N = 0.8$, using fixed substrate limitation and inhibition constants in the case II-1 112

Figure 6-6. Calculated results of pH and calcite. Legend indicates the conditions of [stoichiometry, considered mechanisms, corresponding constants] 116

SUPPLEMENTAL DATA

S1. Supplemental data of the single treatment experiments – Pore and back pressure changes during the reacting period

In the single treatment experiments, back pressure was controlled at the defined value during the whole reacting period. Nevertheless, due to the gas production and gas in excess venting out, the pore and back pressure were intervened. These results are presented in Figure S-1

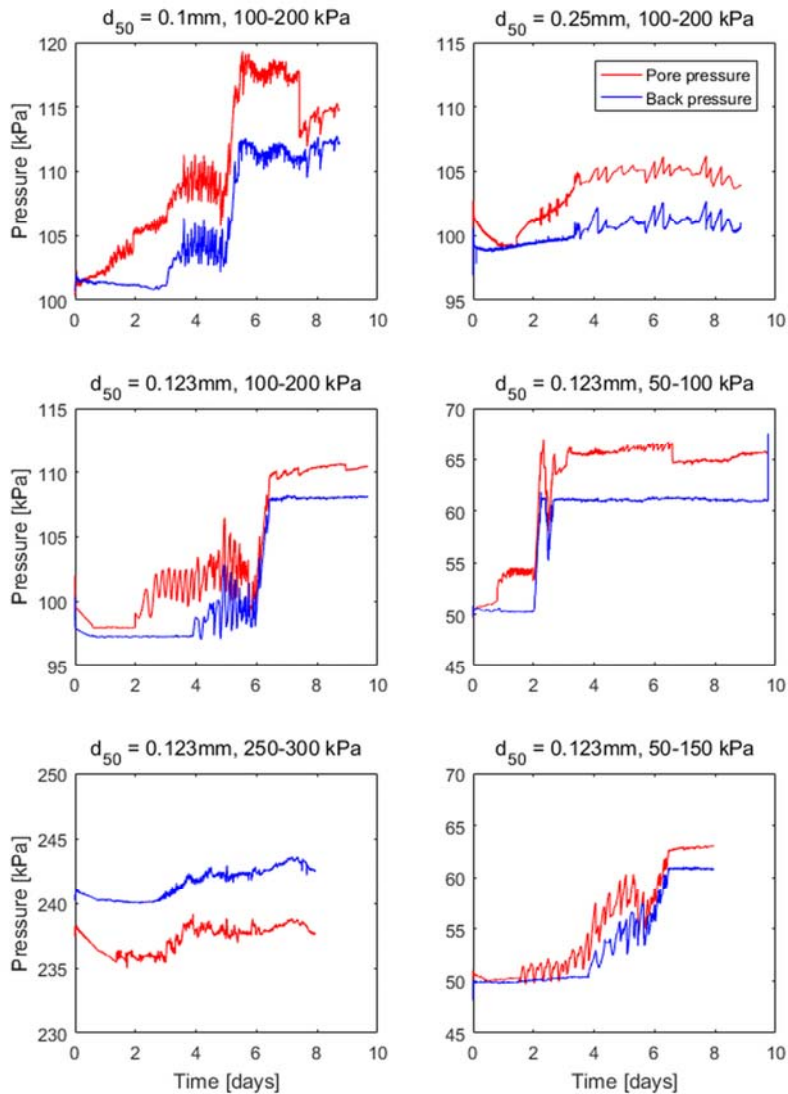


Figure S-1. Back and pore pressure changes during reacting periods of the single treatment experiments

S2. Supplemental data of the multiple treatment experiments

S2.1. Change of pore water volume and hydraulic conductivity

Table S-1 presents the detail reduction of water saturation and hydraulic conductivity of the samples throughout the experiments.

Table S-1. Changes of pore water volume and permeability

Exp.	Treat- ment	V _{inis} [mL]	V _{expelled} [mL]	V _{ends} [mL]	V _{replaced} [mL]	S _w [%]	S _{w-end} [%]	B _{ini} [%]	B _{end} [%]	K _{initial/revision} [cm/d]	K _{end} [cm/d]
(1) High conc.	1	196.5	57.2	139.2	30.5	100	71	98.4	1.3	83.30	24.75
	2	169.8	22.3	147.5	21.6	86	75	6.5	1.2	48.08	26.71
	3	169.0	21.4	147.6	20.7	86	75	6.0	3.2	55.42	7.98
	end	168.4				86		n.d.		43.73	
(2) Low conc.	1	201.9	49.8	152.1	18.3	100	75	94.7	n.d.	84.07	23.83
	2	170.4	17.2	153.2	20.6	84	76	n.d.	4.5	67.31	32.23
	3	173.8	15.9	157.8	23.6	86	78	5.7	n.d.	61.77	27.38
	4	181.5	16.8	164.7	20.4	90	82	7.3	3.8	58.17	23.13
	5	185.1	20.0	165.1	19.1	92	82	5.5	3.8	53.98	14.20
	6	184.1	19.7	164.4	20.3	91	81	5.7	3.6	43.06	14.17
	7	184.7	25.5	159.2	18.6	91	79	4.5	3.5	30.27	4.99
	8	177.8	12.9	164.9	12.8	88	82	4.9	3.8	20.49	4.57
	9	177.7	11.0	166.7	17.5	88	83	5.0	3.4	14.33	2.23
	10	184.2	11.7	172.5	5.6	91	85	4.1	3.0	5.29	0.91
	11	178.2	12.2	165.9	n.d.	88	n.d.	4.6	3.0	1.31	1.39
	12	n.d.	13.3	n.d.	n.d.	n.d.	n.d.	5.4	3.5	1.87	0.44
	13	n.d.	23.7	n.d.	n.d.	n.d.	n.d.	6.9	2.8	8.41	1.51
	14	n.d.	13.6	n.d.	n.d.	n.d.	n.d.	3.4	2.8	7.67	1.09
	15	n.d.	10.7	n.d.	n.d.	n.d.	n.d.	3.0	2.0	4.34	1.24
end	n.d.					n.d.		n.d.		5.81	

V_{inis} : the initial value of pore water of the sample in the beginning of the resident period of a treatment. In the first treatment of both the cases, V_{inis}⁽¹⁾ was the total pore volume after the consolidation step, corresponding with the fully saturated state;

V_{expelled}: pore water volume that was expelled from the sample to the back pressure controller due to the gas production during the resident time of each treatments;

V_{endS} : the final value of pore water in the sample at the end of a resident period:

$$V_{\text{endS}} = V_{\text{iniS}} - V_{\text{expelled}};$$

S_w and $S_{w\text{-end}}$: the water saturation degrees corresponding with the water pore volume V_{ini} and V_{end} over the total pore volume $V_{\text{ini}}^{(1)}$;

V_{replaced} : the mass difference between the total volume going in and out in the flushing step following a resident period, captured by the difference in the weight balances of the two pressure controller. This is the amount of water that replaced the unstable gas bubbles and remained inside the sample after flushing. Consequently, $V_{\text{iniS}}^{(i+1)}$ of the next resident period ($i+1$) is the result of $V_{\text{endS}}^{(i)}$ of the resident period (i) plus the refilled amount of $V_{\text{replaced}}^{(i)}$ in that period:

$$V_{\text{iniS}}^{(i+1)} = V_{\text{endS}}^{(i)} + V_{\text{replaced}}^{(i)};$$

B : the pore pressure coefficient, which is the ratio of pore pressure change over the change of cell pressure. $B_{\text{end}}^{(i)}$ was obtained at the end of the treatment (i) before flushing, and $B_{\text{ini}}^{(i+1)}$ was obtained after that flush.

K_{initial} : the hydraulic conductivity, or permeability, of the untreated sand, corresponding with the fully saturated state;

K_{end} : the hydraulic conductivity of the sample corresponding with the water saturation degree $S_{w\text{-end}}$. It is calculated with the outflow rate in the first 10 seconds of the flush.

K_{revised} : the regained value of permeability due to the gas replacement during flushing. It is calculated with the outflow rate in the last 10 seconds of the flush, corresponding with the water saturation S_w and the initial water pore volume of the next resident period (i.e. the next treatment).

In this table, V_{expelled} and V_{replaced} are the measured parameters, V_{iniS} and V_{endS} are directly interpreted from the measured volumes and used for water saturation S interpretation; B -coefficient is interpreted from pore and cell pressure measurements; K is calculated from the flow rates according to Darcy's law.

S2.2. Concentrations and volumes of the substrates in the flushes

Table S-2 presents the measured concentrations of substances in the newly substrates prepared for each resident period and in the residual liquid remaining inside the set-up at the end of those periods, together with the corresponding volumes .

Table S-2. Initial and end values of substances concentration in each treatments

	Treat-Resident ment period		Newly substrates						Liquid in back pressure controller		Residual substances				
			V _{in} [mL]	V _{ini} T [mL]	[Ca ⁺²] _{ini} [mM]	[Ac ⁻] _{ini} [mM]	[NO ₃ ⁻] _{ini} [mM]	[NO ₂ ⁻] _{ini} [mM]	V _{backw} [mL]	[Ca ⁺²] _{backw} [mM]	V _{end} T [mL]	[Ca ⁺²] _{end} [mM]	[Ac ⁻] _{end} [mM]	[NO ₃ ⁻] _{end} [mM]	[NO ₂ ⁻] _{end} [mM]
(1)	1	16	⁽¹⁾ 201.5	201.5	124.8	140.9	103.7	0.00	550.6	13.70	144.2	3.2	0.0	2.30	1.81
High	2	10	369.8	225.0	134.1	139.0	108.9	0.07	381.4	28.80	152.5	94.5	99.4	31.54	33.43
conc.	3	10	285.3	195.0	139.2	137.2	106.3	0.00	474.0	20.30	152.7	114.6	115.1	62.66	23.45
	end		342.9	225.0	0.18	n.d.	0.01	0.00							

Table S-3 (cont.). Initial and end values of substances concentration in each treatments

	Treat-Resident ment period	[days]	Newly substrates					Liquid in back pressure controller		Residual substances					
			V _{in}	V _{iniT}	[Ca ⁺²] _{ini}	[Ac ⁻] _{ini}	[NO ₃ ⁻] _{ini}	[NO ₂ ⁻] _{ini}	V _{backw}	[Ca ⁺²] _{backw}	V _{endT}	[Ca ⁺²] _{end}	[Ac ⁻] _{end}	[NO ₃ ⁻] _{end}	[NO ₂ ⁻] _{end}
			[mL]	[mL]	[mM]	[mM]	[mM]	[mM]	[mL]	[mM]	[mL]	[mM]	[mM]	[mM]	[mM]
(2)	1	5	⁽¹⁾ 210.0	210.0	28.8	25.2	20.0	0.00	521.8	6.9	174.4	4.74	n.d.	2.40	0.126
Low conc.	2	2	300.9	220.0	27.6	20.6	20.1	0.00	319.3	7.7	202.8	7.21	4.37	1.18	0.015
	3	2	294.4	240.0	25.3	20.3	19.3	0.00	366.1	8.3	224.1	7.35	5.57	1.54	0.069
	4	3	319.1	240.0	25.6	22.7	20.2	0.00	401.1	9.4	223.2	9.03	5.92	1.74	0.010
	5	2	314.0	240.0	26.5	27.9	20.6	0.00	408.6	9.9	220.0	9.68	7.50	1.27	0.037
	6	2	307.8	240.0	24.0	27.1	21.1	0.00	412.4	7.7	220.3	8.44	n.d.	0.87	0.037
	7	3	306.9	240.0	26.9	27.4	20.7	0.00	399.2	8.0	214.5	8.45	5.35	0.96	0.000
	8	2	282.5	230.0	26.9	n.d.	n.d.	n.d.	369.2	9.0	217.1	7.64	4.90	0.34	0.003
	9	2	290.8	220.0	26.8	25.8	19.9	0.00	506.8	8.8	209.0	7.25	3.78	0.37	0.003
	10	3	362.7	210.0	27.0	27.7	21.3	0.00	455.9	4.0	198.3	7.00	3.42	0.04	0.002
	11	2	⁽²⁾ 211.0	210.0	27.2	27.8	20.7	0.00	446.4	9.2	197.8	7.69	4.80	0.03	0.002
	12	2	314.9	220.0	29.1	27.5	20.8	0.00	390.6	8.7	206.7	7.98	4.20	0.03	0.004
	13	3	298.2	220.0	28.7	27.5	20.9	0.00	483.5	8.8	196.3	7.10	3.68	0.04	0.004
	14	2	314.3	190.0	29.0	27.2	20.7	0.00	442.6	10.0	176.4	7.28	3.95	0.02	0.001
	15	2	335.6	210.0	29.0	26.7	21.4	0.01	409.8	2.5	199.3	7.39	n.d.	0.03	0.004
	end			288.7	210.0	0.19	n.d.	0.01	0.00						

⁽¹⁾This is the volume being mixed with the sand in the preparation step.

⁽²⁾This is the volume in the 10th flush preparing for the 11th treatment, the hydraulic conductivity became very low that this volume took about 5 hours. The flush was stopped due to the time limit of the experiment.

In this table:

- V_{in} : total volume of newly substrate solution which had been flushed in each treatment. In the first treatment, this is the volume to be used when preparing samples in the step (1). In other following treatments, this is the mass difference of the third controller before and after the flush.
- V_{iniT} : volume of newly substrate solution staying inside the set-up after flushing ready for the resident period, it covered all the pore volume of the sample and the tubing. It was identified from the EC breakthrough curves presented in the following section. In each curve, V_{iniT} is the volume corresponding with the mean value of the max and minimum EC in that curve.
- V_{backw} : volume of the liquid in the back pressure controller at the end of flushing. This liquid was the mixture of the demi-deaired water from the beginning of a resident period, the expelled liquid from the sample during that resident period, and the excess newly substrate liquid after flushing.
- $[Ca^{+2}]_{backw}$: calcium concentration measured in the V_{backw} .
- V_{endT} : volume of the residual liquid inside the set-up at the end of the resident period;
 $V_{iniT} - V_{endT} = V_{expelled}$.
- $[Ca^{+2}]_{ini}$, $[Ac]_{ini}$, $[NO_3^-]_{ini}$, $[NO_2^-]_{ini}$: initial concentrations of calcium, acetate, nitrate and nitrite at the beginning of a resident period. They were measured from the newly substrate solution that had been added into the third controller for flushing.
- $[Ca^{+2}]_{end}$, $[Ac]_{end}$, $[NO_3^-]_{end}$, $[NO_2^-]_{end}$: the final concentration at the end of a resident period. They were measured from the samples that had been taken during flushing, whose EC values stay constant in the first part of the breakthrough curve.

S2.3. Breakthrough curves of electrical conductivity EC of the outflows during flushing

EC breakthrough curves of the outflows during flushing were used to identify when the newly substrate solution completely replaces the residual liquid from the previous treatment in the whole set-up. The replacing volume of the newly substrate solution that stays inside the set-up for a new resident period (V_{iniT}) is the volume corresponding with the mean value of the max and minimum EC in that curve.

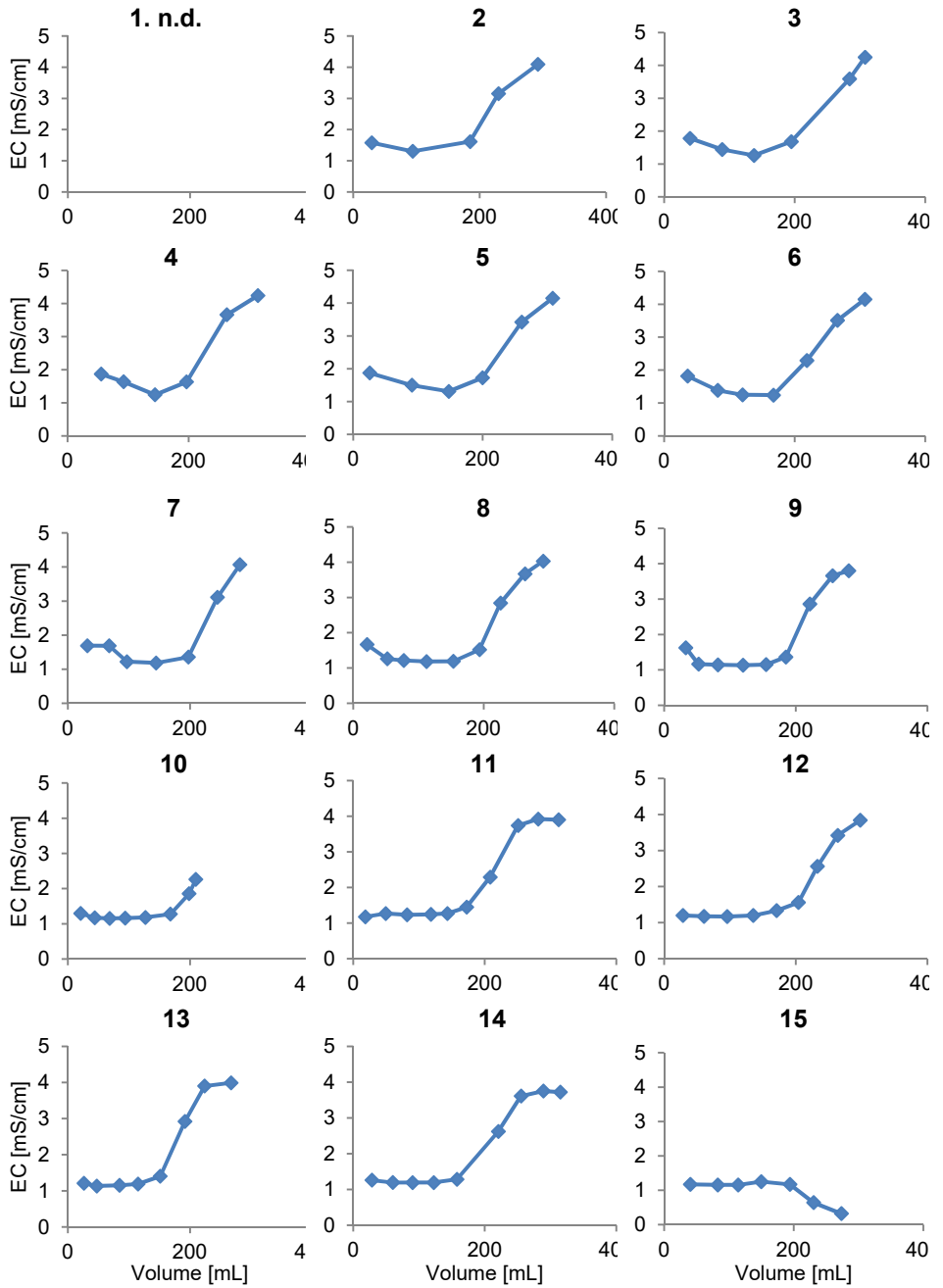


Figure S-2. EC breakthrough curve during flushing after each treatments of the low concentration experiment

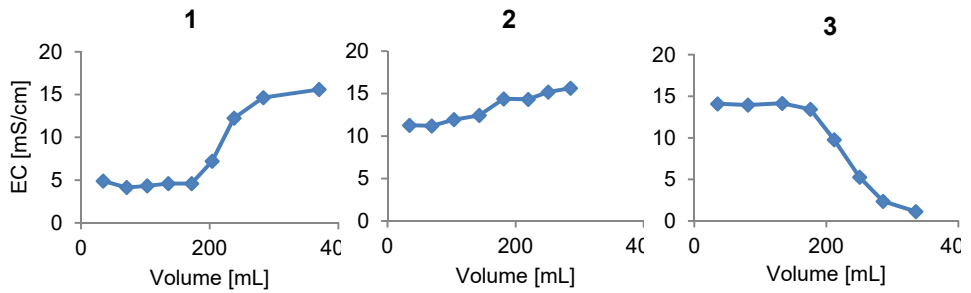


Figure S-3. EC breakthrough curve during flushing after each treatments of the high concentration experiment

S2.4. Substrate consumption during the treatments

Substrate consumption during the treatments of the two regimes are calculated in Table S-4. These results were calculated from the volumes and corresponding measured concentrations which are presented in Table S-2, Figure S-2 and Figure S-3.

Table S-4. Substrate consumption during treatment

Treat- ment	Resident period [days]	Acetate [mmol]					Nitrate [mmol]					Nitrite	Ac/N				
		$n_{\text{iniT}^{\text{Ac}}}$	$n_{\text{endT}^{\text{Ac}}}$	$n_{\text{expelled}^{\text{Ac}}}$ max min		$n_{\text{reacted}^{\text{Ac}}}$	Rate ^{Ac}	$n_{\text{iniT}^{\text{N}}}$	$n_{\text{endT}^{\text{N}}}$	$n_{\text{expelled}^{\text{N}}}$ max min		$n_{\text{reacted}^{\text{N}}}$	Rate ^N	$n_{\text{endT}^{\text{N}}}$			
Stock inoculum in batch liquid (1)	7	27.2	11.4	-		15.9	6.0	19.9	0.00	-		19.9	7.5	0.00	0.8		
High conc.	16	28.4	0.0	8.06	0.00	28.4	20.3	>6.3	20.9	0.33	5.94	0.13	20.4	14.6	>4.5	0.26	1.5±0.4
	10	31.3	20.1	3.10	2.22	8.91	8.03	3.6÷4.6	24.5	6.39	2.43	0.70	17.4	15.7	7.0÷7.7	6.74	0.5±0.05
	10	26.8	20.0	2.93	2.46	4.31	3.84	2.0÷2.2	20.7	10.9	2.27	1.34	8.51	7.57	3.9÷4.4	4.07	0.5±0.05

Table S-5 (cont.). Substrate consumption during treatment

Treatment	Resident period [days]	Acetate [mmol]								Nitrate [mmol]						Nitrite	Ac/N				
		n _{init} ^{Ac}		n _{end} ^{Ac}		n _{expelled} ^{Ac}		n _{reacted} ^{Ac}		Rate ^{Ac}	n _{init} ^N		n _{end} ^N		n _{expelled} ^N		n _{reacted} ^N		Rate ^N	n _{end} ^N	
		max	min	max	min	max	min	max	min	[mM/d]	max	min	max	min	max	min	max	min	[mM/d]		
Low conc.	1	5	5.29	n.d.	1.26	n.d.	n.d.	n.d.	(-)	4.19	0.42	0.99	0.12	3.66	2.78	(-)	0.02	n.d.			
	2	2	4.53	0.89	0.35	0.08	3.57	3.29	>7.5	4.42	0.24	0.35	0.02	4.16	3.84	>8.7	0.00	0.8±0.05			
	3	2	4.88	1.25	0.32	0.09	3.54	3.31	>6.9	4.64	0.34	0.31	0.02	4.27	3.99	>8.3	0.02	0.8±0.05			
	4	3	5.45	1.32	0.38	0.10	4.03	3.75	(-)	4.84	0.39	0.34	0.03	4.43	4.12	(-)	0.00	0.8±0.10			
	5	2	6.71	1.65	0.56	0.15	4.91	4.50	>9.4	4.94	0.28	0.41	0.03	4.63	4.25	>8.6	0.01	1.0±0.10			
	6	2	6.52	n.d.	0.54	n.d.	n.d.	n.d.	n.d.	5.05	0.19	0.42	0.02	4.84	4.45	>9.2	0.01	n.d.			
	7	3	6.58	1.15	0.70	0.14	5.29	4.73	(-)	4.97	0.21	0.53	0.02	4.74	4.24	(-)	0.00	1.0±0.10			
	8	2	n.d.	1.06	n.d.	0.06	n.d.	n.d.	n.d.	n.d.	0.07	n.d.	0.00	n.d.	n.d.	n.d.	0.00	n.d.			
	9	2	5.69	0.79	0.29	0.04	4.85	4.61	>10.5	4.37	0.08	0.22	0.00	4.29	4.08	>9.3	0.00	1.1±0.05			
	10	3	5.82	0.68	0.32	0.04	5.11	4.82	(-)	4.47	0.01	0.25	0.00	4.46	4.21	(-)	0.00	1.1±0.05			
	11	2	5.83	0.95	0.34	0.06	4.82	4.54	>10.8	4.36	0.01	0.25	0.00	4.35	4.10	>9.6	0.00	1.0±0.10			
	12	2	6.05	0.87	0.37	0.06	5.13	4.81	>10.9	4.57	0.01	0.28	0.00	4.56	4.29	>9.7	0.00	1.1±0.05			
	13	3	6.06	0.72	0.65	0.09	5.25	4.69	(-)	4.60	0.01	0.50	0.00	4.59	4.10	(-)	0.00	1.0±0.15			
	14	2	5.16	0.70	0.37	0.05	4.41	4.10	>10.8	3.94	0.00	0.28	0.00	3.94	3.66	>9.6	0.00	1.0±0.10			
	15	2	5.62	0.20	0.29	0.01	5.41	5.13	>12.2	4.49	0.01	0.23	0.00	4.48	4.25	>10.1	0.00	1.1±0.10			

- n_{iniT} Amount of the substrate in the set-up in the beginning of a resident period, it is correspondent with V_{iniT} and initial concentration of the substrate;
- n_{endT} Amount of the substrate in the set-up in the end of a resident period, it is correspondent with V_{endT} and the final concentration of the substrate;
- $n_{expelled}$ Amount that had been expelled out of the set-up to the back pressure controller during a resident period. In the expelled liquid $V_{expelled}$, concentrations of the solute substances had to be between the initial and residual concentrations, so $n_{expelled\ max}$ was calculated with the initial concentration, and $n_{expelled\ min}$ was calculated with the residual concentration
- $n_{reacted}$ The amount of the substrates that had been consumed in a resident period between each flush, it was calculated as: $n_{reacted} = n_{iniT} - n_{endT} - n_{expelled}$.
- Rate The consumption rates were calculated as the quotients of the reacted amounts and the corresponding resident times and the total liquid volumes of the set-up at the beginning of those resident periods and thus assumed a constant rate between flushes and did not take into account effects of desaturation. Between flushes in which one of the substrates were nearly consumed, only the minimum rates were identified. In the low concentration regime, the amounts of residual substances in the 2-day and 3-day duration treatments were similar, so the consumption rate was calculated only for the 2-day durations. From these results, ranges of the substrate consumption ratio Ac/N were calculated accordingly.

Stoichiometry corresponding with this substrate consumption ratio and leftover NO_2^- is calculated following the microbial energy approach suggested by Heijnen et.al. (2010). Result of the stoichiometric coefficients in each treatments are as followed:

Table S- 6. Calculated stoichiometry of the reactions in each treatments

Treatments		$C_2H_3O_2^-$	NO_3^-	NO_2^-	N_2	H_2O	H_2CO_2	H^+	$CH_{1.8}O_{0.5}N_{0.2}$
Regime H	1	-1.386	-1.258	0	0.529	0.729	1.773	-2.644	1
	2, 3	-2.537	-4.391	2.153	1.019	1.219	4.074	-4.775	1
Regime L	1-3	-2.344	-2.790	0	1.295	1.495	3.688	-5.134	1
	4	-1.913	-2.101	0	0.950	1.150	2.826	-4.014	1
	5-15	-1.386	-1.258	0	0.529	0.729	1.773	-2.644	1

S2.5. Estimating the amount of Ca^{+2} reacted for CaCO_3 precipitation from the concentration measurements

The amount of precipitated CaCO_3 in the whole set-up, presented in Table S-7, was estimated similarly to the identification of the reacted substrates above but for the whole experiments, which considered the total amounts of all the resident periods. This interpretation considered the calcium balance within the total reaction times, i.e.: $\text{total } n_{\text{iniT}} = \text{total } n_{\text{endT}} + \text{total } n_{\text{expelled}} + \text{total } n_{\text{reacted}}$. From this balance, the reacted calcium is estimated, n_{reacted} [estimated], in the range of 29.8÷38.0 mmol for the high concentration regime, and 59.6÷65.1 mmol for the low concentration regime.

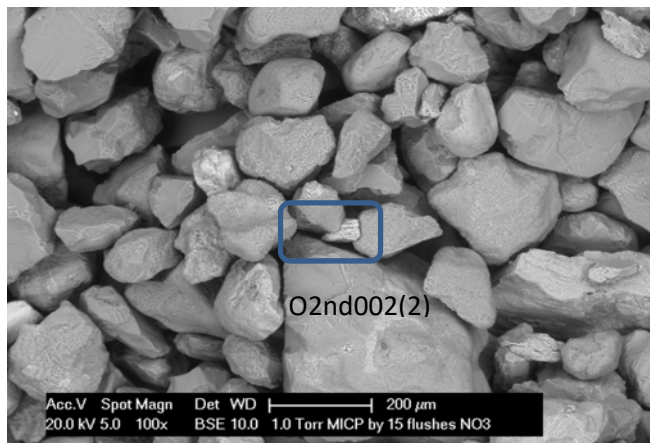
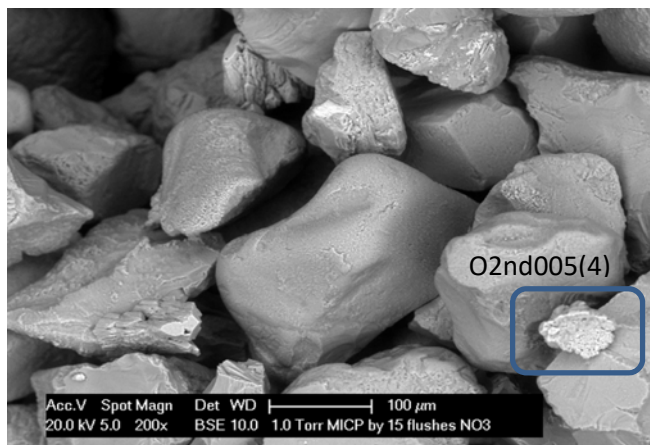
Besides, total amount of precipitated calcium in the whole set-up was also identified directly from the balance of total supplied calcium. In this balance, the total supply n_{in} covers the reacted amount n_{reacted} , the leftover during resident durations and the unused amount in the excess liquid during flushing. Back pressure controller was the container for those leftover and unused amounts, n_{backw} , as after each flush it contained the unreacted amount in the expelled liquid and the residual in the set-up from the previous treatment together with excess amount of the current flush. Therefore: $\text{total } n_{\text{in}} = \text{total } n_{\text{reacted}} + \text{total } n_{\text{backw}}$. In this interpretation, total n_{in} and total n_{backw} was calculated from direct measurements of volume and concentration (results presented in Table S-2 of the Supplementary Data), so the calculated n_{reacted} is assigned as the measured value n_{reacted} [measured] in Table S-7.

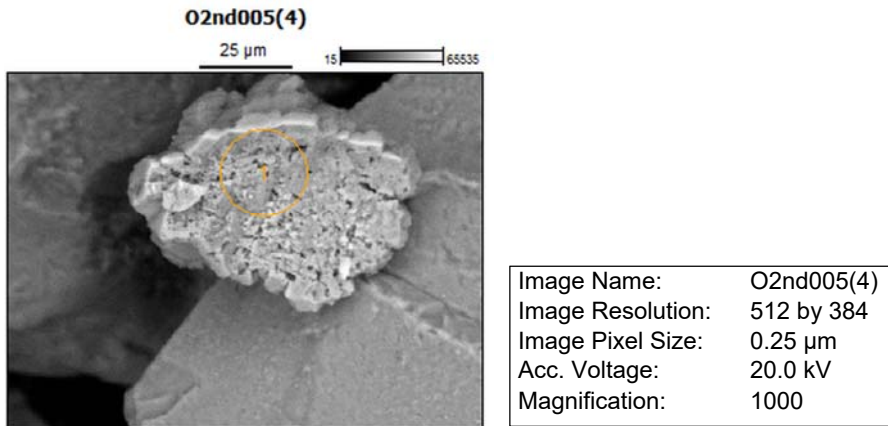
Table S-7. Reacted calcium for CaCO₃ precipitation

	Treat- ment	n_{in}^{Ca}	n_{iniT}^{Ca}	n_{endT}^{Ca}	$n_{expelled}^{Ca}$ [mmol]		n_{backw}^{Ca}	$n_{reacted}^{Ca}$ [mmol]	
		[mmol]	[mmol]	[mmol]	max	min	[mmol]	estimated	measured
(1) High conc.	1	25.14	25.14	0.45	7.14	0.18	22.63		
	2	49.59	30.17	19.16	2.99	2.11	32.95		
	3	39.71	27.14	19.90	3.00	2.45	28.86		
	End	0.06	0.04						
Total		114.4	82.5	39.55	13.1	4.74	84.4	29.8÷38.	30.0
(2) Low conc.	1	6.05	6.05	0.83	1.43	0.24	3.62		
	2	8.30	6.07	1.46	0.47	0.12	2.45		
	3	7.46	6.08	1.65	0.40	0.12	3.04		
	4	8.18	6.16	2.01	0.43	0.15	3.75		
	5	8.32	6.36	2.13	0.53	0.19	4.04		
	6	7.39	5.76	1.86	0.47	0.17	3.16		
	7	8.26	6.46	1.81	0.69	0.22	3.19		
	8	7.60	6.19	1.66	0.35	0.10	3.32		
	9	7.79	5.90	1.52	0.30	0.08	4.43		
	10	9.79	5.67	1.39	0.31	0.08	1.84		
	11	5.74	5.71	1.52	0.33	0.09	4.12		
	12	9.16	6.40	1.65	0.39	0.11	3.38		
	13	8.56	6.31	1.39	0.68	0.17	4.23		
	14	9.11	5.51	1.28	0.39	0.10	4.43		
	15	9.73	6.09	1.47	0.31	0.08	1.02		
End		0.05	0.04						
Total		121.5	90.76	23.63	7.50	2.01	50.02	59.6÷65.	71.5

S2.6. ESEM images and XRF analysis results of large precipitated crystals

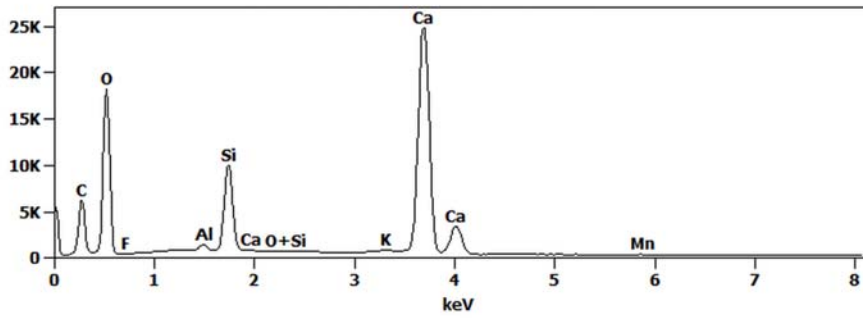
A dried lump taken in the middle of treated sand was scanned using Philips ESEM XL30. Two large crystals were zoomed in and XRF analysis was performed to analyse their chemical components.





Full scale counts: 24723

O2nd005(4)_pt1



SUPPLEMENTAL DATA

Weight %

	<i>C-K</i>	<i>O-K</i>	<i>F-K</i>	<i>Al-K</i>	<i>Si-K</i>	<i>K-K</i>	<i>Ca-K</i>	<i>Mn-K</i>
<i>O2nd005(4)_p</i>								
<i>t1</i>	14.15	57.76	0.00	0.32	4.85	0.09	22.75	0.08

Atom %

	<i>C-K</i>	<i>O-K</i>	<i>F-K</i>	<i>Al-K</i>	<i>Si-K</i>	<i>K-K</i>	<i>Ca-K</i>	<i>Mn-K</i>
<i>O2nd005(4)_p</i>								
<i>t1</i>	21.25	65.12	0.00	0.21	3.11	0.04	10.24	0.03

Formula

	<i>C-K</i>	<i>O-K</i>	<i>F-K</i>	<i>Al-K</i>	<i>Si-K</i>	<i>K-K</i>	<i>Ca-K</i>	<i>Mn-K</i>
<i>O2nd005(4)_pt1</i>	C	O	F	Al	Si	K	Ca	Mn

Compound %

	<i>C</i>	<i>O</i>	<i>F</i>	<i>Al</i>	<i>Si</i>	<i>K</i>	<i>Ca</i>	<i>Mn</i>
<i>O2nd005(4)_p</i>								
<i>t1</i>	14.15	57.76	0.00	0.32	4.85	0.09	22.75	0.08

Norm. Compound %

	<i>C</i>	<i>O</i>	<i>F</i>	<i>Al</i>	<i>Si</i>	<i>K</i>	<i>Ca</i>	<i>Mn</i>
<i>O2nd005(4)_p</i>								
<i>t1</i>	14.15	57.76	0.00	0.32	4.85	0.09	22.75	0.08

Cations

	<i>C-K</i>	<i>O-K</i>	<i>F-K</i>	<i>Al-K</i>	<i>Si-K</i>	<i>K-K</i>	<i>Ca-K</i>	<i>Mn-K</i>
<i>O2nd005(4)_pt</i>								
<i>1</i>	0.00	0.00	0.00	0.00	0.00	0.00	0.00	0.00

Standard Name

	<i>C-K</i>	<i>O-K</i>	<i>F-K</i>	<i>Al-K</i>	<i>Si-K</i>	<i>K-K</i>	<i>Ca-K</i>	<i>Mn-K</i>
<i>O2nd005(4)_pt1</i>								

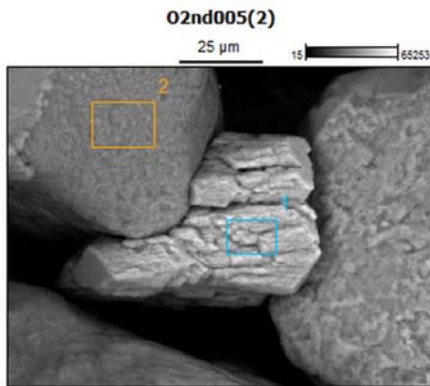
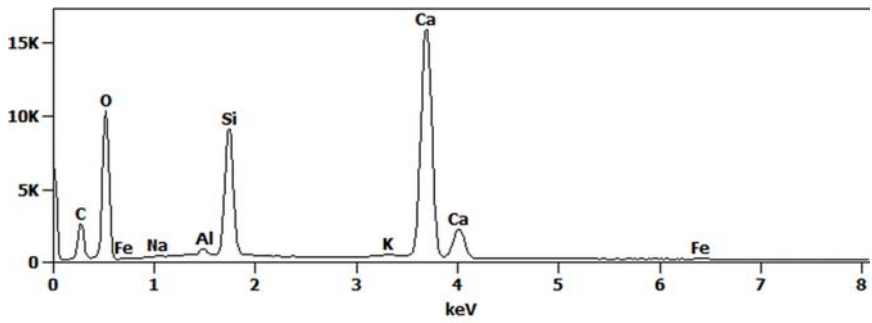


Image Name:	O2nd005(2)
Image Resolution:	512 by 384
Image Pixel Size:	0.25 μm
Acc. Voltage:	20.0 kV
Magnification:	1000

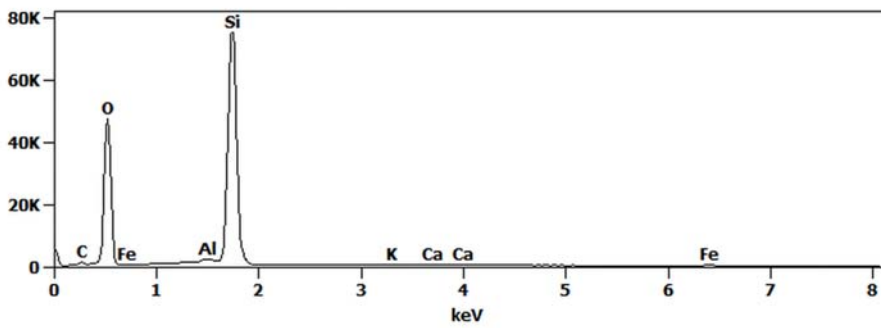
Full scale counts: 15889

O2nd005(2)_pt1



Full scale counts: 75244

O2nd005(2)_pt2



SUPPLEMENTAL DATA

Weight %

	<i>C-K</i>	<i>O-K</i>	<i>Na-K</i>	<i>Al-K</i>	<i>Si-K</i>	<i>K-K</i>	<i>Ca-K</i>	<i>Fe-K</i>
<i>O2nd005(2)_p</i>					7.58			
<i>t1</i>	11.11	55.93	0.12	0.37		0.18	24.46	0.26
<i>O2nd005(2)_p</i>	3.19						0.14	
<i>t2</i>		63.47		0.45	32.40	0.07		0.27

Atom %

	<i>C-K</i>	<i>O-K</i>	<i>Na-K</i>	<i>Al-K</i>	<i>Si-K</i>	<i>K-K</i>	<i>Ca-K</i>	<i>Fe-K</i>
<i>O2nd005(2)_p</i>					5.06			
<i>t1</i>	17.36	65.60	0.09	0.26		0.09	11.45	0.09
<i>O2nd005(2)_p</i>	4.90						0.07	
<i>t2</i>		73.29		0.31	21.31	0.03		0.09

Formula

	<i>C-K</i>	<i>O-K</i>	<i>Na-K</i>	<i>Al-K</i>	<i>Si-K</i>	<i>K-K</i>	<i>Ca-K</i>	<i>Fe-K</i>
<i>O2nd005(2)_pt1</i>	C	O	Na	Al	Si	K	Ca	Fe
<i>O2nd005(2)_pt2</i>	C	O		Al	Si	K	Ca	Fe

Compound %

	<i>C</i>	<i>O</i>	<i>Na</i>	<i>Al</i>	<i>Si</i>	<i>K</i>	<i>Ca</i>	<i>Fe</i>
<i>O2nd005(2)_p</i>					7.58			
<i>t1</i>	11.11	55.93	0.12	0.37		0.18	24.46	0.26
<i>O2nd005(2)_p</i>	3.19						0.14	
<i>t2</i>		63.47		0.45	32.40	0.07		0.27

Norm. Compound %

	<i>C</i>	<i>O</i>	<i>Na</i>	<i>Al</i>	<i>Si</i>	<i>K</i>	<i>Ca</i>	<i>Fe</i>
<i>O2nd005(2)_p</i>					7.58			
<i>t1</i>	11.11	55.93	0.12	0.37		0.18	24.46	0.26
<i>O2nd005(2)_p</i>	3.19						0.14	
<i>t2</i>		63.47		0.45	32.40	0.07		0.27

Cations

	<i>C-K</i>	<i>O-K</i>	<i>Na-K</i>	<i>Al-K</i>	<i>Si-K</i>	<i>K-K</i>	<i>Ca-K</i>	<i>Fe-K</i>
<i>O2nd005(2)_pt</i>								
<i>1</i>	0.00	0.00	0.00	0.00	0.00	0.00	0.00	0.00
<i>O2nd005(2)_pt</i>								
<i>2</i>	0.00	0.00		0.00	0.00	0.00	0.00	0.00

Standard Name

	<i>C-K</i>	<i>O-K</i>	<i>Na-K</i>	<i>Al-K</i>	<i>Si-K</i>	<i>K-K</i>	<i>Ca-K</i>	<i>Fe-K</i>
<i>O2nd005(2)_pt1</i>								
<i>O2nd005(2)_pt2</i>								

S2.7. Pore pressure response during the resident time

During the resident time, gas formation and transport of the gas and liquid phase interfered both the pore pressure and the controlled back pressure inside the samples. These results are presented in the following figure.

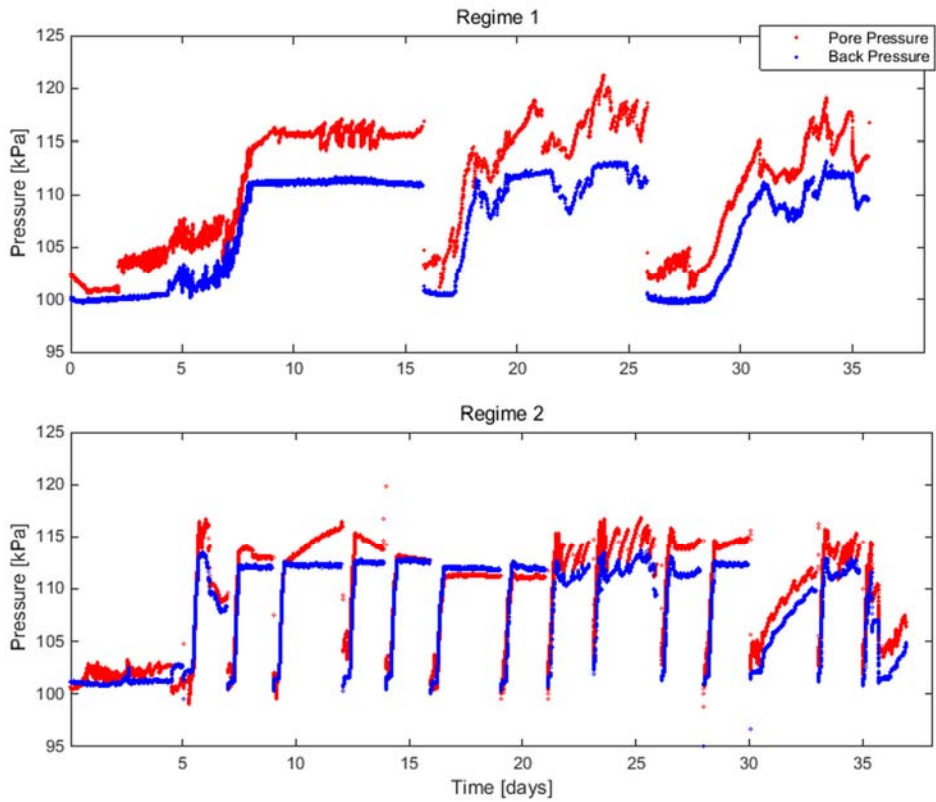


Figure S-4. Pressure changes inside samples during the resident time

References

- Almeida, J. S., Julio, S. M., Reis, M. a. M. & Carrondo, M. J. T. 1995. Nitrite inhibition of denitrification by *Pseudomonas fluorescens*. *Biotechnology and Bioengineering*, 46, 194-201.
- Andrews, J. F. 1968. A mathematical model for the continuous culture of microorganisms utilizing inhibitory substrates. *Biotechnology and Bioengineering*, 10, 707-723.
- Archana, S. K. S. & Sobti, R. C. 2012. Nitrate Removal from Ground Water: A Review. *E-Journal of Chemistry*, 9, 1667-1675.
- Armstrong, R. T., Evseev, N., Koroteev, D. & Berg, S. 2015. Modeling the velocity field during Haines jumps in porous media. *Advances in Water Resources*, 77, 57-68.
- Baveye, P., Vandevivere, P., Hoyle, B. L., Deleo, P. C. & De Lozada, D. S. 1998. Environmental impact and mechanisms of the biological clogging of saturated soils and aquifer materials. *Critical reviews in environmental science and technology*, 28, 123-191.
- Betlach, M. R. & Tiedje, J. M. 1981. Kinetic Explanation for Accumulation of Nitrite, Nitric Oxide, and Nitrous Oxide During Bacterial Denitrification. *Applied and Environmental Microbiology*, 42, 1074-1084.
- Blander, M. & Katz, J. L. 1975. Bubble nucleation in liquids. *AIChE Journal*, 21, 833-848.
- Broadbent, S. R. & Hammersley, J. M. 1957. Percolation processes: I. Crystals and mazes. *Mathematical Proceedings of the Cambridge Philosophical Society*, 53, 629-641.
- Brooks, R. H. & Corey, A. T. 1964. *Hydraulic Properties of Porous Media*, Colorado State University.
- Burbank, M. B., Weaver, T. J., Green, T. L., Williams, B. C. & Crawford, R. L. 2011. Precipitation of Calcite by Indigenous Microorganisms to Strengthen Liquefiable Soils. *Geomicrobiology Journal*, 28, 301-312.
- Carrera, J., Jubany, I., Carvallo, L., Chamy, R. & Lafuente, J. 2004. Kinetic models for nitrification inhibition by ammonium and nitrite in a suspended and an immobilised biomass systems. *Process Biochemistry*, 39, 1159-1165.
- Castegnier, F., Ross, N., Chapuis, R. P., Deschênes, L. & Samson, R. 2006. Long-term persistence of a nutrient-starved biofilm in a limestone fracture. *Water Research*, 40, 925-934.
- Cen 2004. ISO/TS 17892-9:2004 Geotechnical investigation and testing - Laboratory testing of soil - Part 9: Consolidated triaxial compression tests on water saturated soil. European Committee For Standardization.
- Cheng, L., Cord-Ruwisch, R. & Shahin, M. A. 2013. Cementation of sand soil by microbially induced calcite precipitation at various degrees of saturation. *Canadian Geotechnical Journal*, 50, 81-90.
- Chu, J., Stabnikov, V. & Ivanov, V. 2012. Microbially Induced Calcium Carbonate Precipitation on Surface or in the Bulk of Soil. *Geomicrobiology Journal*, 29, 544-549.

- Chung, Y.-C. & Chung, M.-S. 2000. BNP test to evaluate the influence of C/N ratio on N₂O production in biological denitrification. *Water Science and Technology*, 42, 23-27.
- Cole, J. A. 1990. Physiology, Biochemistry and Genetics of Nitrate Dissimilation to Ammonia. In: REVSBECH, N. P. & SØRENSEN, J. (eds.) *Denitrification in Soil and Sediment*. Boston, MA: Springer US.
- Das, B. M. 2007. *Principles of Foundation Engineering, 6th Edition*, Thomson.
- Davis, A. M. 1992. Shallow gas: an overview. *Continental Shelf Research*, 12, 1077-1079.
- Dejong, J., Martinez, B., Ginn, T., Hunt, C., Major, D. & Tanyu, B. 2014. Development of a Scaled Repeated Five-Spot Treatment Model for Examining Microbial Induced Calcite Precipitation Feasibility in Field Applications.
- Dejong, J. T., Fritzes, M. B. & Nüsslein, K. 2006. Microbially Induced Cementation to Control Sand Response to Undrained Shear. *Journal of Geotechnical and Geoenvironmental Engineering*, 132, 1381-1392.
- Dejong, J. T., Martinez, B. C., Mortensen, B. M., Nelson, D. C., Waller, J. T., Weil, M. H., Ginn, T. R., Weathers, T., Barkouki, T., Fujita, Y., Redden, G., Hunt, C., Major, D. & Tanyu, B. 2009. Upscaling of Bio-Mediated Soil Improvement. In: HAMZA, M., SHAHIEN, M. & EL-MOSSALLAMY, Y. (eds.) *17th International Conference on Soil Mechanics and Geotechnical Engineering*. Egypt: IOS Press.
- Dejong, J. T., Soga, K., Kavazanjian, E., Burns, S., Van Paassen, L. A., Qabany, A. A., Aydilek, A., Bang, S. S., Burbank, M., Caslake, L. F., Chen, C. Y., Cheng, X., Chu, J., Jefferis, S., Kuo, M., Laloui, L., Larrahondo, J., Manning, D. a. C., Martinez, B., Montoya, B. M., Nelson, D. C., Palomino, A., Renforth, P., Santamarina, J. C., Seagren, E. A., Tanyu, B., Tsesarsky, M. & Weaver, T. 2013. Biogeochemical process and geotechnical applications: progress, opportunities and challenges. *Geotechnique*, 63.
- Dhamole, P. B., Nair, R. R., D'souza, S. F. & Lele, S. S. 2007. Denitrification of high strength nitrate waste. *Bioresource Technology*, 98, 247-252.
- Dominguez, A., Bories, S. & Prat, M. 2000. Gas cluster growth by solute diffusion in porous media. Experiments and automaton simulation on pore network. *International Journal of Multiphase Flow*, 26, 1951-1979.
- Edwards, V. H. 1970. The influence of high substrate concentrations on microbial kinetics. *Biotechnology and Bioengineering*, 12, 679-712.
- Erşan, Y. Ç., Belie, N. D. & Boon, N. 2015. Microbially induced CaCO₃ precipitation through denitrification: An optimization study in minimal nutrient environment. *Biochemical Engineering Journal*, 101, 108-118.
- Feng, K. & Montoya, B. M. 2016. Influence of Confinement and Cementation Level on the Behavior of Microbial-Induced Calcite Precipitated Sands under Monotonic Drained Loading. *Journal of Geotechnical and Geoenvironmental Engineering*, 142, 04015057.
- Ferguson, S. J. 1994. Denitrification and its control. *Antonie van Leeuwenhoek*, 66, 89-110.
- Fredlund, D. G., Rahardjo, H. & Fredlund, M. D. 2012. *Unsaturated Soil Mechanics in Engineering Practice*, John Wiley & Sons, Inc.

- Gauglitz, P. A. & Radke, C. J. 1989. Dynamics of Haines Jumps for Compressible Bubbles in Contracted Capillaries. *American Institute of Chemical Engineers Journal*, 35.
- Gerlach, R. & Cunningham, A. B. 2010. Chapter 5. Influence of Biofilms on Porous Media Hydrodynamics. In: VAFAI, K. (ed.) *Porous Media: Application in Biological Systems and Biotechnology*. CRC Press Taylor Francis Group.
- Glass, C. & Silverstein, J. 1998. Denitrification kinetics of high nitrate concentration water: pH effect on inhibition and nitrite accumulation. *Water Research*, 32, 831-839.
- Grozic, J. L., Robertson, P. K. & Morgenstern, N. R. 1998. The behavior of loose gassy sand. *Canadian Geotechnical Journal*, 36, 482-492.
- Guelon, T., Mathias, J.-D. & Stoodley, P. 2011. Advances in Biofilm Mechanics. In: FLEMMING, H.-C., WINGENDER, J. & SZEWZYK, U. (eds.) *Biofilm Highlights*. Berlin: Springer Berlin Heidelberg.
- Haines, W. B. 1930. Studies in the physical properties of soil. V. The hysteresis effect in capillary properties, and the modes of moisture distribution associated therewith. *The Journal of Agricultural Science*, 20, 97-116.
- Halling-Sorensen, B. & Jorgensen, S. E. 1993. 4. Process Chemistry and Biochemistry of Denitrification. *Studies in Environmental Science*. Elsevier.
- Hamdan, N., Kavazanjian, E., Rittmann, B. E. & Karatas, I. 2016. Carbonate Mineral Precipitation for Soil Improvement through Microbial Denitrification. *Geomicrobiology Journal*, 00-00.
- Hammes, F. & Verstraete, W. 2002. Key roles of pH and calcium metabolism in microbial carbonate precipitation. *Reviews in Environmental Science and Biotechnology*, 1, 3-7.
- Harkers, M. P., Van Paassen, L. A., Booster, J. L., Whiffen, V. S. & Van Loosdrecht, M. C. M. 2010. Fixation and distribution of bacterial activity in sand to induce carbonate precipitation for ground reinforcement. *Ecological Engineering*, 36, 112-117.
- Haynie, D. T. 2008. *Biological Thermodynamics*. 2 ed. Cambridge: Cambridge University Press.
- He, J. & Chu, J. 2014. Undrained Responses of Microbially Desaturated Sand under Monotonic Loading. *Journal of Geotechnical and Geoenvironmental Engineering*, 140, 04014003.
- He, J., Chu, J. & Ivanov, V. 2013. Mitigation of liquefaction of saturated sand using biogas. *Geotechnique*, 63, 267-275.
- Heijnen, J. J. & Kleerebezem, R. 2010. Bioenergetics of Microbial Growth. *Encyclopedia of Industrial Biotechnology*. John Wiley & Sons, Inc.
- Heijnen, J. J., Van Loosdrecht, M. C. M. & Tjihuis, L. 1992. A black box mathematical model to calculate auto- and heterotrophic biomass yields based on Gibbs energy dissipation. *Biotechnology and Bioengineering*, 40, 1139-1154.
- Hovland, M. & Judd, A. G. 1988. *Seabed pockmarks and seepages : impact on geology, biology, and the marine environment*, London ;, Graham & Trotman.
- IneˆS M. Soares, M., Belkin, S. & Abeliovich, A. 1988. Biological Groundwater Denitrification: Laboratory Studies. *Water Science & Technology*, 20, 189-195.

- IneˆS M. Soares, M., Braester, C., Belkin, S. & Abeliovich, A. 1991. Denitrification in laboratory sand columns: Carbon regime, gas accumulation and hydraulic properties. *Water Research*, 25, 325-332.
- Istok, J. D., Park, M. M., Peacock, A. D., Oostrom, M. & Wietsma, T. W. 2007. An Experimental Investigation of Nitrogen Gas Produced during Denitrification. *Ground Water*, 45, 461-467.
- Ivanov, V. & Chu, J. 2008. Applications of microorganisms to geotechnical engineering for bioclogging and biocementation of soil in situ. *Review in Environmental Science and Bio/Technology*, 7, 139-153.
- James, G. A., Warwood, B. K., Hiebert, R. & Cunningham, A. B. 2000. Microbial Barriers to the Spread of Pollution. In: VALDES, J. J. (ed.) *Bioremediation*. Dordrecht: Springer Netherlands.
- Kaelin, D., Manser, R., Rieger, L., Eugster, J., Rottermann, K. & Siegrist, H. 2009. Extension of ASM3 for two-step nitrification and denitrification and its calibration and validation with batch tests and pilot scale data. *Water Research*, 43, 1680-1692.
- Karatas, I. 2008. *Microbiological Improvement of the Physical Properties of Soils*. Doctor of Philosophy, Arizona State University.
- Kavazanjian, E., O'donnell, S. T. & Hamdan, N. 2015. Biogeotechnical Mitigation of Earthquake-Induced Soil Liquefaction by Denitrification: A Two-Stage Process. *6th International Conference on Earthquake Geotechnical Engineering*. Christchurch, New Zealand.
- Keddy, P. A. 2010. *Wetland Ecology - Principles and Conservation, 2nd edition*, Cambridge University Press.
- Kim, D.-S. & Fogler, H. S. 2000. Biomass evolution in porous media and its effects on permeability under starvation conditions. *Biotechnology and Bioengineering*, 69, 47-56.
- Knowles, R. 1982. Denitrification. *Microbiological reviews*, 46, 43.
- Kornaros, M., Zafiri, C. & Lyberatos, G. 1996. Kinetics of denitrification by *Pseudomonas denitrificans* under growth conditions limited by carbon and/or nitrate or nitrite. *Water Environment Research*, 68, 934-945.
- Körner, H. & Zumft, W. G. 1989. Expression of denitrification enzymes in response to the dissolved oxygen level and respiratory substrate in continuous culture of *Pseudomonas stutzeri*. *Applied and Environmental Microbiology*, 55, 1670-1676.
- Kuenen, J. G. & Robertson, L. A. 1988. Ecology of nitrification and denitrification. In: COLE, J. A. & FERGUSON, S. J. (eds.) *SSGM 42 The Nitrogen and Sulphur (Society for General Microbiology Symposia)* Cambridge University Press.
- Lee, P. C., Tseng, F. G. & Pan, C. 2004. Bubble dynamics in microchannels. Part I: single microchannel. *International Journal of Heat and Mass Transfer*, 47, 5575-5589.
- Li, X. & Yortsos, Y. C. 1995. Theory of multiple bubble growth in porous media by solute diffusion. *Chemical Engineering Science*, 50, 1247-1271.
- Lin, H., Suleiman, M. T., Brown, D. G. & Jr., E. K. 2016. Mechanical Behavior of Sands Treated by Microbially Induced Carbonate Precipitation. *Journal of Geotechnical and Geoenvironmental Engineering*, 142, 04015066.

- Lubetkin, S. D. 2003. Why Is It Much Easier To Nucleate Gas Bubbles than Theory Predicts? *Langmuir*, 19, 2575-2587.
- Luong, J. H. T. 1987. Generalization of monod kinetics for analysis of growth data with substrate inhibition. *Biotechnology and Bioengineering*, 29, 242-248.
- Madigan, M. T., Martinko, J. M., Stahl, D. A. & Clark, D. P. 2012. *Brock - Biology of Microorganisms*, Pearson.
- Martin, D., Dodds, K., Butler, I. B. & Ngwenya, B. T. 2013. Carbonate Precipitation under Pressure for Bioengineering in the Anaerobic Subsurface via Denitrification. *Environmental Science & Technology*, 47, 8692-8699.
- Matějů, V., Čížinská, S., Krejčí, J. & Janoch, T. 1992. Biological water denitrification—A review. *Enzyme and Microbial Technology*, 14, 170-183.
- Mcconnaughey, T. A. & Whelan, J. F. 1997. Calcification generates protons for nutrient and bicarbonate uptake. *Earth-Science Reviews*, 42, 95-117.
- Meeussen, J. C. L. 2003. ORCHESTRA: An Object-Oriented Framework for Implementing Chemical Equilibrium Models. *Environmental Science & Technology*, 37, 1175-1182.
- Mitchell, J. K. & Santamarina, J. C. 2005. Biological Considerations in Geotechnical Engineering. *Journal of Geotechnical and Geoenvironmental Engineering*, 131, 1222-1233.
- Monod, J. 1949. The Growth of Bacterial Cultures. *Annual Review of Microbiology*, 3, 371-394.
- Montoya, B. M. & Dejong, J. T. 2015. Stress-Strain Behavior of Sands Cemented by Microbially Induced Calcite Precipitation. *Journal of Geotechnical and Geoenvironmental Engineering*, 141, 04015019.
- Montoya, B. M., Dejong, J. T. & Boulanger, R. W. 2013. Dynamic response of liquefiable sand improved by microbial-induced calcite precipitation. *Géotechnique*, 63, 267-275.
- Mortensen, B. M., Haber, M. J., Dejong, J. T., Caslake, L. F. & Nelson, D. C. 2011. Effects of environmental factors on microbial induced calcium carbonate precipitation. *Journal of Applied Microbiology*, 111, 338-349.
- Mosdorf, R. & Wyszowski, T. 2013. Self-organising structure of bubble departures. *International Journal of Heat and Mass Transfer*, 61, 277-286.
- O'donnell, S. 2016. *Mitigation of Earthquake-Induced Soil Liquefaction via Microbial Denitrification: A Two-Stage Process*. Doctor of Philosophy, Arizona State University.
- Op Den Camp, H. J. M., Kartal, B., Guven, D., Van Niftrik, L. a. M. P., Haaijer, S. C. M., Van Der Star, W. R. L., Van De Pas-Schoonen, K. T., Cabezas, A., Ying, Z., Schmid, M. C., Kuypers, M. M. M., Van De Vossenberg, J., Harhangi, H. R., Picioreanu, C., Van Loosdrecht, M. C. M., Kuenen, J. G., Strous, M. & Jetten, M. S. M. 2006. Global impact and application of the anaerobic ammonium-oxidizing (anammox) bacteria. *Biochemical Society Transactions*, 34, 174-178.
- Paassen, L. a. V. 2009a. *Biogrout: Ground Improvement by Microbially Induced Carbonate Precipitation*. Doctor of Philosophy, Delft University of Technology.

- Paassen, L. a. V. 2009b. Microbes turning sand into sandstone, using waste as cement. *4 iYGEC'09 - 4th International Young Geotechnical Engineer's Conference*. Egypt: ISSMGE.
- Paassen, L. a. V. 2011. Bio-mediated ground improvement: From laboratory experiment to pilot applications. *Geo-Frontiers Congress 2011*. Dallas, Texas, United States: American Society of Civil Engineers.
- Paassen, L. a. V., Daza, C. M., Staal, M., Sorokin, D. Y., Son, W. V. D. & Loosdrecht, M. C. M. V. 2010. Potential soil reinforcement by biological denitrification. *Ecological Engineering*, 36, 168-175.
- Payne, W. J. 1981. *Denitrification Canada*, A Wiley-Interscience Publication.
- Pham, V. P., Nakano, A., Star, W. R. L. V. D., Heimovaara, T. J. & Paassen, L. a. V. 2016a. Applying MICP by denitrification in soils: a process analysis. *Environmental Geotechnics*, 0, 1-15.
- Pham, V. P., Nakano, A., Van Der Star, W. R. L., Heimovaara, T. J. & Van Paassen, L. A. 2016b. Applying MICP by denitrification in soils: a process analysis. *Environmental Geotechnics*, 1-15, in press.
- Phillips, A. J., Gerlach, R., Lauchnor, E., Mitchell, A. C., Cunningham, A. B. & Spangler, L. 2013a. Engineered applications of ureolytic biomineralization: a review. *Biofouling*, 29, 715-733.
- Phillips, A. J., Gerlach, R., Lauchnor, E., Mitchell, A. C., Cunningham, A. B. & Spangler, L. 2013b. Engineered applications of ureolytic biomineralization: a review. *Biofouling*, 29, 715-33.
- Pinar, G., Duque, E., Haidour, A., Oliva, J., Sanchez-Barbero, L., Calvo, V. & Ramos, J. L. 1997. Removal of high concentrations of nitrate from industrial wastewaters by bacteria. *Applied and Environmental Microbiology*, 63, 2071-3.
- Pirt, S. J. 1975. *Principles of microbe and cell cultivation*, Oxford :, Blackwell Scientific.
- Puyol, D., Carvajal-Arroyo, J. M., Sierra-Alvarez, R. & Field, J. A. 2014. Nitrite (not free nitrous acid) is the main inhibitor of the anammox process at common pH conditions. *Biotechnology Letters*, 36, 547-551.
- Qabany, A. A., Soga, K. & Santamarina, C. 2012. Factors Affecting Efficiency of Micronially Induced Calcite Precipitation. *Journal of Geotechnical and Geoenvironmental Engineering*, 138.
- Rebata-Landa, V. & Santamarina, J. C. 2011. Mechanical effects of biogenic nitrogen gas bubbles in soils. *Journal of Geotechnical and Geoenvironmental Engineering*, 138, 128-137.
- Reed, D. 2002. Shallow Geohazard Risk Mitigation; A Drilling Contractor's Perspective. Society of Petroleum Engineers.
- Robertson, G. P. & Groffman, P. M. 2015. Nitrogen Transformations. In: PAUL, E. A. (ed.) *Soil Microbiology, Ecology and Biochemistry (Fourth Edition)*. Boston: Academic Press.
- Robertson, L. A., Dalsgaard, T., Revsbech, N.-P. & Kuennen, J. G. 1995. Confirmation of 'aerobic denitrification' in batch cultures, using gas chromatography and ¹⁵N mass spectrometry. *FEMS Microbiology Ecology*, 18, 113-120.
- Roth, K. 2012. Soil Physic - Lecture notes. Institute of Environmental Physics, Heidelberg University.

- Shapleigh, J. P. 2009. Dissimilatory and Assimilatory Nitrate Reduction in the Purple Photosynthetic Bacteria. In: HUNTER, C. N., DALDAL, F., THURNAUER, M. C. & BEATTY, J. T. (eds.) *The Purple Phototrophic Bacteria*. Dordrecht: Springer Netherlands.
- Sijbesma, W. F. H., Almeida, J. S., Reis, M. a. M. & Santos, H. 1996. Uncoupling effect of nitrite during denitrification by *Pseudomonas fluorescens*: An in vivo ³¹P-NMR study. *Biotechnology and Bioengineering*, 52, 176-182.
- Šimek, M. & Cooper, J. E. 2002. The influence of soil pH on denitrification: progress towards the understanding of this interaction over the last 50 years. *European Journal of Soil Science*, 53, 345-354.
- Sin, G., Kaelin, D., Kampschreur, M. J., Takács, I., Wett, B., Gernaey, K. V., Rieger, L., Siegrist, H. & Van Loosdrecht, M. C. M. 2008. Modelling nitrite in wastewater treatment systems: a discussion of different modelling concepts. *Water Science and Technology*, 58, 1155-1171.
- Skempton, A. W. 1954. The Pore-Pressure Coefficients A and B. *Géotechnique*, 4, 143-147.
- Soares, M. I. M. 2000. Biological Denitrification of Groundwater. *Water, Air, and Soil Pollution*, 123, 183-193.
- Soto, O., Aspé, E. & Roeckel, M. 2007. Kinetics of cross-inhibited denitrification of a high load wastewater. *Enzyme and Microbial Technology*, 40, 1627-1634.
- Thullner, M., Zeyer, J. & Kinzelbach, W. 2002. Influence of Microbial Growth on Hydraulic Properties of Pore Networks. *Transport in Porous Media*, 49, 99-122.
- Tiedje, J. M. J. J. M. 1988. Ecology of denitrification and dissimilatory nitrate reduction to ammonium. *Ecology of Denitrification and Dissimilatory Nitrate Reduction to Ammonium*, 179-244.
- Turnhout, A. G. V., Kleerebezem, R. & Heimovaara, T. J. 2016. A toolbox to find the best mechanistic model to predict the behavior of environmental systems. *Environ. Model. Softw.*, 83, 344-355.
- Van Der Star, W. R. L., Taher, E., Harkes, M. P., Blauw, M., Van Loosdrecht, M. C. M. & Van Paassen, L. A. 2009. Use of Waste Stream and Microbes for *In Situ* Transformation of Sand into Sandstone. In: LEUNG, C. F., CHU, J. & SHEN, R. F. (eds.) *Ground Improvement Technologies and Case Histories*. Research Publishing Services.
- Van Paassen, L. A., Ghose, R., Van Der Linden, T. J. M., Van Der Star, W. R. L. & Van Loosdrecht, M. C. M. 2010. Quantifying Biomediated Ground Improvement by Ureolysis: Large-Scale Biogrout Experiment. *Journal of Geotechnical and Geoenvironmental Engineering*, 136, 1721-1728.
- Van Paassen, L. A., Van Hermert, W. J., Van Der Star, W. R. L., Zwieten, G. V. & Baalen, L. V. 2012. Direct Shear Strength of Biologically Cemented Gravel. *GeoCongress 2012: State of the Art and Practice in Geotechnical Engineering*. ASCE.
- Van Spanning, R. J. M., Richardson, D. J. & Ferguson, S. J. 2007. Chapter 1 - Introduction to the Biochemistry and Molecular Biology of Denitrification. In: BOTHE, H., FERGUSON, S. J. & NEWTON, W. E. (eds.) *Biology of the Nitrogen Cycle*. Amsterdam: Elsevier.

- Van Turnhout, A. G., Kleerebezem, R. & Heimovaara, T. J. 2016. A toolbox to find the best mechanistic model to predict the behavior of environmental systems. *Environmental Modelling & Software*, 83, 344-355.
- Voorhees, E. B. 1902. Studies in Denitrification. *Journal of the American Chemical Society*, 24, 785-823.
- Wang, J. H., Baltzis, B. C. & Lewandowski, G. A. 1995. Fundamental denitrification kinetic studies with *Pseudomonas denitrificans*. *Biotechnology and Bioengineering*, 47, 26-41.
- Whiffin, V. S., Van Paassen, L. A. & Harkes, M. P. 2007. Microbial Carbonate Precipitation as a Soil Improvement Technique. *Geomicrobiology Journal*, 24, 417-423.
- Yaws, C. L. 2012. Yaws' Handbook of Properties for Aqueous Systems. Knovel.
- Yegian, M. K., Eseller-Bayat, E. & Alshawabkeh, A. 2007. Induced-Partial Saturation for Liquefaction Mitigation: Experimental Investigation. *Journal of Geotechnical and Geoenvironmental Engineering*, 133, 372-380.
- Yortsos, Y. C. & Parlur, M. 1989. Phase Change in Binary Systems in Porous Media: Application to Solution-Gas Drive. Society of Petroleum Engineers.
- Zhu, T. & Dittrich, M. 2016. Carbonate Precipitation through Microbial Activities in Natural Environment, and Their Potential in Biotechnology: A Review. *Frontiers in Bioengineering and Biotechnology*, 4, 4.
- Zumft, W. G. 1997. Cell biology and molecular basis of denitrification. *Microbiology and Molecular Biology Reviews*, 61, 533-616.

Curriculum Vitae

Vinh Phú Phạm

16/09/1986 Born in Hanoi, Vietnam

Education

- 9/2012 – 7/2017 PhD student
Delft University of Technology, Department of Geoscience and
Engineering, the Netherlands
- 8/2010 – 7/2012 Master of Science in Civil Engineering
Delft University of Technology, the Netherlands
Specialization: Geo-Engineering
- 9/2004 – 7/2009 Bachelor's Degree in Civil Engineering
Hanoi Water Resources University, Vietnam
Specialization: Hydraulic Construction.

Experience

- 3/2017 – 6/2017 Groundwater Technology BV
Project member;
- 5/2015 – 6/2015 Deltares
Performing cyclic triaxial test to investigate rockwool material
- 6/2011- 5/2012 Deltares
Internship
Subject: Investigation of rice husk ash applicability in
geotechnology.
- 2009 – 2010 Water Resources University, Hanoi, Vietnam
Assistant Lecturer on the subject of Soil Mechanics and
Foundation Engineering.

Publication

V.P. Pham, A. Nakano, W.R.L van der Star, T.J. Heimovaara, L.A. van Paassen (2016)
Applying MICP by denitrification in soils: a process analysis. *Environmental
Geotechnics*. 10.1680/jenge.15.000780. [article in press].

Pham, V.P., van Paassen, L.A., van der Star, W.R.L., and Heimovaara, T.J. & (2017).
Evaluating strategies to improve process efficiency of denitrification based MICP.
Journal of Geotechnical and Geoenvironmental Engineering. [under review].

G. Greeuw, A. Venmans, L.A. van Paassen, V. Pham (2016). Steenwol als tijdelijke
waterbuffer in de grond. *Land+Water* nr. 7/8 2016.

Vinh P. Pham, Wouter RL van der Star, Guang Ye, Leon A. van Paassen (2016). Rice

husk ash with high carbon content proves favourable for soil stabilization. *Jaarboek van de Mijnbouwkundige Vereeniging te Delft*, 77 Editie.

Sy Huu Pham, Vinh Phu Pham, Le Minh Vu. The ellipsoidal surface method solving by intergration for slope stability analysis. *Proceeding of the 2nd International Conference HanoiGeo 2015*, 27-28 November 2015. ISBN 978-604-913-418-0.

Le Minh Vu, Vinh Phu Pham (2009). The study of interpretation of cone penetration records to determine soil properties using for construction design. Vietnamese. *Proceeding of National Youth Technology Scientific Symposium for Colleges and Universities*, p. 785-788.